Ingeniería e Investigación
Journal
Abbreviated Journal Title: **Ing. Investig.**

Frequency
Quarterly, 3 issues per year
April, August and December

Cover Layout
Carlos Andrés Ortiz Valle

Proofreader
Janeth Alejandra García

Layout Artist
Patricia Chávez R.

Photography
Courtesy of the Dept. of Electrical and Electronic Engineering (Anonymous Author)

Printing
Corcas Editores S.A.S.

For additional information contact
revii_bog@unal.edu.co
Bogotá - Colombia
December - 2019

Table of Contents

Papers published in *Ingeniería e Investigación journal* are abstracted/indexed in

- Science Citation Index Expanded (SciSearch®), Clarivate Analytics
- Scopus - Elsevier
- Scientific Electronic Library Online - SciELO, Colombia
- Chemical Abstract
- Índice de Revistas Latinoamericanas en Ciencias Periódica
- Redalyc-Red de Revistas Científicas de América Latina y el Caribe, España y Portugal
- Dialnet
- Sistema Regional de Información en Línea para Revistas Científicas de América Latina, El Caribe, España y Portugal - Latindex
- Ebsco Publishing
- DOAJ - Directory of Open Access Journals
- Redib - Red Iberoamericana de Innovación y Conocimiento Científico

Ingeniería e Investigación journal was created in 1981. This is an entity in charge of spreading the teaching, scientific and technical research developed in the Universidad Nacional de Colombia's Engineering Faculty and other national and international institutions. *Ingeniería e Investigación journal* deals with original, unedited scientific research and technological developments in the various disciplines related to engineering. *Ingeniería e Investigación journal* contributes towards the development of knowledge, generating a global impact on academia, industry and society at large, through an exchange of knowledge and ideas maintaining a set of serious and recognized quality standards.

Ingeniería e Investigación journal publications are developed for the academic community who is interested in research and engineering knowledge development. We invite readers to be part of this Journal and participate either as authors, peer reviewers or subscribers.

For additional information contact:
www.revistas.unal.edu.co/index.php/ingeinv
E-mail: revii_bog@unal.edu.co
Tel: 57(1) 3 16 5000 Ext. 13674

Tabla de Contenido

Editorial

Español

Una mirada a la Misión de Sabios

Resumen

Esta nota editorial presenta una revisión somera del informe de la Misión de Sabios 2019. La nota reúne los aspectos más generales y plantea una discusión acerca del rol que las Facultades de Ingeniería pueden desempeñar en el marco de referencia trazado por la Misión.

La Misión de Sabios

La Misión de Sabios fue una iniciativa convocada por el Gobierno Nacional de Colombia para "aportar a la construcción e implementación de la política pública de Educación, Ciencia, Tecnología e Innovación y a las estrategias que debe construir Colombia a largo plazo, para responder a los desafíos productivos y sociales de manera escalable, replicable y sostenible". (Gobierno de Colombia, 2019a). Para tal fin, se convocaron a 47 especialistas nacionales e internacionales en las distintas disciplinas profesionales que definieron focos estratégicos para el desarrollo acelerado de la ciencia, tecnología e innovación (CTI) en el país. Los focos estratégicos definidos son:

- Biotecnología, bioeconomía y medio ambiente
- Ciencias básicas y del espacio
- Ciencias de la vida y de la salud
- Ciencias sociales, desarrollo humano y equidad
- Energía sostenible
- Industrias creativas y culturales
- Océanos y recursos hidrobiológicos
- Tecnologías convergentes e industria 4.0

Se dice en uno de los documentos de la Misión de Sabios que hay al menos tres aspectos en los que el mundo actual es diferente al de 1994 (Gobierno de Colombia, 2019b). El primero es el progreso acelerado de diferentes tecnologías (digitalización, biología y materiales avanzados). El avance de la banda ancha para internet y de conectividad a través del internet de las cosas ha reconfigurado numerosas cadenas de valor y ha habilitado la creación de negocios en plataformas. Las posibilidades de las tecnologías convergentes para solucionar problemas y crear valor económico y social son gigantescas (Gobierno de Colombia, 2019b).

El segundo es la evidencia creciente sobre los impactos del cambio climático y de la urgencia de un enfoque de economía

English

A Look at the Mission of Wise Men

Summary

This editorial note presents a brief review of the report by the 2019 Mission of Wise men. The note gathers the more general aspects and poses a discussion about the role that the Schools of Engineering can play in the framework of reference raised by the Mission.

The Mission of Wise Men

The Mission of Wise Men was an initiative convened by the National Government of Colombia to "contribute to the construction and implementation of the public policy of Education, Science, Technology and Innovation and to the strategies that Colombia must build in the long term, to respond to productive and social challenges in a scalable, replicable and sustainable way". (Gobierno de Colombia, 2019a). For this purpose, 47 national and international specialists were summoned from various professional disciplines that defined the strategic foci for the accelerated development of science, technology and innovation (STI) in the country. The strategic foci defined are:

- Biotechnology, bioeconomy and environment
- Basic and space sciences
- Life and health sciences
- Social sciences, human development and equity
- Sustainable energy
- Creative and cultural industries
- Oceans and hydrobiological resources
- Converging technologies and industry 4.0

One of the documents of the Mission of Wise Men states that there are at least three aspects in which the current world is different from that of 1994 (Gobierno de Colombia, 2019b). The first one is the accelerated progress of different technologies (digitization, biology and advanced materials). The advancement of the internet broadband and connectivity through internet of things has reconfigured numerous value chains and enabled the creation of businesses on platforms. The possibilities of converging technologies to solve problems and create economic and social value are enormous (Gobierno de Colombia, 2019b).

The second one is the growing evidence of the impacts of climate change and the urgency of a circular economy

circular para modelos que alinean la creación de valor con la reducción de los efectos de la contaminación creciente del agua y del aire urbano (Gobierno de Colombia, 2019b).

El tercero es la presión por descubrir nuevas formas de expresión y participación de los ciudadanos. La ciencia, la tecnología, las industrias creativas y culturales y la reflexión de las ciencias sociales pueden contribuir a que los ciudadanos desarrollen su capacidad de imaginar su sociedad y su papel en ella Cambiar por: (Gobierno de Colombia, 2019b).

De acuerdo con la Misión (Gobierno de Colombia, 2019b; Colciencias, 2019), el 80% de las exportaciones de Colombia en 2018 proviene de la minería, lo que significa que nuestra economía es poco diversificada y de baja complejidad. Existe un gran potencial para el desarrollo de una industria manufacturera de productos de mayor valor agregado. La Misión resalta la dependencia del país en el desarrollo económico debida a las deficiencias en conocimiento básico. Para generar riqueza es necesario tener capacidades propias en ciencias básicas y productividad científica. Con el fin de superar estas deficiencias, la Misión presenta cuatro propuestas que se describen brevemente a continuación.

Propuestas de la Misión de Sabios

La Misión de Sabios formula cuatro propuestas transversales relacionadas con el marco institucional, la financiación, la educación y las misiones o centros.

Medidas institucionales

La Misión (Colciencias, 2019) identificó deficiencias estructurales en el Sistema Nacional de Ciencia, Tecnología e Innovación (SNCTI) y sugiere tres principios para superarlas:

a. Separación entre la formulación de políticas y su ejecución, mediante la creación de una agencia ejecutora con amplias capacidades de estructuración financiera.

b. Reconocimiento de funciones diferenciadas de creación de conocimiento básico, desarrollo y transferencia de tecnología, impulso a la I+D privada y adopción de tecnologías de frontera.

c. Actividades e iniciativas que faciliten a la ciudadanía el aprovechamiento de la CTI para la formación de talento, organización de redes y apropiación del conocimiento.

Financiación

Entre los documentos producidos por la Misión se dice que "la meta de la inversión en CTI es aumentar la productividad de la economía, la sostenibilidad ambiental y el progreso social a través de mejores productos, servicios y actividades creativas" (Gobierno de Colombia, 2019b, p. 14). La Misión (Gobierno de Colombia, 2019b; Colciencias, 2019) sugiere orientar la financiación pública estatal definiendo prioridades de la siguiente manera:

approach to models that align value creation with the reduction of the effects of increased urban water and air pollution (Gobierno de Colombia, 2019b). The third is the pressure to discover new forms of expression and citizen participation. Science, technology, creative and cultural industries and reflection of the social sciences can help citizens to develop their ability to imagine their society and their role in it.

According to the Mission (Gobierno de Colombia, 2019b; Colciencias, 2019), 80% of Colombian exports in 2018 come from mining, which means that our economy is little diversified and has low complexity. There is great potential for the development of a manufacturing industry with higher value-added products. The Mission highlights the country's dependence on economic development, due to deficiencies in basic knowledge. To generate wealth, it is necessary to have own skills in basic sciences and scientific productivity. In order to overcome these shortcomings, the Mission presents four proposals which are briefly described below.

Proposals by the Mission of Wise Men

The Mission of Wise Men formulate four cross-cutting proposals related to the institutional framework, funding, education and, missions or centers.

Institutional Measures

The Mission (Colciencias, 2019) identified structural deficiencies in the National System of Science, Technology and Innovation (SNCTI) and suggests three basic principles to overcome them:

a. Separation between policy making implementation, through the creation of an executing agency with extensive capabilities of financial structuring.

b. Recognition of differentiated functions of basic knowledge creation, technology development and transfer, boosting private R&D, and adoption of frontier technologies.

c. Activities and initiatives to facilitate enable citizens to take advantage for talent training, networking and appropriation of knowledge.

Financing

Some of the documents produced by the Mission (Gobierno de Colombia, 2019b; Colciencias, 2019) state that the goal of investment in STI is to increase the productivity of the economy, environmental sustainability and social progress through better products, services and creative activities. The Mission suggests orienting the state public funding by defining priorities as follows:

- The state public funding should support STI that lacks high private profitability but has high social benefits.

- La financiación pública estatal debe apoyar la CTI que carezca de rentabilidad privada alta, pero que tenga beneficios sociales altos.
- El sector público no debe financiar la CTI de baja rentabilidad privada con aportes sociales inferiores al costo de los fondos públicos.
- El sector privado debe financiar la CTI de rentabilidad privada alta.

Se presentan críticas hacia los esquemas de incentivos utilizados, para los cuales se recomiendan cinco tipos (Gobierno de Colombia, 2019b):

- Las grandes empresas recibirán incentivos cuando inviertan en investigación básica, realicen aportes a centros e institutos de investigación, proyectos desarrollados por universidades o Pymes.
- Los incentivos tributarios por innovación deben limitarse a Pymes.
- Se abrirán líneas especiales de crédito con riesgo compartido para Pymes.
- Se promoverá el capital de riesgo, administrado en delegación a actores experimentados en este tipo de financiación.
- Se cofinanciará la I+D con las grandes empresas para investigación a largo plazo y se abrirán convocatorias para que las grandes empresas sirvan de ancla en proyectos con Pymes.

La Misión de Sabios (Gobierno de Colombia, 2019b) considera que el Estado debe ser líder y responsable de empezar y sostener las propuestas presentadas. Se vislumbraron dos fases para alcanzar tales propósitos:

- Fase 1: Capital público paciente, para el cual se espera lograr un 1,2% de inversión total en I+D como porcentaje del PIB para 2028. Este porcentaje está compuesto por 0,8% de inversión pública y 0,4% de inversión privada.
- Fase 2: Despegue de I+D privado. Se espera alcanzar una inversión de 1,8% con respecto al PIB, con una inversión pública del 0,85% y una inversión privada del 0,95%. Para el 2022 la inversión pública debe llegar al 0,37% y la privada a un 0,26% del PIB. La Misión resalta que, con base en experiencias internacionales, una inversión pública de 0,8% activa las inversiones privadas.

La Misión (Gobierno de Colombia, 2019b; Colciencias, 2019) también sugiere cambiar el porcentaje de los recursos de regalías destinado a CTI de un 10% a un 25% mediante una reforma constitucional. Tales recursos se destinarían a

- The public sector should not finance STI with low-private profitability and social contributions below the cost of public funds.
- The private sector must finance high private profitability STI.

Some criticism is presented towards the schemes used for incentives, to which five types are recommended (Gobierno de Colombia, 2019b):

- Large companies will receive incentives when investing in basic research, making contributions to research centres and institutes, projects developed by universities, or SMEs.
- Innovation tax incentives should be limited to SMEs.
- Special lines of credit with shared risk will be opened for SMEs.
- Venture capital will be promoted under delegated management from experienced actors in this type of funding.
- R&D will be co-financed with large companies for long-term research and calls will be opened for large companies to serve as an anchor in projects with SMEs.

The Mission of Wise Men (Gobierno de Colombia, 2019b): believes that the State should lead and responsible for starting and supporting the presented proposals. Two phases were envisaged to achieve these purposes:

- Phase 1: Patient public capital, for which 1,2% of the total investment in R&D is expected as a percentage of the GDP for 2028. This percentage is composed of 0,8% public investment and 0,4% of private investment.
- Phase 2: Private R&D takeoff. An investment of 1,8% regarding GDP is expected, with public investment of 0,85% and private investment of 0,95%. By 2022, public investment must reach 0,37% and private investment should reach 0,26% of the GDP. The Mission highlights that, based on international experience, a public investment of 0,8% activates private investment.

The Mission (Gobierno de Colombia, 2019b; Colciencias, 2019) also suggests changing the percentage of royalty resources allocated to STI from 10% to 25%, through a constitutional reform. Those resources would be devoted to integral education for children under 5 years of age, funding of regional research and innovation centers and institutes, and challenge and mission programmes. Additionally, the Mission of Wise Men deems it necessary to obtain international loans in an estimated amount of $300 million dollars for the next four years (until 2024).

educación integral para menores de 5 años, a la financiación de centros e institutos de investigación e innovación regionales y a los programas de retos y misiones. Además, la Misión de Sabios considera necesaria la consecución de préstamos internacionales en un monto estimado de 300 millones de dólares para los próximos cuatro años (hasta 2024).

Educación

La educación representa un factor esencial en la transformación de las sociedades y en el desarrollo humano. La Misión de Sabios (Gobierno de Colombia, 2019b; Colciencias, 2019) resalta el rol de la educación, particularmente en el contexto de un cambio tecnológico acelerado. La educación debe avanzar en aspectos como pedagogías nuevas, universalización del acceso, calidad de la educación, nutrición, salud, afecto y demás componentes de una atención integral a niños de 0 a 5 años, así como en la diversificación y universalización de la educación secundaria.

La Misión (Gobierno de Colombia, 2019b) presenta en relación con la educación varias propuestas:

- La creación del Instituto Superior de Investigación en Educación y Alta Formación de Maestros (IESI).
- Programas agresivos de becas y estímulos para el estudio de las ciencias básicas como medio para aproximar la investigación y la docencia.
- Reformar el sistema educativo para soportar el aprendizaje y actualización permanente a lo largo de la vida.
- Transformar la educación media, los métodos, herramientas y gestión educativa a través de las alternativas que ofrecen las tecnologías convergentes y la Industria 4.0.
- Fortalecer las Universidades en su rol de guardianes de la investigación básica, las humanidades, la democracia y la libertad, articuladas con los institutos.

Misiones y Centros

Con el fin de evitar el actual uso disperso de los fondos, la Misión de Sabios sugiere como estrategia las misiones y los centros. En este sentido, la Misión (Gobierno de Colombia, 2019b; Colciencias, 2019) realizó esfuerzos importantes en la definición de tres grandes retos:

1. El primer reto es una Colombia biodiversa que propone identificar, conocer, documentar y aprovechar la diversidad cultural y natural del país para impulsar la bioeconomía y la economía creativa.
2. El segundo reto es una Colombia productiva y sostenible que busca modificar la estructura productiva del país hacia industrias y servicios con contenido

Education

Education is an essential factor in the transformation of societies and human development. The Mission of Wise Men (Gobierno de Colombia, 2019b; Colciencias, 2019) highlights the role of education, particularly in the context of an accelerated technological change. Education must advance in aspects such as new pedagogies, universalization of access, quality of education, nutrition, health, affection and other components of comprehensive assistance for children aged from 0 to 5 years, as well as in the diversification and universalization of secondary education.

The Mission (Gobierno de Colombia, 2019b) presents several proposals in relation to education:

- The creation of the Higher Research Institute in Education and High Training of Teachers (IESI).
- Aggressive scholarship and stimulus programs for the study of basic sciences as a means of approximating research and teaching.
- Reforming the education system to support lifelong learning and permanent updating.
- Transforming middle education, methods, tools and educational management using alternatives offered by converging technologies and Industry 4.0.
- Strengthening Universities in their role as guardians of basic research, the humanities, democracy, and freedom, articulated with centers and institutes.

Missions and Centers

In order to avoid the currently disperse use of funds, the Mission of Wise Men suggests missions and centers as a strategy. In this sense, the Mission (Gobierno de Colombia, 2019b; Colciencias, 2019) made important efforts to define three major challenges:

- The first challenge is a biodiverse Colombia that proposes to identify, know, document and take advantage of the cultural and natural diversity of the country to promote the bioeconomy and the creative economy.
- The second challenge is a productive and sustainable Colombia that seeks to modify the productive structure of the country toward industries and services with high technological content and toward companies of circular economy with the maximum use of waste and environmental sustainability.
- The third challenge is an equitable Colombia that aims to improve in large sections of the population the levels of education and health, and strengthen their cultural identity, so that they integrate with economic growth and human and sustainable development with equity.

tecnológico alto y hacia empresas de economía circular con máximo aprovechamiento de residuos y con sostenibilidad ambiental.

3. El tercer reto es una Colombia equitativa que apunta a que amplias capas de la población mejoren sus niveles de educación y de salud, y afiancen su identidad cultural, de forma que se integren al crecimiento económico y al desarrollo humano y sostenible con equidad.

Rol de la Ingeniería

La pregunta que queremos formular a los profesionales de la Ingeniería en Colombia es: ¿Cuál es el rol de la Ingeniería en el panorama presentado por la actual Misión de Sabios?

Existen diversas oportunidades para participar en el escenario propuesto por la Misión. Una lista somera que dista de ser la más completa es la siguiente:

- Experiencia en formación de profesionales. Las Facultades de Ingeniería estamos perfectamente alineadas con los principios planteados acerca de la educación gracias a las revisiones que se han hecho a los programas de estudio, orientándolos al desarrollo de competencias y al logro de resultados de aprendizaje. Es un reto cambiar de paradigma (Arzola y Pavas, 2019), pero los beneficios potenciales justifican emprender la transformación.

- Experiencia en Investigación, Desarrollo e Innovación. Las Facultades de Ingeniería albergan a una parte importante de los grupos de investigación del país. Estos han realizado contribuciones significativas al conocimiento nacional y han alcanzado reconocimiento a nivel mundial. Los investigadores de Ingeniería son un actor esencial en el panorama de CTI del país. Además, la amplia experiencia en proyectos de extensión ofrece cercanía y competencia en la gestión de recursos públicos y privados para el desarrollo de soluciones de alto impacto social. Perfiles como los de los grupos e investigadores de las Facultades de Ingeniería son deseables para atraer la inversión privada con fines de investigación y desarrollo.

- Misiones y centros. Las Facultades de Ingeniería conocen el país en todas sus dimensiones: recursos, clima, medio ambiente, riesgos, diversidad social y económica, etc. El trabajo interdisciplinario es parte de nuestra práctica, de forma que integrarnos con otras disciplinas profesionales en el marco de referencia propuesto por la Misión no nos es ajeno.

- Las tecnologías convergentes están presentes en las Facultades de Ingeniería, tanto en calidad de insumo como de resultado. El desarrollo de cadenas de valor es parte de la formación básica en Ingeniería. Se investiga sobre el tema y se desarrollan proyectos relacionados con la industria y el sector público. Alrededor de estas

Role of Engineering

The question we want to ask to Engineering professionals in Colombia is: What is the role of Engineering in the framework presented by the current Mission of Wise Men?

There are several opportunities to participate in the scenario proposed by the Mission of Wise Men. A short list that is far from being the most complete is the following:

- Experience in educating professionals. The Schools of Engineering are perfectly aligned with the principles raised about education thanks to the revisions made to the curricula, which oriented them to the development of competences and the achievement of learning outcomes. It is a challenge to change the paradigm (Arzola and Pavas, 2019), but the potential benefits justify undertaking the transformation.

- Research, Development and Innovation Experience. The Schools of Engineering encompass an important part of the country's research groups. They have made significant contributions to national knowledge and have achieved worldwide recognition. Engineering researchers have an essential role in the STI landscape of the country. Besides, extensive experience in projects of specialized consultancy offers closeness and competence in the management of public and private resources for the development of solutions with high social impact. Profiles such as those of groups and researchers of the Schools of Engineering are desirable to attract private investment for research and development purposes.

- Missions and centers. The Schools of Engineering know the country in all its dimensions: resources, climate, environment, risks, social and economic diversity, etc. Interdisciplinary work is part of our practice, thus integrating other professional disciplines in the reference framework proposed by the Mission is not strange to us.

- Converging technologies are present in the Schools of Engineering, both as input and result. The development of value chains is part of the basic education in Engineering, Research is carried out on the subject and projects related to industry and the public sector are developed. Around these converging technologies, the Schools of Engineering offer significant experience and have great opportunities for contributing.

With regard to scientific publications, the Mission makes no explicit mention of their role in the general guidelines of its proposals. However, scientific publications are indeed benchmark for justifying those proposals and emerge as indicators for reviewing and as targets to be achieved in the future. An increase is suggested in the quantity and quality of publications. Regarding the number of publications, it is understood that the more it is published, the more likely it is to make contributions that translate into new

tecnologías convergentes, las Facultades de Ingeniería ofrecen una experiencia significativa y tienen grandes oportunidades de contribución.

En cuanto a las publicaciones científicas, la Misión no hace mención explícita sobre su rol en los lineamientos generales de sus propuestas. No obstante, las publicaciones científicas sí son el referente para justificar dichas propuestas y emergen como indicadores de revisión y como metas a alcanzar a futuro. Se sugiere incrementar la cantidad y calidad de las publicaciones. En cuanto a la cantidad de publicaciones, se entiende que cuanto más se publique existen más posibilidades de realizar contribuciones que se traduzcan en nuevo conocimiento, desarrollos o innovaciones. Con respecto a la calidad de las publicaciones, se menciona de forma reiterativa en los documentos de la Misión la indexación en bases de datos científicas con trazabilidad internacional y el número de citas recibidas por las publicaciones. En este sentido, presentamos a los lectores las siguientes reflexiones:

- Incrementar la cantidad de publicaciones de autores nacionales, así como mejorar su calidad es un propósito loable desde el punto de vista académico y científico. Esto requiere mayor cantidad de manuscritos y capacidad para su correspondiente gestión y visibilidad. ¿De qué manera van a apoyarse los proyectos editoriales nacionales para atender las demandas de productividad que la Misión sugiere?
- Los criterios de calidad de las publicaciones mencionados en los documentos de la Misión de Sabios se centran en la presencia en bases de datos científicas y el número de citas. Sin embargo, no existe una correspondencia directa entre las citas y presencia en bases de datos, y los propósitos que persigue la Misión, ya que los trabajos más citados no necesariamente son aquellos que logran traducirse en desarrollos productivos, ni todos los desarrollos productivos han sido sujeto de publicación o han recibido citas. Por ende, surge la siguiente pregunta: ¿Las metas sugeridas por la Misión para el mejoramiento de la calidad de las publicaciones deben medirse siguiendo criterios cuantitativos de citas y visibilidad en bases de datos?

Invitamos respetuosamente a los lectores a leer los documentos presentados por la Misión, a compartirlos y discutirlos en sus instituciones, y a reflexionar sobre la mejor manera posible de participar y contribuir en este panorama nacional.

Referencias

Arzola de la Peña, Nelson, and Pavas, Andrés. (2019). La enseñanza de la Ingeniería en su encrucijada. *Ingeniería e Investigación*, *39*(2), 3-10. 10.15446/ing.investig.v39n2.83786

Colciencias (2019). *Colombia hacia una Sociedad del Conocimiento. Informe Misión Internacional de Sabios 2019 por la Educación, la Ciencia, la Tecnología y la Innovación* [Preliminar]. https://minciencias.gov.co/sites/default/files/upload/paginas/191205_informe_mision_de_sabios_2019_vpreliminar.pdf

Gobierno de Colombia (2019a). *Misión de Sabios* [Brochure]. https://minciencias.gov.co/sites/default/files/upload/paginas/brochure_mision_de_sabios_16_abril.pdf

Gobierno de Colombia (2019b). *Propuestas de la Misión Internacional de Sabios*. https://minciencias.gov.co/sites/default/files/upload/paginas/propuesta-sabios-txt_y_portada-alta.pdf

knowledge, developments or innovations. With regard to the quality of publications, the documents of the Mission reiteratively mention indexation in internationally traceable scientific databases and the number of citations received by the publications. In this sense, we present the following reflections to the readers:

- Increasing the number of publications by national authors, as well as improving their quality, is a laudable purpose from an academic and scientific point of view. This requires more manuscripts and the capacity for their corresponding management and visibility. How will national editorial projects be supported to meet the productivity demands suggested by the Mission?
- The quality criteria of the publications mentioned in the documents of the Mission of Wise Men focus on the presence in scientific databases and the number of citations. However, there is no direct correspondence between citations or database presence and the purposes pursued by the Mission, since the most cited works are not necessarily those able to translate into productive developments, nor all productive developments have been published or have received citations. Therefore, the following question arises: Regarding the goals suggested by the Mission for improvement of the quality of publications, should they be measured according to quantitative criteria of citation and visibility in databases?

We respectfully invite readers to read the documents presented by the Mission, to share them and discuss them in their institutions, and to reflect upon the best possible way to participate and contribute in this national landscape.

References

Arzola de la Peña, Nelson, and Pavas, Andrés. (2019). The teaching of Engineering at its crossroads. *Ingeniería e Investigación*, *39*(2), 3-10. 10.15446/ing.investig.v39n2.83786

Colciencias (2019). *Colombia hacia una Sociedad del Conocimiento. Informe Misión Internacional de Sabios 2019 por la Educación, la Ciencia, la Tecnología y la Innovación* [Preliminar]. https://minciencias.gov.co/sites/default/files/upload/paginas/191205_informe_mision_de_sabios_2019_vpreliminar.pdf

Gobierno de Colombia (2019a). *Misión de Sabios* [Brochure]. https://minciencias.gov.co/sites/default/files/upload/paginas/brochure_mision_de_sabios_16_abril.pdf

Gobierno de Colombia (2019b). *Propuestas de la Misión Internacional de Sabios*. https://minciencias.gov.co/sites/default/files/upload/paginas/propuesta-sabios-txt_y_portada-alta.pdf

2019 por la Educación, la Ciencia, la Tecnología y la Innovación [Preliminar]. https://minciencias.gov.co/sites/default/files/upload/paginas/191205_informe_mision_de_sabios_2019_vpreliminar.pdf

Gobierno de Colombia (2019a). *Misión de Sabios* [Brochure]. https://minciencias.gov.co/sites/default/files/upload/paginas/brochure_mision_de_sabios_16_abril.pdf

Gobierno de Colombia (2019b). *Propuestas de la Misión Internacional de Sabios*. https://minciencias.gov.co/sites/default/files/upload/paginas/propuesta-sabios-txt_y_portada-alta.pdf

ANDRÉS PAVAS
Director Revista *Ingeniería e Investigación*
Profesor Asociado
Departamento de Ingeniería Eléctrica y Electrónica
Universidad Nacional de Colombia
http://orcid.org/0000-0002-0971-0725

NELSON ARZOLA DE LA PEÑA
Editor Asociado Revista *Ingeniería e Investigación*
Profesor Titular
Departamento de Ingeniería Mecánica y Mecatrónica
Universidad Nacional de Colombia
https://orcid.org/0000-0002-5004-113X

ANDRÉS PAVAS
Head Editor of *Ingeniería e Investigación*
Associate Professor
Department of Electrical and Electronic Engineering
Universidad Nacional de Colombia
http://orcid.org/0000-0002-0971-0725

NELSON ARZOLA DE LA PEÑA
Associate Editor of *Ingeniería e Investigación*
Full Professor
Department of Mechanical and Mechatronics Engineering
Universidad Nacional de Colombia
https://orcid.org/0000-0002-5004-113X

Ingeniería e Investigación vol. 39 No. 3, December - 2019 (10-19)

DOI: http://dx.doi.org/10.15446/ing.investig.v39n3.81424

Engineering applications of chemically-bonded phosphate ceramics

Aplicaciones en ingeniería de las cerámicas de fosfato químicamente enlazadas

Carlos Andrés Cárdenas-Balaguera[1] and Maryory Astrid Gómez-Botero[2]

ABSTRACT

Phosphate cements originated more than a century ago for specific applications to the field of dentistry. These cements have other applications including: biomaterials with bone applications, stabilization of hazardous waste, and structural cements. However, the applications in civil infrastructure are recent and not widely known. Therefore, this review discusses and analyzes phosphate cements, presenting the most significant findings of the research to address their mechanical behavior of these cements. It also describes the impact and application of phosphate cements as a structural product (pastes, mortars and concretes), in addition to typical values of mechanical strength, workability, commercial applications, etc. As a result, the review allows to elucidate advantages and disadvantages in comparison with existing technologies and the mechanical possibilities of these cements as biomaterials and for the immobilization of radioactive waste.

Keywords: Phosphate cements, structural applications, mechanical properties.

RESUMEN

Los cementos de fosfato se originaron hace más de un siglo para aplicaciones propias en el campo de la odontología. Estos cementos registran otras aplicaciones entre las que se destacan: biomateriales con aplicaciones óseas, estabilización de desechos peligrosos y como cemento estructural. Sin embargo, las aplicaciones en obras de infraestructura civil son recientes y poco conocidas. Por este motivo, esta revisión discute y analiza los cementos de fosfato, presentando los hallazgos más significativos de las investigaciones realizadas para abordar y comprender su comportamiento mecánico. También se describen el impacto y la aplicación de los cementos de fosfato como producto estructural (pastas, morteros y hormigones), así como valores típicos de resistencia mecánica, trabajabilidad, aplicaciones comerciales, etc. Como resultado, esta revisión permite dilucidar ventajas y desventajas en comparación con las tecnologías existentes y las posibilidades mecánicas de estos cementos como biomateriales y para la inmovilización de residuos radioactivos.

Palabras clave: Cementos de fosfato, aplicaciones estructurales, propiedades mecánicas.

Received: August 1st, 2019
Accepted: September 24th, 2019

Introduction

Ceramic and hydrated cements are the most recognized products of inorganic solids. Ceramics are obtained by compaction of powders and subsequent sintering at high temperatures, resulting in hard and dense ceramics with good properties against corrosion. Its structure is usually highly crystalline with vitreous phases, presenting ionic and covalent bonds. Hydrated cements are chemically-bonded materials with hydrogen bonds that are formed by the chemical reaction of water with some characteristic powders that harden at room temperature, obtaining a product with sufficient compressive strength, to be used in structural applications (Wagh, 2016). These cements are usually united by van der Waals forces, exhibiting a non-crystalline, very porous structure. It is worth noting that the most noticeable difference between ceramics and hydrated cements lies in their consolidation process as a material. To obtain ceramic hard products, materials must be exposed to high temperatures. In contrast, hydrated cements reach hardness at room temperature (Wagh, 2016), although raw materials are subjected to high temperatures for their manufacture and considerable energy consumption is needed to obtain the clinker (Schneider, Romer, Tschudin, and Bolio, 2011), which is the main component of conventional Portland cement.

However, there is an intermediate product among those mentioned above, which consolidates similarly to a hydraulic

[1]Industrial Engineer and Industrial Designer, Universidad Pedagógica y Tecnológica de Colombia. Master in Strategic Management, Universidad Internacional Iberoamericana, Puerto Rico. Affiliation: CIDEMAT Research Center, Universidad de Antioquia, Colombia. DITMAV Research Group, Univerisdad Pedagógica y Tecnológica, Colombia. E-mail: carlos.cardenasb@udea.edu.co
[2]Metallurgical Engineer, Universidad de Antioquia, Colombia. M.Sc. in Laser processing, Universidad de Barcelona, España. Ph.D. in Instrumental Techniques of Physics, Universidad de Barcelona, España. Affiliation: Professor and researcher of the CIDEMAT Research Center, Universidad de Antioquia, Colombia. E-mail: maryory.gomez@udea.edu.co

How to cite: Cardenas-Balaguera, C. A. and Gómez-Botero, M. A. (2019). Engineering applications of chemically-bonded phosphate ceramics. *Ingeniería e Investigación*, *39*(3). DOI: 10.15446/ing.investig.v39n3.81424

cement, but resists and behaves structurally as a ceramic. As it presents bonds of the ionic and covalent type, its structure varies from very crystalline to vitreous, showing compressive strengths similar to conventional cement and setting times faster than hydraulic cements (Wagh, 2016). This intermediate product that contains crystalline or non-crystalline phases and sets at temperatures close to that of the environment is known as chemically-bonded ceramics (CBC) (Roy, 1987; Wagh, 2013).

The chemically-bonded phosphate ceramics (CBPC) are a specific type of chemically-bonded ceramics (CBC), formed from reactions of phosphate anions with metal cations. The CBPC have had an important development in the last two decades, mainly due to the search for environmental alternatives for the manufacture of cements (Wagh, 2013).

A significant environmental impact in terms of energy consumption and generation of greenhouse gases is a widely known result of the production of conventional Portland cement (Habert, Billard, Rossi, Chen, and Roussel, 2010; Gartner, 2004). Therefore, the search for different cement alternatives that are friendly to the environment has led researchers to coin the term "eco-efficient cements" or "green cements". Magnesium phosphate cements are recognized as eco-efficient commercial products, due to their low environmental impact, in addition to their good mechanical performance, availability of raw materials and manufacturing facility. Under the names of "Ceramicrete'' and "Grancrete'', these types of cements are some of the more promising eco cements (Imbabi, Carrigan, and McKenna, 2012).

There is a positive impact of phosphate cements in the environmental context (Wagh, 2013). This article reviews the mechanical performance of phosphate cements and their structural requirements in contrast to Portland-type conventional cements.

Basic concepts of phosphate cements

Acid-base reaction system of chemically-bonded ceramics (CBC)

Chemically-bonded ceramics are structured as an acid-base reaction. These reactions originate from a base, usually powders of a metal oxide or a silicate, with an acid. The product of the reaction is a complex salt that acts as binding agent or cementing matrix, besides the presence of water. The excesses of the alkaline base that do not react become part of the cement fillers. The great majority of these reactions are fast and exothermic (Wilson and Nicholson, 1994).

The process for forming cements under the acid-base reaction system is described below (Wilson and Nicholson, 1993) and illustrated in Figure 1 (Wagh, 2004).

- Dissolution of the alkaline base in an acid solution, to facilitate the formation of cations.
- Interaction of anions and cations in the solution to form neutral compounds.
- Gelification of the compound and saturation of the solution with the compound.
- Precipitation of solids in the saturated gel solution forming connected networks of the types: crystalline, semicrystalline and disordered solids.

In the specific case of phosphate cements, the reactions to combine the cations and phosphate anions can take place in solution at normal or hydrothermal pressures or by combinations at high temperatures to overcome the kinetic barriers. The transformations of phosphates into new structures can be achieved thermally or through ion exchange reactions (Attfield, 2001).

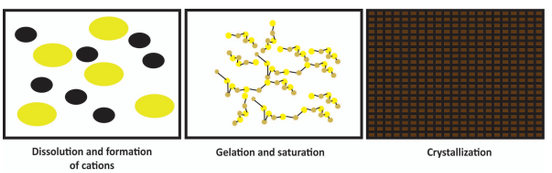

Figure 1. Steps in the formation of chemically-bonded ceramics.
Source: Adapted from Wagh (2004)

Chemically-bonded phosphate ceramics (CBPC) or phosphate cements

Phosphate cements are essentially an acid-base system that reacts at room temperature (Wagh, 2016). These cements are formed by the reaction of phosphoric acid or an acid phosphate with metal oxides, where the acid component contributes to the phosphate anions and the basic component to the metal cations, necessary for the cement shaping reaction (Figure 2).

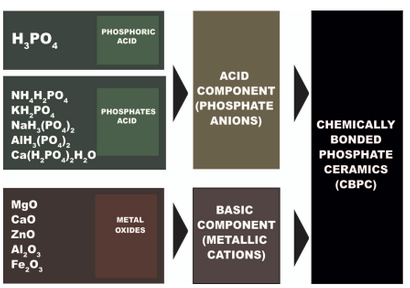

Figure 2. Components in the formation of phosphate cements.
Source: Authors

Although phosphate cements are more expensive than Portland cements, the former are projected as one of the special cements with the highest development potential (Attfield, 2001; Glasser, 2011). Some of the main reasons are the ease and safety to handle their reagents and that they are non-toxic and stable at high temperatures (1 000 °C) (Attfield, 2001) and have a wide pH range, available raw materials and low environmental impact, in addition to good reported mechanical properties. Five types of cement are recognized as typical phosphate cements: magnesium

phosphate, calcium phosphate, zinc phosphate, aluminum phosphate and iron phosphate. Among them, magnesium and calcium phosphate cements stand out for having the highest development in structural applications. Some of the reactions and main products responsible for the mechanical properties in phosphate cements have been presented by Wagh (2016) and Alshaaer, Cuypers, Mosselmans, Rahier and Wastiels (2011), and are listed in Table 1.

Table 1. Typical reactions and products of phosphate cements

Phosphate cement	Chemical reaction	Main formed product	Reference
Calcium Phosphate	$CaSiO_3+H_3PO_4+2H_2O \leftrightarrow SiO_2.H_2O+CaHPO_4.2H_2O$	Brushite	(Colorado, Wang, and Yang, 2015)
Zinc Phosphate	$3ZnSO_4.7H_2O+2NaHPO_4.2H_2O \rightarrow Zn_3(PO_4)_2\cdot4H_2O+H_2SO_4+2Na_2SO_4+21H_2O$	Hopeite	(Parhi, Manivannan, Kohli, and McCurdy, 2008)
Aluminum Phosphate	$Al_2O_3+2AlH_3(PO_4)_2\cdot H_2O \rightarrow 4AlPO_4+4H_2O$	Berlinite	(Liu and Chen, 2016)
Iron Phosphate	$Fe_2O_3+Fe+6H_3PO_4 \rightarrow 3Fe(H_2PO_4)_2+3H_2O$	Iron Dihydrogen phosphate	(Wagh and Jeong, 2003)
Magnesium Phosphate	$Mg_3(PO4)_2\cdot4H_2O \rightarrow NH_4MgPO_4\cdot6H_2O$	Struvite	(Soudée and Péra, 2000)

Source: Authors

Environmental impact of phosphate cements and Portland cements

It is unfeasible to establish a definitive relation of the environmental impact of phosphate cements compared with Portland, due to the low development of the former. However, some of the phosphate cements with the highest impact and development are magnesium phosphate cements, which can be used as reference, specifically the commercial application Ceramicrete with the addition of fly ash, for a comparison with Portland cements. Production of greenhouse gases for Ceramicrete consists mainly in carbon dioxide, under two premises. First, there are greenhouse gases produced in the transformation of raw materials, that is, by the decarbonization of limestone and dolomite, called direct emissions. Second, some gases are associated with the combustion of fossil fuels in different stages of the process, such as calcination, milling, screening, transport and packaging among others. These are called process emissions, in addition to the energy consumed in the transformation processes to obtain the cements (Wagh, 2013). Wagh (2013) establishes a first approach to the environmental impact of the phosphate cements. Table 2 presents a parallel comparing the environmental impact of the two technologies. This parallel allows to conclude that the energy consumed and the greenhouse gases released by the processes of magnesium phosphate cement are approximately 40% less, in comparison with conventional Portland technology (Wagh, 2016).

In addition, phosphate cements can be referred to as eco-efficient or eco-friendly products. Several authors have tried to link alternative raw materials and additives of low environmental impact in the formation of cements. The review of some researches evidenced the use of substitute raw materials that reduce manufacturing costs and reuse of industrial waste as source of raw materials (Formosa et al., 2008; Gardner et al., 2015; Choi, Um, and Choung, 2014; Kinnunen et al., 2018). This fact has a substantial impact, since it allows to diminish the environmental impact produced by the exploitation and transformation of conventional raw materials.

Table 2. Environmental impact of the production of phosphate cements

Product	Composition	Energy consumption (MJ/ton)	Greenhouse gases (ton/ton)	Main process
Ceramicrete	$MgKPO_4\cdot6H_2O$ + Fly ash	2 186	0,32	Calcination, release of CO_2 and chemical process
General purpose Portland cement	Mixture of oxides, sulphates and silicates	4 800	0,85	Calcination, CO_2 release and mechanical processes

Source: Adapted from Wagh (2016)

Biomaterials of phosphate cements

There is a group of phosphate cements that exhibit relevant mechanical properties, although it is not completely applicable in civil engineering. These cements have generated a great scientific interest in recent years (Dorozhkin and Epple, 2002; Al-Sanabani, Madfa, and Al-Sanabani, 2013; Viani, Sotiriadis, Kumpová, Mancini and Appavou, 2017). The applications are confined to the human body due to biocompatibility, among other reasons. This group of phosphate cements is identified in the group of biomaterials, briefly described below.

Dental cements: Zinc phosphates

Zinc phosphate cements are the oldest known dental cements, as they were developed in 1880. Although at present they are not widely used in comparison with new materials that have emerged (Viani et al., 2017), they still find a subsistence niche in cemented restorations.

Dental cements of zinc phosphate are obtained by mixing phosphoric acid and zinc oxide. Due to the strong reaction that originates, aluminum hydroxide has been used to neutralize the reaction. These cements have reached compressive strengths between 71 and 131 MPa and tensile strength between 4,3 and 8,3 MPa (Wagh, 2016). Dental porcelain cements consisting of alumina, vitreous silica, calcium oxide, sodium oxide, fluorine, zinc oxide and phosphoric acid are probably the inorganic cements with the highest reported mechanical strength. They have a compression strength of 255 MPa, bending stress of 24,5 MPa and tension of 13,6 MPa. However, the fracture tenacity of 0,12 to 0,3 MPa/m^2 indicates the fragility of this cement (Wagh, 2016).

Cements for orthopedic applications: Calcium phosphates

Calcium phosphate cements mainly precipitate as hydroxyapatite, which is a basic mineral constituent of the bones. That is why this type of cement will always be one of the main alternatives of use in this field. In addition, these cements are easily grafted with rapid hardening in the bones of the human body and minimal intrusion implications. These cements are used in special applications such as bone augmentation, bone reinforcement, metal implant fixation and spinal fractures (Ginebra, Canal, Espanol, Pastorino, and Montufar, 2012).

The cortical bone is the external part of the bone that represents its main mechanical properties. Table 3 describes these properties compared to calcium phosphate cement. The main aspect is the similarity in the density of these two materials, which is inferior when compared with typical metal prostheses such as titanium (A. Wagh, 2004). There are also great similarities in compression strength and Young's modulus. Advances in future research are expected to improve resistance to stress and fracture.

Table 3. Mechanical properties of calcium phosphate cements

Property	**Cortical bone**	Calcium phosphate cement
Specific Gravity (g/cm3)	1,7-2,1	1,7-2,0
Tensile Strength (MPa)	60-160	2,1-14
Compressive strength (MPa)	13-18	20-91
Young's Modulus (GPa)	3-30	35-105
Fracture energy (J/m2)	390-560	–
Resistance to fracture (Mpa/m2)	2-12	0,3-0,8
Composition	Inorganic + organic	Inorganic

Source: Adapted from Wagh (2016)

Phosphate cement for structural applications

Research in phosphate cements began at the start of the 20th century and resulted in the main development of dental cements and biocements. In the year 2003, Wagh, Grover and Jeong published a literature review of abstracts of articles from the years 1988-2002 (Table 4). They described the low percentage of research developed in structural applications. Only 5,6% of applications are structural, perhaps due to the difficulty of industrially scaling this type of cement, where production volumes are considerable. However, the low percentage can also suggest an important development potential.

The first cements for structural purposes were developed at Brookhaven National Laboratory (BNL) in the United States (1970). Looking for applications of magnesium phosphate cements, aluminum, pb and iron phosphates were also researched without finding practical applications at the structural level. From the Argonne National Laboratory

Table 4. Phosphate Cement Research

Items	Percentage
Articles on biomaterials and dental cements	68 %
Structural materials	5,6%
Refractory materials	12,6%
Structure of materials, properties, etc.	13,9%
Total number of articles found relevant to low temperature phosphate cements and ceramics (2 264)	100%

Source: Adapted from Wagh (2016)

research in the decade of 1990, the possibilities of application of magnesium phosphate cements for structural uses were extended, specifically in the immobilization of dangerous and radioactive waste (Wagh, 2016). The research developed in the Argonne National Laboratory, which is evidenced by numerous publications and patents, is substantially important to describe the progress of this type of material.

Trying to define a frame that contains the generalities of the mechanical properties of the phosphate cements is a complex challenge, because phosphate cements have a great variability of compositions, offering a wide range of mechanical properties. However, the significant development experienced by magnesium phosphate and calcium phosphate cements can be used as reference to explain the mechanical behavior of these compounds. Table 5 presents a general framework of phosphate cements, with the purpose of contrasting their main differences and similarities.

In many cases, phosphate cements show mechanical properties superior to the conventional Portland cements. However, producing phosphate cements as commercial products (pastes, mortars and concretes) is more expensive than producing a conventional cement. Therefore, specific applications with added value are projected as commercially viable possibilities (Wagh, 2013).

Magnesium Phosphate Cements

Phosphate cement pastes: Phosphate cement pastes comprise the reaction between the acidic and basic components without other additional components. This frames the fundamental model for the analysis and understanding of these cements. However, in practical terms, making cements with only these components promotes additional costs that oppose to the approach of making products of this type of cements more commercially available. Below significant findings are explained on their mechanical properties.

The proportion of raw materials is an important factor that requires differences in terms of mechanical strength. A. Wang, Yuan, et al. (2013) calcined the MgO (1 200 °C) for 3 hours and dried particles of KH_2PO_4 (100 °C) as acidic component for 6 hours. Then, by grinding, they pre-mixed the two components and dried them for 3 hours forming a powder compound (grams) that was mixed with deionized water in different proportions. The optimum liquid - solid ratio was 1:7, keeping the mixture under stirring until

solidification, and the optimum ratio for the MgO/KH_2PO_4 was 4:1, registering compressive strengths close to 40 MPa (A. Wang, Yuan, et al., 2013). These same authors studied the liquid-solid relationship. They used KH_2PO_4 and MgO in a weight to weight ratio of 1:1, which constituted the solid component, and used deionized water as liquid component, reporting the formation of cements for liquid (milliliter)-to-solid (grams) ratio of 1:4, 1:3, 2:5, 1:2, 3:5 and 2:3, with compressive strengths between 8 MPa and 22 MPa . The study showed that the compressive strength increased as the water content decreased, linking low porosities with high mechanical resistance (A. Wang, Zhang, Li, Ma, and Liu, 2013).

Composite cements (*mortars, concretes and others*)*:* Phosphate cements also form composite materials similar to Portland cement mortars and concretes. Del Valle et al. formed a composite material from the magnesium phosphate cement matrix and hemp fibers (Hemp) as a structural phase. The researchers added proportions by weight (wt.%) of the fiber of 8, 12, 16 and 20%; although the additions with 20% do not substantially outperform mechanical performance. They offer improvements to those found in the literature (Del Valle-Zermeño et al., 2016). Maximum strength $\sigma_{MAX} = 0,71$ MPa was recorded. The researchers highlight the excellent thermal and hygroscopic properties of this fiber demonstrated during the tests.

Table 5. Phosphate Cements

Phosphate	Main applications	Main features	Typical ranges of compressive strenght (MPa)	Reference
Zinc Phosphate	Biomaterial: dental cement	Exothermic reactions, low scale production.	50-130	(Viani et al., 2017) (Wagh, 2016)
Calcium Phosphate	Biomaterial: bone cement, structural products in addition to Wollastonite.	Exothermic reactions, high manufacturing cost.	20-150	(Tamimi, Sheikh, and Barralet, 2012) (Colorado et al., 2015) (Colorado et al., 2012) (Wagh, 2016)
Aluminum Phosphate	Dental porcelain, products resistant to corrosion at high temperatures, refractories and electric insulators.	Products superior to most phosphate cements, difficulties to scale products industrially.	30-110	(Y.S. Wang, Dai, Ding, and Xu, 2017) (Wagh et al., 2003) (Wagh, 2016)
Magnesium Phosphate	Encapsulation of radioactive materials and hazardous waste, sealant in oil wells, corrosion protection coatings, road repair.	Cement of greater development and projection as structural material, wide range of applications from Ceramicrete.	20-90	(U.S. Patent No. 5,645,518, 1997) (Li, Shi, and Li, 2016) (Liu and Chen, 2016) (A. Wang, Zhang, et al., 2013) (A. Wang, Yuan, et al., 2013) (Del Valle-Zermeño, Aubert, Laborel-Préneron, Formosa, and Chimenos, 2016)
Iron Phosphate	Encapsulation of radioactive material and hazardous waste.	Availability of raw materials at low cost, broad spectrum in the reuse of waste materials.	20 -50	(Wagh and Jeong, 2003) (He et al., 2016) (Choi et al., 2014) (US Patent No. 6,498,119 B2, 2002) (Wagh, 2016)

Source: Authors

Formosa et al. (2008) proposed the evaluation of a magnesium phosphate cement, composed of potassium hydrogen phosphate (KH_2PO_4) and magnesium oxide (MgO), with contribution percentages between 65%-45% (MgO) and 45%-35% (KH_2PO_4) and a water/solids ratio between 0,24-0,28. The authors found that increasing the water content and/or magnesium oxides decreases the compressive strength. They also show that the increase of the curing time is not a significant parameter to increase the mechanical strength, however an increase in the compressive strength is obtained between 10-12% (28 days) reaching values of 79 MPa. The increase of the porosity is due to a greater amount of water and MgO, influencing a decrease in the mechanical strength (Formosa et al., 2008).

The modulus of elasticity has also been studied for the mineralogical phases of the reaction of magnesium phosphate cement, Morales et al. (2015) analyzed the mechanical behavior of the different minerals present in the cement using the Statistical Nanoindentation Technique (SNT) and Scanning Electron Microscope equipped with Energy Dispersive X-ray analysis (SEM-EDX). The elastic modulus that registered a greater resistance corresponds to the Periclase (MgO). It is a phase of aggregation or filler significantly higher than the K-struvite ($KMgPO_4 \cdot 6H_2O$) that is, the cement matrix. It is worth noting the fundamental role of Periclase for the development of mechanical strength of cement (Morales et al., 2015).

Some reactive materials that are part of the acid-base system in phosphate cements, in some circumstances, can provide material that do not react by generating phases of the source material, which behave as filler, These phases of material that do not react contribute significantly to the resistant activity of the cements, classifying these mixtures as mortars (Formosa, Chimenos, Lacasta, and Niubó, 2012).

Various composite materials have been developed from the matrix of magnesium phosphate cement. Lu, Hou, Ma, Fan, and Li (2016) added different proportions of graphene oxide in order to increase their mechanical strength, determining an ideal proportion of 5 wt.% of graphene. The addition of graphene oxide decreases the workability of the magnesium

phosphate cement paste, modifying setting times from 15 minutes to 11 minutes. Likewise, fluidity decreases with the increase in graphene oxide. This is attributed to the addition of Graphene oxide that accelerates the hydration of cement by possessing a larger specific area, thus absorbing more water and generating an aggregation of the phosphate cement. The addition of graphene oxide has a negative effect on the workability, similar to what happened in Portland cement. However, the compressive and flexural strength improves, with values of 40,61 MPa and 6,82 MPa, respectively. This can also be explained by the decrease in porosity and a greater degree of hydration of the paste (Lu et al., 2016).

Active additions as in Portland technology are also used in phosphate cements. Hou, Li, Tong, and Zhang (2012) used calcined coal gangue (with 58,73% SiO_2 and 26,48% Al_2O_3) and calcined magnesia as active addition to obtain magnesium phosphate cements. The addition of calcinated coal gangue increases the setting times from 6,5 to more than 8 minutes, since it decreases the concentration of the used acid phosphate ($NH_4H_2PO_4$). With the addition of the coal gangue, the initial compressive strength (24 hours) increases slightly, then decreases. However, considerable increases in resistance are reported after day 28, reaching resistance of 95 MPa after 360 days with percentages of 10% coal gangue. The authors attribute this phenomenon, to the hydration of the gangue due to the high contents of amorphous silica and alumina (Hou et al., 2012).

Donahue and Aro (2010), applied Ceramicrete (magnesium phosphate cement binder, perfected and patented by Argonne Laboratories) and aggregates such as fly ash, OSB (oriented standard board), fiberboard chip and paper pulp waste to develop consolidated boards under pressure. Physical and mechanical properties were evaluated, complying with all the minimum requirements of the standards for low density boards, except for the modulus of rupture (MOR). The authors showed the great potential of the boards for specific applications.

Additives in magnesium phosphate cements: One of the characteristic factors of phosphate cements is the fast setting time, Formosa et al. (2015) contrasted the setting times and the mechanical properties in phosphate cement pastes added with boric acid. The cement was prepared from magnesium oxide (MgO), monopotassium phosphate (KH_2PO_4) and boric acid (H_3BO_3) as retardant. The results showed that the modulus of elasticity increased with the curing time for each formulation, but decreased in the measure that the additive (H3BO3) increased. Therefore, increasing the H_3BO_3 decreases the strength (Formosa et al., 2015). Likewise, applying statistical techniques such as Design of Experiments (DoE), the same authors refined the findings mentioned above, defining ideal additions of 60 wt.% magnesium oxide (MgO), 40 wt.% monopotassium phosphate (KH_2PO_4) and boric acid between 0,5 wt.% and 1,0 wt.%, with a liquid - solid ratio of 0,24. They obtained a cement with good workability reaching final setting times of up to 60 minutes, with constant compressive strengths since the seventh day setting higher than 40 MPa (Formosa et al., 2012).

Calcium Phosphate Cements

Calcium phosphate cements for applications in civil engineering, have been generalized under the name of IPC (Inorganic Phosphate Cement), which are made with an initial mixture of wallastonite (CaSiO3) source of calcium and phosphoric acid (H3PO4) source of phosphorus. These compounds react mainly forming brushite ($CaHPO_4.2H_2O$), in addition to amorphous silica. Alshaaer, Cuypers, Mosselmans et al., (2011) researched the mechanical response of calcium phosphate cement for high temperature applications. The researchers reported that for a temperature range between 80 and 200 °C the flexural strength decreases from 14 MPa to 7 MPa. This attributed to the appearance of microcracks due to the dehydration of brushite, a situation that does not affect the compressive strength. Between 800 and 1 000 °C, an increase in resistance is observed reaching values of 80 MPa and 12 MPa for compressive and flexural strength, respectively. This occurs due to the healing effect when reaching glass transition temperatures for some phases of the cement. Similarly, the aging effect at room temperature is described, registering an increase in compressive strength of up to 50%. Continuing with the line of research, Alshaaer Cuypers, Rahier and Wastiels (2011) proposed a new , hydrothermal post curing (HTPC) system to provide a solution to problems of dimensional and chemical stability of the IPC. With the application of the HTPC, the cement changes phase to monetite, which describes a decrease in the compressive strength of about 60%. This occurs due to the change in the pore structure, which is a situation that positively affects the flexural strength increase by 30%.

Cements reinforced with fiberglass can present problems of durability due to the chemical attack on the fiber by the hydroxide ions present in alkaline environments. Calcium phosphate cements (IPC) do not present an alkaline environment, favoring the durability of fiberglass. Cuypers et al. (2006) researched the phosphate cement matrix added with fiberglass to study typical damage mechanisms in relation to mechanical properties. After performing simple tensile tests, Portland cement and a calcium phosphate cement (IPC) were compared, both reinforced with fiberglass. It was reported that Portland cement resistance decreased to 50% of the initial strength after an accelerated aging for 90 days, opposed to phosphate cement that maintained 90-95% of its initial resistance (Cuypers et al., 2006).

Colorado, Hiel and Han (2011) mixed nano graphite platelets into a phosphate cement paste composed of powders of wollastonite ($CaSiO_3$) and phosphoric acid (H_3PO_4). They formed a composite material of IPC by a very rapid exothermic reaction that produces bubbles, which promote porosity and negatively affect mechanical strength. In addition to evaluating the effect of graphite, the authors provide information on alternative mixing methods (RAM, Resonant Acoustic Mixer), which reduce the formation of bubbles and

therefore result in better mechanical characteristics. The research reported mean flexural strengths of 23 MPa and good thermal stability at high temperatures (600 °C).

Functional ceramics that exhibit additional properties to those commonly studied are also analyzed in calcium phosphate cements. Colorado et al. (2015) added on a matrix of IPC, barium titanate (BaTiO3) selected for its good dielectric properties and high thermochemical stability. They effectively showed that the dielectric constant increased as the ($BaTiO_3$) load increased. At the same time, compression strengths of approximately 150 MPa for addition values of $BaTiO_3$ between 15-30 wt.% were reported (Colorado et al., 2015).

Phosphate Geopolymers

The geopolymeric cements include a series of materials in which a reactive source of alumina and silica is mixed with an activator, in an aqueous solution such as sodium or potassium hydroxide and silicate (Glasser, 2011). The alkaline activation of aluminosilicates, such as fly ash or metakaolin, is widely registered to obtain inorganic products known as geopolymers. Similar to conventional geopolymers, phosphate geopolymers have been conceived. These materials have a tetrahedral molecular structure of $PO4^{5-}$, together with $AlO4^{3-}$ and $SiO4^{4-}$ as their basic components (Y.S. Wang et al., 2017).

From metakaolin and silica, fume reacted with phosphate monoaluminate (mixture of different acidic aluminum phosphates, $Al(H_2PO_4)_3$, $AlPO_4$, $Al_2(HPO_4)_3$. Y.S. Wang et al. (2017) performed a geopolymer with mechanical resistances at 7 and 28 days of 7 MPa and 30 MPa, respectively. They also showed good mechanical behavior at high temperatures (1 000 °C) (Y.S. Wang et al., 2017). This geopolymer can be described as an aluminum phosphate cement.

Commercial products and frequent applications of phosphate cements

Commercial applications

There are two types of phosphate cements in structural mechanical applications that register commercial products: potassium magnesium and potassium cements. They are developed by Argonne laboratories, who have patented a binder known as Ceramicrete and a calcium phosphate cement, widely studied by the University of Vrije Brussels, which in combination with fiberglass has resulted in a composite material that was patented under the name of VUBONITE.

The Ceramicrete has been widely disseminated in the immobilization of hazardous waste and as a material sprayed on sheets of polystyrene foam to produce housing walls that rise in record time, known as Grancrete (Wagh, 2016). Related to the Ceramicrete matrix, Qiao Chau, and Li (2010) evaluated mortars of magnesium phosphate cements as possible material for the repair of potholes or patches on the roads. They payed special attention to the relations (M/P) magnesium oxide (MgO) and potassium dihydrogen phosphate (KH_2PO_4), in addition to their corresponding ratio (S/B) sand and binder. They showed that these relationships influence the mechanical properties and setting times of mortars. Magnesium phosphate cement mortars showed superior bond strengths to those of mortars and Portland concretes. The pull-off tests showed flexural strengths of up to 5 MPa (28 days) in contrast to Portland mortars that reached 2 MPa at 28 curing days (Qiao et al., 2010).

The composite material, VUBONITE has had various applications in civil buildings at a structural level. De Roover et al. (2002) used this material for the construction of modular bridges, which took advantage of the tensile strength provided by fiberglass, added to the resistance to corrosion and fire of phosphate cements. In spite of the relatively low rigidity of the material, much lower than for steel or reinforced polymers, a cost-effective, resistant and easy-to-assemble bridge was made.

Immobilization of radioactive waste and hazardous elements

One of the main applications of phosphate cements has been the immobilization of radioactive waste and hazardous elements. A good number of authors have reported research in this field, in addition several to patents registered in this regard. Some of the researches carried out are cited below.

In a patent, Singh, Wagh, and Jeong (2000) present a method to produce phosphate cements and immobilize large amounts of waste of low radioactivity and hazardousness. They reported compressive strengths of 30 MPa obtained in a potassium magnesium phosphate cement (U.S. Patent No. 6,133,498, 2000). The patents of Wagh and Singh (U.S. Patent No. 5,645,518, 1997) and Wagh Singh and Jeong (U.S. Patent No. 5,830,815, 1998) disclose processes for using phosphate ceramics to encapsulate wastes, recording compressive strengths for magnesium phosphate ceramics and phosphate and magnesium ceramics of the order of 2923 psi (20 MPa) and 6734 psi (46,4 MPa), respectively. In U.S. Patent No. 5,830,815 (1998), the inventors describe a method for producing phosphate-bonded structural products for high volumes of benign waste.

Colorado and Singh (2014) stabilized nuclear waste streams with high sodium content by means of magnesium phosphate cement, elaborated from anhydrous monobasic sodium phosphate (NaH_2PO_4), magnesium oxide (MgO), waste, water and fly ash as filler. The authors recorded compressive strengths obtained between 40MPa and 5MPa depending on the monobasic sodium phosphate concentration, with observed higher strength at higher concentrations. The nuclear regulation commission (NRC) establishes a minimum compressive strength of 3,45 MPa for cements for immobilization of waste. In the same line of research, Choi et al. (2014) intervened the final waste of the processing of nuclear fuels, through the development of phosphate iron cements obtained mainly from the reaction of basic steel slag (BOF Slag) and phosphoric acid (H3PO4). The slag /

acid weight ratios used were 1:1,5, 2 and 2,5, registering compressive strengths between 16 MPa and 19 MPa.

Likewise, in a calcium phosphate cement matrix, lead was added to evaluate its ability to block gamma rays. The powders constituted by wollastonite ($CaSiO_3$) and lead (in proportion of solids weight of 2%, 10% and 50%) reacted with phosphoric acid in a powder-to-acid ratio of 100:120, forming a calcium phosphate cement. The authors reported excellent gamma-ray attenuation coefficients, in addition to compression strengths close to 80 MPa for mixtures with 10% lead dust (Colorado et al., 2012).

Conclusions

In civil building applications, magnesium phosphate cement and calcium phosphate cement stand out. The mechanical strength reported in phosphate cements is important, since most of them have compressive strengths with values equal to or higher than Portland cements used for structural purposes. Besides, their low environmental impact makes cements of phosphate an important material for structural works in Civil Engineering. The final cost of phosphate cements as product is higher than the cost of a traditional Portland cement. However, new applications in specific environments, in addition to the use of fillers, can potentiate this type of cements as commercially viable products.

Phosphate cements that exhibit the best mechanical response at elevated temperatures are calcium phosphate cements, registering much higher values of compressive strength at 1 000 °C than other cements. However, they present problems of dimensional instability.

In the synthesis of composite materials with phosphate cement matrix, the reinforcement materials showed significant support to improve the mechanical resistance, while influencing the decrease in cement costs.

The presence of water is necessary for the formation of phosphate cements, especially in the dissolution of acidic compounds and it helps to provide an aqueous environment for the dissolution of the alkaline bases. The amount of water present in the mixture substantially affects the mechanical strength. Lower water contents increase the resistance to compression and produces low porosities. Water also influences as a retardant in setting. Although the curing time is not a factor of wide interest and frequent research in the available literature, it increases the compression resistance, especially after 28 curing days, and there are no significant changes for curing times of less than 7 days.

One of the most frequently used additives is boric acid. This setting retardant, in adequate proportions, increases the fluidity of cement, improving its workability. The use of this additive does not significantly influence the mechanical strengths of the cement. The durability of the phosphate cements is superior to the Portland cements, and it is another positive aspect of these materials. It presents an environment with neutral pH, which favors the inactivity of other materials present in the cement.

The most frequent application of phosphate cements is the immobilization and neutralization of hazardous and radioactive waste, in which the demands of mechanical resistance of 3,45 Mpa are not so stringent (500 psi) (Colorado and Singh, 2014).

Acknowledgements

This work was carried out thanks to the support for research of the Government of Boyacá – Colciencias Call 733 (Formation of High-Level Human Capital for the Regions).

References

Al-Sanabani, J. S., Madfa, A. A., and Al-Sanabani, F. A. (2013). Application of calcium phosphate materials in dentistry. *International Journal of Biomaterials*, 2013. DOI: 10.1155/2013/876132

Viani, A., Sotiriadis, K., Kumpová, I., Mancini, L., Appavou, M.-S. (2017). Microstructural characterization of dental zinc phosphate cements using combined small angle neutron scattering and microfocus X-ray computed tomography. *Dental Materials, 33*(4), 402-417. DOI: 10.1016/j.dental.2017.01.008

Alshaaer, M., Cuypers, H., Mosselmans, G., Rahier, H., and Wastiels, J. (2011). Evaluation of a low temperature hardening Inorganic Phosphate Cement for high-temperature applications. *Cement and Concrete Research, 41*(1), 38-45. DOI: 10.1016/j.cemconres.2010.09.003

Alshaaer, M., Cuypers, H., Rahier, H., and Wastiels, J. (2011). Production of monetite-based Inorganic Phosphate Cement (M-IPC) using hydrothermal post curing (HTPC). *Cement and Concrete Research, 41*(1), 30-37. DOI: 10.1016/j.cemconres.2010.09.002

Attfield, J. P. (2001). Phosphates. In K.H. Jürgen Buschow, R.W. Cahn, M.C. Flemings, B. Ilschner, E. J. Kramer, S. Mahajan and P. Veyssière (Eds.). *Encyclopedia of Materials: Science and Technology* (2nd Ed, Vol. 3). Oxford, UK: Pergamon Press, 6896-6901. DOI: 10.1016/B0-08-043152-6/01222-5

Choi, J., Um, W., and Choung, S. (2014). Development of iron phosphate ceramic waste form to immobilize radioactive waste solution. *Journal of Nuclear Materials, 452*(1-3), 16-23. DOI: 10.1016/j.jnucmat.2014.04.033

Colorado, H. A., Hiel, C., and Hahn, H. T. (2011). Chemically bonded phosphate ceramics composites reinforced with graphite nanoplatelets. *Composites Part A: Applied Science and Manufacturing, 42*(4), 376-384. DOI: 10.1016/j.compositesa.2010.12.007

Colorado, H. A., Pleitt, J., Hiel, C., Yang, J. M., Hahn, H. T., and Castano, C. H. (2012). Wollastonite based-Chemically Bonded Phosphate Ceramics with lead oxide contents under gamma irradiation. *Journal of Nuclear Materials, 425*(1-3), 197-204. DOI: 10.1016/j.jnucmat.2011.08.043

Colorado, H. A. and Singh, D. (2014). High-sodium waste streams stabilized with inorganic acid-base

phosphate ceramics fabricated at room temperature. *Ceramics International, 40*(7, Part B), 10621-10631. DOI: 10.1016/j.ceramint.2014.03.045

Colorado, H. A., Wang, Z., and Yang, J. M. (2015). Inorganic phosphate cement fabricated with wollastonite, barium titanate, and phosphoric acid. *Cement and Concrete Composites, 62*, 13-21. DOI: 10.1016/j.cemconcomp.2015.04.014

Cuypers, H., Wastiels, J., Van Itterbeeck, P., De Bolster, E., Orlowsky, J., and Raupach, M. (2006). Durability of glass fibre reinforced composites experimental methods and results. *Composites Part A: Applied Science and Manufacturing, 37*(2), 207-215. DOI: 10.1016/j.compositesa.2005.03.027

De Roover, C., Vantomme, J., Wastiels, J., Croes, K., Cuypers, H., Taerwe, L., and Blontrock, H. (2002). Modelling of an IPC-concrete modular pedestrian bridge. *Computers and Structures, 80*(27-30), 2133-2144. DOI: 10.1016/S0045-7949(02)00258-4

Del Valle-Zermeño, R., Aubert, J. E., Laborel-Préneron, A., Formosa, J., and Chimenos, J. M. (2016). Preliminary study of the mechanical and hygrothermal properties of hemp-magnesium phosphate cements. *Construction and Building Materials, 105*, 62-68. DOI: 10.1016/j.conbuildmat.2015.12.081

Donahue, P. K. and Aro, M. D. (2010). Durable phosphate-bonded natural fiber composite products. *Construction and Building Materials, 24*(2), 215-219. DOI: 10.1016/j.conbuildmat.2007.05.015

Dorozhkin, S. V. and Epple, M. (2002). Biological and medical significance of calcium phosphates. *Angewandte Chemie - International Edition, 41*(17), 3130-3146. DOI: 10.1002/1521-3773(20020902)41:17<3130::AID-ANIE3130>3.0.CO;2-1

Formosa, J., Aranda, M. A., Chimenos, J. M., Rosell, J. R., Fernández, A. I., and Ginés, O. (2008). Cementos químicos formulados con subproductos de óxido de magnesio. *Boletin de La Sociedad Espanola de Ceramica y Vidrio, 47*(5), 293-297. https://dialnet.unirioja.es/servlet/articulo?codigo=2732922

Formosa, J., Chimenos, J. M., Lacasta, A. M., and Niubó, M. (2012). Interaction between low-grade magnesium oxide and boric acid in chemically bonded phosphate ceramics formulation. *Ceramics International, 38*(3), 2483-2493. DOI: 10.1016/j.ceramint.2011.11.017

Formosa, J., Lacasta, A. M., Navarro, A., Del Valle-Zermeño, R., Niubó, M., Rosell, J. R., and Chimenos, J. M. (2015). Magnesium Phosphate Cements formulated with a low-grade MgO by-product: Physico-mechanical and durability aspects. *Construction and Building Materials, 91*, 150-157. DOI: 10.1016/j.conbuildmat.2015.05.071

Gardner, L. J., Bernal, S. A., Walling, S. A., Corkhill, C. L., Provis, J. L., and Hyatt, N. C. (2015). Characterisation of magnesium potassium phosphate cements blended with fly ash and ground granulated blast furnace slag. *Cement and Concrete Research, 103*, 78-87. DOI: 10.1016/j.cemconres.2015.01.015

Gartner, E. (2004). Industrially interesting approaches to "low-CO2" cements. *Cement and Concrete Research, 34*(9), 1489-1498. DOI: 10.1016/j.cemconres.2004.01.021

Ginebra, M. P., Canal, C., Espanol, M., Pastorino, D., and Montufar, E. B. (2012). Calcium phosphate cements as drug delivery materials. *Advanced Drug Delivery Reviews, 64*(12), 1090-1110. DOI: 10.1016/j.addr.2012.01.008

Glasser, F. (2011). 4 - Application of inorganic cements to the conditioning and immobilisation of radioactive wastes. In: M. I. Ojovan (Ed.). *Handbook of Advanced Radioactive Waste Conditioning Technologies*. Swaston, CA: Woodhead Publishing, 67-135. DOI: 10.1533/9780857090959.1.67

Habert, G., Billard, C., Rossi, P., Chen, C., and Roussel, N. (2010). Cement production technology improvement compared to factor 4 objectives. *Cement and Concrete Research, 40*(5), 820-826. DOI: 10.1016/j.cemconres.2009.09.031

Hou, L., Li, J. H., Tong, L. X., and Zhang, Q. (2012). Effect of Calcined Coal Gangue on the Mechanical Property and Microstructure of Magnesium Phosphate Cement. *Applied Mechanics and Materials*, 174-177, 943-946. DOI: 10.4028/www.scientific.net/AMM.174-177.943

Imbabi, M. S., Carrigan, C., and McKenna, S. (2012). Trends and developments in green cement and concrete technology. *International Journal of Sustainable Built Environment, 1*(2), 194-216. DOI: 10.1016/j.ijsbe.2013.05.001

Kinnunen, P., Ismailov, A., Solismaa, S., Sreenivasan, H., Räisänen, M.-L., Levänen, E., and Illikainen, M. (2018). Recycling mine tailings in chemically bonded ceramics - A review. *Journal of Cleaner Production, 174*, 634-649. DOI: 0.1016/j.jclepro.2017.10.280

Li, Y., Shi, T., and Li, J. (2016). Effects of fly ash and quartz sand on water-resistance and salt-resistance of magnesium phosphate cement. *Construction and Building Materials, 105*, 384-390. DOI: 10.1016/j.conbuildmat.2015.12.154

Liu, N., and Chen, B. (2016). Experimental research on magnesium phosphate cements containing alumina. *Construction and Building Materials, 121*, 354-360. DOI: 10.1016/j.conbuildmat.2016.06.010

Lu, Z., Hou, D., Ma, H., Fan, T., and Li, Z. (2016). Effects of graphene oxide on the properties and microstructures of the magnesium potassium phosphate cement paste. *Construction and Building Materials, 119*, 107-112. DOI: 10.1016/j.conbuildmat.2016.05.060

Morales, M., Formosa, J., Xuriguera, E., Niub, M., Segarra, M., and Chimenos, J. M. (2015). Elastic modulus of a chemically bonded phosphate ceramic formulated with low-grade magnesium oxide determined by Nanoindentation. *Ceramics International, 41*(9 Part B), 12137-12146. DOI: 10.1016/j.ceramint.2015.06.031

Parhi, P., Manivannan, V., Kohli, S., and McCurdy, P. (2008). Room temperature metathetic synthesis and characterization of α-hopeite, Zn3(PO4)2·4H2O. *Materials Research Bulletin, 43*(7), 1836-1841. DOI: 10.1016/j.materresbull.2007.07.005

Qiao, F., Chau, C. K., and Li, Z. (2010). Property evaluation of magnesium phosphate cement mortar as patch repair material. *Construction and Building Materials, 24*(5), 695-700. DOI: 10.1016/j.conbuildmat.2009.10.039

Roy, D. M. (1987). New strong cement materials: chemically bonded ceramics. *Science (New York), 235*(4789), 651-658. DOI: 10.1126/science.235.4789.651

Schneider, M., Romer, M., Tschudin, M., and Bolio, H. (2011). Sustainable cement production-present and future. *Cement and Concrete Research, 41*(7), 642-650. DOI: 10.1016/j.cemconres.2011.03.019

Singh, D., Wagh, A. S., and Jeong, S. Y. (2000). U. S. Patent No. 6,133,498. Washington, D. C.: U. S. Patent and Trademark Office.

Soudée, E. and Péra, J. (2000). Mechanism of setting reaction in magnesia-phosphate cements. *Cement and Concrete Research, 30*(2), 315-321. DOI: 10.1016/S0008-8846(99)00254-9

Tamimi, F., Sheikh, Z., and Barralet, J. (2012). Dicalcium phosphate cements: Brushite and monetite. *Acta Biomaterialia, 8*(2), 474-487. DOI: 10.1016/j.actbio.2011.08.005

Wagh, A. S. (2004). Introduction to Chemically Bonded Phosphate Ceramic. In Chemically Bonded Phosphate Ceramics. *Amsterdam: Elsevier Science*, 1-13. DOI: 10.1016/B978-008044505-2/50005-3

Wagh, A. S. (2004). Chemically Bonded Phosphate Ceramics. In Chemically Bonded Phosphate Ceramics. Amsterdam: *Elsevier Science*, 15-27. DOI: 10.1016/B978-008044505-2/50006-5

Wagh, A. S. (2004). Dental Cements and Bioceramics. In Chemically Bonded Phosphate Ceramics. Amsterdam: *Elsevier Science*, 245-253. DOI: 10.1016/B978-008044505-2/50022-3

Wagh, A. S. (2013). Recent Progress in Chemically Bonded Phosphate Ceramics. *ISRN Ceramics*, 2013, 1-20. DOI: 10.1155/2013/983731

Wagh, A. S. (2016). *Chemically Bonded Phosphate Ceramics* (2nd ed.). Amsterdam: Elsevier. DOI: 10.1016/C2014-0-02562-2

Wagh, A. S., Grover, S., and Jeong, S. Y. (2003). Chemically Bonded Phosphate Ceramics: II, Warm-Temperature Process for Alumina Ceramics. *Journal of the American Ceramic Society, 86*(11), 1845-1849. DOI: 10.1111/j.1151-2916.2003.tb03570.x

Wagh, A. S., and Jeong, S. Y. (2002). *U. S. Patent No. 6,498,119*. Washington, D. C.: U. S. Patent and Trademark Office.

Wagh, A. S. and Jeong, S. Y. (2003). Chemically Bonded Phosphate Ceramics: III, Reduction Mechanism and Its Application to Iron Phosphate Ceramics. *Journal of the American Ceramic Society, 86*(11), 1850-1855. DOI: 10.1111/j.1151-2916.2003.tb03571.x

Wagh, A. S., and Singh, D. (1997). *U. S. Patent No. 5,645,518*. Washington, D. C.: U. S. Patent and Trademark Office.

Wagh, A. S., Singh, D., and Jeong, S.-Y. (1998). *U.S. Patent No. 5,830,815*. Washington, D. C.: U. S. Patent and Trademark Office

Wang, A., Yuan, Z., Zhang, J., Liu, L., Li, J., and Liu, Z. (2013). Effect of raw material ratios on the compressive strength of magnesium potassium phosphate chemically bonded ceramics. *Materials Science and Engineering: C, 33*(8), 5058-5063. DOI: 10.1016/j.msec.2013.08.031

Wang, A., Zhang, J., Li, J., Ma, A., and Liu, L. (2013). Effect of liquid-to-solid ratios on the properties of magnesium phosphate chemically bonded ceramics. *Materials Science and Engineering: C, 33*(5), 2508-2512. DOI: 10.1016/j.msec.2013.02.014

Wang, Y. S., Dai, J.-G., Ding, Z., and Xu, W.-T. (2017). Phosphate-based geopolymer: Formation mechanism and thermal stability. *Materials Letters, 190*(January), 209-212. DOI: 10.1016/j.matlet.2017.01.022

Wilson, A. and Nicholson, J. (1993). Theory of acid-base cements. In *Acid-Base Cements: Their Biomedical and Industrial Applications* (Chemistry of Solid State Materials, pp. 5-29). Cambridge: Cambridge University Press. DOI: 10.1017/CBO9780511524813.003

Ingeniería e Investigación vol. 39 No. 3, December - 2019 (20-26)

DOI: http://dx.doi.org/10.15446/ing.investig.v39n3.81380

Application of grid convergence index to shock wave validated with LS-DYNA and ProsAir

Aplicación del índice de convergencia de malla frente a onda de choque validado con LS-DYNA y ProsAir

Ricardo Castedo[1], Carlos Reifarth[2], Anastasio P. Santos[3], Jorge Losada[4], Lina M[a]. López[5], María Chiquito[6], and Juan M. Mancilla[7]

ABSTRACT

The discretization error is not always calculated, even though it is essential for the studies of computational solid mechanics. However, it is well known that an error committed by the mesh used can be as large as the measured variable, which greatly invalidates the results obtained. The grid convergence index (GCI) method makes possible to determine on a solid basis, the order of convergence and the asymptotic solution. This method seems to be a suitable estimator despite further research is needed in the context of blast situations and finite element (FE) calculations. For this purpose, field trials were performed consisting in the detonation of a spherical hanging load of homemade explosive. The pressure generated by the shock wave was measured in different positions at two distances. With these data, a TNT equivalent has been obtained and used to calculate the shock propagation with the solvers LS-DYNA and ProsAir. This work aims to verify the GCI method by comparing its results with field data along with the simulations carried out. The comparison also seeks to validate the methodology used to obtain the TNT equivalent.

This research shows that the GCI gives good results for both solvers despite the complexity of the physical problem. Besides, LS-DYNA displays better correlation with the experimental data than the ProsAir results, with an error of less than 10% in all values.

Keywords: Grid convergence index (GCI), TNT equivalent, LS-DYNA, ProsAir.

RESUMEN

La estimación del error de discretización no siempre se calcula, aunque es algo fundamental para el estudio de la mecánica computacional de los sólidos. Sin embargo, es bien sabido que el error cometido por la malla utilizada puede ser del mismo orden que la variable medida, lo que llega a invalidar los resultados obtenidos. El método del ındice de convergencia de la malla (GCI) permite determinar sobre una base sólida el orden de convergencia y la solución asintótica, por lo que parece ser un buen estimador, a pesar de que es necesario seguir investigando en el contexto de las situaciones de ondas de choque (explosivos) y de los cálculos de elementos finitos (FE). Para este fin, se realizaron pruebas de campo consistentes en la detonación de una carga esférica colgada de explosivo casero. La presión generada por la onda de choque se midió en diferentes posiciones a dos distancias. Con estos datos, se obtuvo un equivalente de TNT que se utilizó para calcular la propagación del choque con los programas LS-DYNA y ProsAir. Este trabajo pretende verificar el método GCI comparando sus resultados con los datos de campo junto con las simulaciones realizadas. También, la comparación busca validar la metodologıa empleada para la obtención del equivalente TNT.

La investigación muestra que el GCI da buenos resultados para ambos programas a pesar de la complejidad del problema fısico. Además, el LS-DYNA produce una mejor correlación con los datos experimentales que los aportados por el ProsAir, con todos los valores por debajo del 10 % de error.

Palabras clave: ındice de convergencia de malla (GCI), equivalente de TNT, LS-DYNA, ProsAir.

Received: July 31st, 2019
Accepted: December 17th, 2019

[1]BSc. in Geological Engineering, Universidad Politécnica de Madrid, Spain. Ph.D. in Engineering, Universidad Politécnica de Madrid, Spain. Affiliation: Assistant Professor, Universidad Politécnica de Madrid, Spain. E-mail: ricardo.castedo@upm.es
[2]B.Sc. student in Energy Engineering, Universidad Politécnica de Madrid, Spain. Affiliation: Researcher, Universidad Politécnica de Madrid, Spain.
E-mail: c.reifarth@alumnos.upm.es
[3]B.Sc. in Mining Engineering, Universidad Politécnica de Madrid, Spain. Ph.D. in Mining Engineering, Universidad Politécnica de Madrid, Spain. Affiliation: Associate Professor, Universidad Politécnica de Madrid, Spain. E-mail: tasio.santos@upm.es
[4]B.Sc. in Energy Engineering, Universidad Politécnica de Madrid, Spain. M.Sc. in Energetic Installations and Projects, CEU Cardenal Herrera University, Spain. Affiliation: Project Developer, Grupo Cobra, Spain. E-mail: jjlosada@grupocobra.com
[5]B.Sc. in Mining Engineering, Universidad Politécnica de Madrid, Spain. Ph.D. in Mining Engineering, Universidad Politécnica de Madrid, Spain. Affiliation: Associate Professor, Universidad Politécnica de Madrid, Spain. E-mail: lina.lopez@upm.es
[6]B.Sc. in Civil Engineering, Universidad Politécnica de Madrid, Spain. Ph.D. candidate in Engineering, Universidad Politécnica de Madrid, Spain. Affiliation: Assistant Professor, Universidad Politécnica de Madrid, Spain. E-mail: maria.chiquito@upm.es
[7]B.Sc. in Biology, Universidad de Málaga, Spain. Affiliation: Ph.D. candidate in Engineering, Universidad Politécnica de Madrid, Spain.
E-mail: jm.mancilla@alumnos.upm.es

How to cite: Castedo, R., Reifarth, C., Santos, A. P., Losada, J., López, L. M., Chiquito, M., and Mancilla, J. M. (2019). Application of grid convergence index to shock wave validated with LS-DYNA and ProsAir. *Ingeniería e Investigación*, *39*(3). DOI: 10.15446/ing.investig.v39n3.81380

Introduction

The interest in high order finite elements methods (FEM) in different areas has increased significantly during the last decade, especially in engineering. FEMs provide good accuracy with a reduced computational cost and save resources in trials usually very expensive in both time and money.

Multiple software can be used for the simulation of detonations. Some of them, such as LS-DYNA (LSTC, 2019) or ANSYS, offer general finite element solvers for different kinds of formulations (Lagrangian; Smooth Particles Hydrodynamic – SPH; Particle Blast – PB; Multi-Material Arbitrary Lagrangian Eulerian – MM-ALE); or methods (Load Blast Enhanced – LBE; explosive Equation of State – EOS) related with explosives or their effects. Others, like ProsAir (Forth, 2012), are stand-alone compressible Computational Fluid Dynamics (CFD) codes developed specifically for assessing blast loading and blast waves with finite volume method. ProsAir uses the AUSMDV Riemman solver, an improved advection upstream splitting method (AUSM) together with the MUSCL-Hancock integration scheme to achieve a second order of accuracy.

In a numerical study, discretization error estimation would be desirable due to the dependency of the solution on the mesh size. This error is present in our solution, even when the results obtained agree with real data, e.g. field test or laboratory experiments. Another error present in the results is the modelling error itself, which is related to the simplifications made to the physical problem or the mathematical implementation of various factors (e.g. boundary and loading conditions, material properties, or constitutive equations) (Anderson et al., 2007). The Grid Convergence Index - GCI (Roache, 1994) is a method to estimate the discretization error even when the successive mesh refinements are not integer multiples. This technique is defined as an error percentage, providing a confidence bound in which the numerical solution will likely to be. Several authors used the mentioned GCI in computer fluid dynamics (Jin and Shaw, 2010; Liang and Tao, 2017; Ndebele and Skews, 2019). However, it is less mentioned in discrete methods (Kwaśniewski, 2013; Schwer, 2008), with no sources found for shock waves produced by explosive detonation. According to Roache (1994), the GCI method would be recommended for shocks and other discontinuities despite further experience with complex shocked flows is needed. In addition, Huang et al. (2012) highlighted the need of further research to contrast simulated results with field data and their validation.

To verify the efficiency and accuracy of the GCI method, the present work presents a comparison of both ProsAir and LS-DYNA approaches with the data obtained from experimental studies of blast wave using homemade explosive. To reproduce the explosive behavior in this software, the TNT equivalent is necessary, since the results are better with the accuracy of this calculation. Therefore, this work also has served to validate the methodology used in that calculation (Chiquito et al., 2019).

Field blast testing program

A total of 18 tests with different explosives were conducted. However, the results in terms of energy released by the explosive were too low for five out of the six mixtures used. In this work, only the mixture that resulted in a higher TNT equivalent in pressure was considered. More information about the tests is available in the paper by Chiquito et al. (2019).

The explosive selected in this work was a mixture of ammonium nitrate with aluminum. The technical ammonium nitrate used in the tests is usually produced for industrial purposes and it is basically pure ammonium nitrate with high porosity. The specifications provided by the manufacturer ensure that a minimum of 98,5% is ammonium nitrate. The aluminum powder was added to the ammonium nitrate at 10% by weight. The aluminum used was already in powder form with a size of 230 microns and a purity of at least 98%. All mixtures were done inside a plastic bag and introduced in powder-free latex gloves, easily found in any store. The charge was approximately spherical in shape with 15 cm diameter and it was hanging on a rope at 46 cm from the ground in all tests.

In order to measure the shock wave produced by the explosive studied, five high frequency PCB® pressure sensors were placed on a flat ground around the explosive in two concentric circles whose radios were 3 and 5 m. Two sensors were located at 3 m from the charge (called P1 and P2) and three at 5 m (P3, P4 and P7) with an angle of 0°, 45° and 90°, as Figure 1 shows.

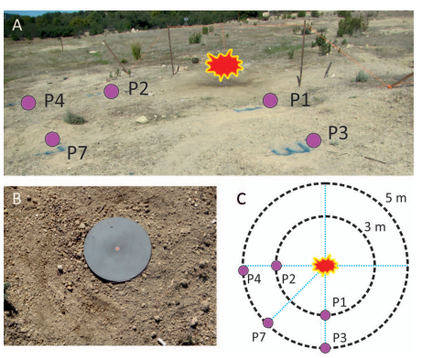

Figure 1. Experimental setup: (A) Photograph of the field settings; (B) cup used to place the pressure sensors, ensuring that they do not move; and (C) detail of the pressure sensor location and distances. **Source:** Authors

After three tests with the same explosive, six signals were available at 3 m, while there were nine signals at 5 meters. The obtained TNT equivalent based on pressure and then used in the numerical models had a weighted average of 5 measurements at 3 m and 9 measurements at 5 m, as one of the measurement at 3 meters was useless. For signals treatment, a code in MATLAB® was developed based on least squares method to fit the modified Friedlander Equation. With this fitting, the key parameters of the positive phase can be extracted. See Chiquito et al. (2019) and Rigby et

al. (2015) for more details. Finally, the TNT equivalent is calculated and the value obtained was 0,855.

Methodology

The success of modelling an event using any technique that require a discretization of the problem, like finite volumes or elements or CFD, depends strongly on the chosen mesh size. Consequently, a convergence study known as Grid Convergence Index (GCI) was carried out in order to find the proper mesh size for this kind of computational models.

The Grid Convergence Index (GCI)

The choice of finite time and space domain introduces a discretization error into simulation. Therefore, a numerical solution can only be treated as an approximation to the real one. In order to find how big this error is depending on the mesh size, the Grid Convergence Index (GCI) method is applied. Presented first by Roache (1994), the GCI can be defined as the relative error bound, i.e. the measure of how far away our computational result is from the asymptotic numerical value. It indicates the error band in which our error is located and how big it could be. Besides, it shows how much the solution will change with a greater refinement of the mesh, as low GCI values will indicate the computational solution near the asymptotic one. If the solution is already good enough, smaller meshes will not result in big different solutions. Assuming that, in general terms, the results obtained with a finer mesh are better although some authors have shown that this is not always the case (Alañón et al., 2018). This technique provides some key advantages when compared with others: an analytical solution is not required, it provides a confidence bound on the estimated error band, and can be used with a minimum of two mesh solutions (though it works better with three).

In the traditional processes of illustration of the convergence error, the analytical solution (exact) was used to determine the error, and then the range of convergence was determined graphically. However, in practical problems, the exact solution is usually unknown. Most traditional discretization methods assume a relation between the analytical solution f_{exact} and its numerical approximation $f(h)$, and then calculate the discretization error $E(h)$, using the Equation (I) and neglecting higher-order terms when the mesh is appropriately refined (Roache, 1994):

$$E\ (h) = f_{exact} - f\ (h) \approx Ah^p \tag{1}$$

where h is a measure of the mesh discretization, A is a constant and p is the rate of convergence. Therefore, three unknowns remain: the constant A, the convergence ratio p, and the exact solution f_{exact}. Estimating these unknowns is the basis of the GCI method.

In this case, the application of the GCI was done with three mesh refinements with a constant grid refinement ratio. The meshes used in this study (called C, D and E) resulted in the following ratio, $r = h_C/h_D = h_D/h_E = 2$. The biggest one was called "Mesh C - h_C" (12,5 mm), followed by "Mesh D - h_D" (6,25 mm), and the smaller one, "Mesh E - h_E" (3,125 mm). To obtain an estimation of the order of convergence, the concept used in Equation (1) is applied to the three mesh sizes CDE, where $h_C > h_D > h_E$. Then, the unknown constant A can be eliminated and the unknown p can be obtained (Schwer, 2008):

$$p = \frac{\left|\ln\left(\frac{f_C - f_D}{f_D - f_E}\right)\right|}{\ln(r)} \tag{2}$$

Additionally, once the order of convergence is known, an estimate of the analytical result can be calculated by finding the asymptotic solution for h approaching zero and using the two finest grids from the threesome CDE (Schwer, 2008):

$$f_{h\to 0} \approx f_{exact} \approx f_E - \frac{f_D - f_E}{r_{ED}^p - 1} \tag{3}$$

After some algebraic work, and starting from Equation (3), it is possible to relate the relative error (ε) of the finer meshes to the mesh (r) and convergence (p) ratios. Details of this can be found in Kwaśniewski (2013) and Schwer (2008). However, the definition of the relative error is as follows (Schwer, 2008):

$$\varepsilon_{ED} = \left|\frac{f_D - f_E}{f_E}\right| \tag{4}$$

which never should be taken as an estimate of the relative error of the methodology, since it does not reflect r or p in the formulation.

The expression that gives the error value of the GCI is presented in Equation (5), whose solution can be expressed as a percentage (Schwer, 2008).

$$GCI_{ED} = F_s \frac{\varepsilon_{ED}}{r_{ED}^p - 1} \tag{5}$$

where F_s expresses the safety factor multiplying the relative error term, based on the application of the GCI in different situations, but always with CFD (Roache, 1994). This error is an estimate of the finest mesh used, relative to the numerical (converged) solution as, in general, the exact solution is unknown. The value of this factor is 3 when two meshes are studied, or 1,25 when there are three or more meshes. The latter value was used in this particular research. This safety factor represents the 95% confidence for the estimated error bound.

Finally, the extrapolated (or computational) solution, called f_{ED}^* for the finer mesh combination, provides an estimate of the numerically asymptotic solution (Schwer, 2008):

$$f_{ED}^* = \frac{r_{ED}^p \cdot f_C - f_D}{r_{ED}^p - 1} \tag{6}$$

This methodology can be applied only when all grids are within the asymptotic range and then Equation (6) is valid asymptotically (also the extrapolated solution for other mesh combination). Based on the idea that the asymptotic range

of convergence requires the ratio between errors and mesh spacing to be constant, it is possible to verify if it is met by comparing the values of two given GCI, as three meshes are available (Kwaśniewski, 2013).

$$GCI_{DC} \approx r^p GCI_{ED} \tag{7}$$

Finally, as the GCI only gives the bound within the error that should be, Equation (8) shows the procedure to obtain the range with a 95% confidence that the converged solution should be (Schwer, 2008).

$$\left[f_E \left(1 - \frac{GCI_{ED}}{100\%} \right), f_E \left(1 + \frac{GCI_{ED}}{100\%} \right) \right] \tag{8}$$

Pros Air modelling process

The first program used to reproduce the field test was ProsAir - *PROpagation of Shocks in AIR* (Forth, 2012). This is a computational fluid dynamics program developed by Cranfield University, which simulates the effects of the detonation of an explosive charge, using a high-resolution, finite volume scheme.

The configuration and use of ProsAir is relatively simple. First, there are four tabs: general settings, spherical geometry, cylindrical geometry and 3D geometry. In the general settings tab the number of CPU cores to be used and the atmospheric conditions (101 325 Pa; 288 k) can be defined, among other less important set-ups. Then, in the spherical and cylindrical geometry tabs, the parameters to be plotted (the overpressure) and its intervals can be assigned. The spherical geometry has been used to mesh the explosive and the cylindrical one to mesh the air. Moreover, the mesh cannot be visualized, but it is a regular structured square. Besides, in the spherical geometry tab, the explosive type and its mass are set. Other control parameters are also established, like simulation time, CFL (or Courant-Friedrichs-Levy) safety number equal to 0,5, cell size (for the explosive, not the one used in the GCI), domain size (defined as 7 m in radial direction and 4 m high – see Figure 2) and type of boundary. Finally, the cylindrical geometry tab has the same control parameters as the spherical one, including the cell size (the one used to define the air – the same as defined in the GCI) and the height of blast.

The ProsAir computational tool was used to reproduce the experimental tests defined above based on the TNT equivalent calculated for the explosive used. In order to check its behavior, the prediction of the pressure caused by the blast wave of a specific spherical TNT mass in two different ranges from the center of the explosion (3 and 5 m) was compared with the GCI prediction, and then with the real (field) data. The data provided by the software depends on the equation of state (EOS) defined for the explosive and the input data used by the program. On the one hand, ProsAir does not allow to modify the Equation of State (EOS) and the manual does not specify what it is. On the other hand, the input data are: density 1 600 kg/m^3, detonation velocity 6 730 m/s and heat of explosion 4 520 kJ/kg.

As mentioned before, the ProsAir software is based on finite volume method, and then it depends on the mesh size. Usually as the mesh size is changed, the pressure also varies, as well as the time consumed by the computer to finish the simulation. As it is not always possible to predict the behavior of the shock wave modelling, the study of mesh convergence (GCI) becomes fundamental.

LS-DYNA modelling process

The second software used for comparison is the finite elements software, called LS-DYNA. This software, in comparison with ProsAir, requires a lot of training and knowledge in order to be used with confidence. It has many different options, but that also increases its complexity. In this case, the general 2D multi-material arbitrary Lagrangian-Eulerian (MMALE) technique was used. The *CONTROL_ALE card was set with Van Leer and half-index-shift advection algorithm of second order accuracy (METH=2). The alternate advection logic was also used, as it is generally recommended for explosives simulation.

The air was meshed as an axisymmetric domain equal to the one defined in the ProsAir (7 m long and 4 m high rectangle – see Figure 2). The explosive was set with the card named *INITIAL_VOLUME_FRACTION_GEOMETRY, defining the container geometry by a sphere and following similar previous works (Mobaraki and Vaghefi, 2015; Rebelo and Cismasiu, 2017). As the data is required by volume, knowing the TNT equivalent and the density of the TNT introduced into the model (Table 1), the explosive volume (m^3) was calculated. The chosen meshing technique was the butterfly one, in order to ensure the good spherical shape of the shock wave as other authors suggest (Lapoujade et al., 2010 and Rigby et al., 2014). The necessary data for the EOS used in this case, the traditional Jones-Wilkins-Lee (Lee et al., 1973), are shown in Table 1.

$$P = A \left(1 - \frac{\omega}{R_1 V} \right) e^{-R_1 V} + B \left(1 - \frac{\omega}{R_2 V} \right) e^{-R_2 V} + \frac{\omega E}{V} \tag{9}$$

where V is the relative volume, E the internal energy, and ω the Grüneisen coefficient.

Table 1. LS-DYNA inputs for the cards *MAT_HIGH_EXPLOSIVE_BURN and *EOS_JWL, see Equation (9)

*MAT_HIGH_EXPLOSIVE_BURN					
Density [Kg/m3]		Detonation velocity [m/s]		Chapman-Jouguet Pressure [GPa]	
1 600		6 730		21	
*EOS_JWL					
A [GPa]	B [GPa]	R_1	R_2	ω	E_0 [GPa]
373,8	3,75	4,15	0,90	0,35	6

Source: Lee et al. (1973)

The air was modelled as a perfect gas using the material *MAT_NULL and including a density of 1,29 kg/m^3, an initial internal energy of 0,25 MPa, and a specific volume of 1

(Huang et al., 2012). The card used to describe the equation of state for the air was the *EOS_LINEAR_POLYNOMIAL, where $C_4 = C_5 = 0{,}4$ and the rest of constants is equal to zero (Huang et al., 2012).

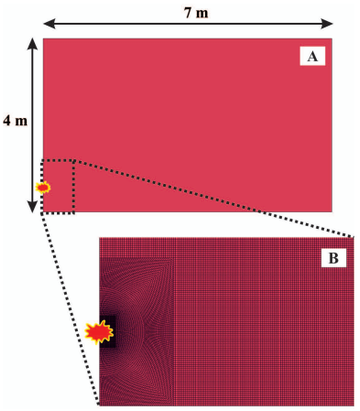

Figure 2. Model domain: (A) Numerical model domain in LS-DYNA. Note that the ProsAir domain is the same; however, the mesh cannot be seen in the software until modelling has been done. B) Mesh detail of the source point with a butterfly mesh to ensure correct wave propagation at the initial stages.
Source: Authors

Results and discussion

Optimal mesh size estimation

The objective of this phase is to find an optimal grid able to reach enough precision to study the pressures caused by a free air explosion. Table 2 shows the real pressure obtained in three tests (five measurements) at 3 meters (mean value and standard deviation, after the ± symbol), and LS-DYNA and ProsAir pressure results for the three meshes used. The shortest distance of 3 meters has been chosen for comparison and validation of the data produced by both software, based on the TNT equivalent calculated. As some authors suggest, at lower distances the calculation is more difficult due to the presence of the highest overpressure and impulse (Huang et al., 2012; Rose, 2001). This point is considered as the most adverse situation and the one that will set the best mesh.

Table 2. Pressure peaks of the three mesh sizes for each solver in comparison with the empirical result

Distance [m]	Mesh code	Mesh size [mm]	Real Pressure [kPa]	ProsAir [kPa]	LS-DYNA [kPa]
3	C	12,5	134,6 ± 6,14	147,21	153,86
	D	6,25		152,57	141,81
	E	3,125		154,78	133,4

Source: Authors

A similar procedure to fit the pressure signals with a Friedlander equation has been done with both data set, ProsAir and LS-DYNA. Analyzing the behavior of the results given by LS-DYNA, we can easily observe a wider range of results than in ProsAir. In each refinement, the variation in the outcome gets closer to the converged solution for LS-DYNA, while a refinement of the ProsAir model just gives a systematically higher pressure. The wide dispersion of LS-DYNA means that this solver has a bigger dependence on the solution with the mesh size than ProsAir. The relevance of choosing a correct mesh using LS-DYNA is a key factor that can make the difference to provide good results. Regarding calculation time for the same mesh size, ProsAir was significantly faster than LS-DYNA.

Table 3 sets the results of the application of the GCI method to the outputs provided by LS-DYNA and ProsAir for the 3 meters pressure peak. In general terms, shocks, non-linear flux limiters and other discontinuities invalidate the basis of GCI (Taylor series in Richardson extrapolation). However, if these phenomena exist at small scale and with simple patterns, the GCI method seems to be valid and recommended (Roache, 1994). In any case, checking if the asymptotic ranged has been reached is generally enough to apply with certainty the GCI method.

Table 3 shows the calculations for each mesh: the order of convergence p, the estimated asymptotic solution $f_h = 0$, the value between subsequent solutions ε, the safety factor (set in 1,25 for three or more meshes) and the GCI for the meshes E and D. It also shows the confidence interval whereby there is a 95% confidence that the converged solution is within this range, and the verification that all calculations are in the asymptotic range of convergence (Equation 7).

Table 3. Results of the application of the GCI method to the outputs provided by LS-DYNA and ProsAir (values at 3 meters)

Software	p	$f_h = 0$ [kPa]	ε [%]	F_s	GCI_{ED} [%]	Confidence Interval		$GCI_{DC}/r^p GCI_{ED}$
ProsAir	1,278	155,52	1,4	1,25	1,25	152,84	156,72	1,014
LS-DYNA	0,519	113,99	6,3	1,25	18,19	109,14	157,66	0,941

Source: Authors

The formulations made with ProsAir, which requires reduced computation load, have lower GCI error value (GCI_{ED}) as shown in Equation (5) and higher convergence order (p) than the LS-DYNA model. This difference is because the results with ProsAir change less with each refinement of the mesh than in LS-DYNA, resulting in an estimation of p that seems to be better. The GCI method provides a different estimation of the asymptotic solution and confidence interval for both solvers. This is logical since the behavior of the software, in this case, is opposite when the mesh changes. The ProsAir estimation ranges from 152,84 to 156,72 while the values for LS-DYNA range from 109,14 to 157,66 presenting a wider range where solutions can be found. In fact, when comparing this confidence interval with the data provided in Table 2, it is possible to affirm that not all the results obtained with ProsAir are within the interval, while all the meshes made with LS-DYNA are in the range.

Finally, it is been verified that all solutions are within the asymptotic range of convergence, so the GCI method can be

properly applied, as GCI_{ED} and GCI_{DC} are compared and the values obtained are similar to 1 (Table 3). Additionally, it is observed that all the estimated asymptotic solutions for the finest meshes are between the 95% confidence intervals. Remark that all the values shown in the table are estimates, and, for instance, despite the real order of convergence used with the solver LS-DYNA $p = 2$, the estimator (p – Table 3) gives a different value. The same happens with the ProsAir. As it is an estimator, the order of convergence is calculated by converging to different asymptotic solutions.

Although the analysis is being carried out on an extremely complex event, such as the shock wave, it can be stated that the GCI is a method that can work despite its dependence on the software used. From the analysis made, the better mesh size is the finest and equal to 3,125 (mesh E) in both, ProsAir and LS-DYNA.

Comparison of the simulation with field data

Table 4 shows the pressure peak results obtained for both software at two different distances (the smaller one, E), thanks to the GCI method. Real pressure peaks are also shown with its standard deviations (after the ± symbol) for 3 and 5 meters. If the pressure is within the measured limits in the field it is signalized with *wml* in the table, otherwise the relative error is displayed right next to the solution.

Table 4. Comparison of the numerical results with real data and its respective relative errors

Distance [m]	Real Pressure [kPa]	ProsAir [kPa]	Error [%]	LS-DYNA [kPa]	Error [%]
3	134,6 ± 6,14	154,78	9,98	133,4	*wml*
5	49,7 ± 1,55	55,32	7,94	46,4	3,63

Source: Authors

On the one hand, the LS-DYNA model gave better results, closer to the experimental pressures. One of them (3 m) was within the measurement limits and the other one had a relative error not exceeding 5%. On the other hand, the ProsAir results differ to a larger extent. Nevertheless, none of the results surpasses the 10% error, which is a very acceptable outcome in the engineering field.

For example, pressure history at 3 and 5 meters from the experiments ProsAir and LS-DYNA is compared in Figure 3. The timing and shape of the overpressure peaks were captured accurately by the simulations. In terms of arrival time, ProsAir tends to go faster, while LS-DYNA behaves in the opposite way. The impulse, defined as the effect of the pressure over some target for a specified time period, is not compared here since the equivalent used was for the pressure peak. However, in Figure 3 it is possible to support that the impulses could be estimated with confidence, knowing that ProsAir overestimates the impulse and LS-DYNA underestimates it. These results are in accordance with others in terms of LS-DYNA and Air3D (similar to ProsAir) behavior (Huang et al., 2012; Rigby et al., 2014; Trajkovski et al., 2014).

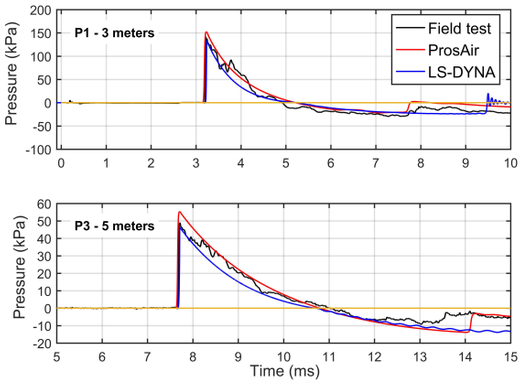

Figure 3. Comparison of experiments results: ProsAir and LS-DYNA analysis. Tests number 3 signals in P1 and P3 (see Figure 1).
Source: Authors

In general terms, the TNT equivalent used here appears to be in the lower range when used in LS-DYNA, while it is in the higher range for ProsAir. The TNT equivalent used here mixed data from two scaled distances, for this reason, the error changes with the distance. It is well-known that the TNT equivalent depends on the distance (Swisdak, 1975). However, as mentioned by Rose (2001), this observation is generally overlooked by most researchers because it adds a level of complexity to already very complicated problems, which makes the whole process of prototype or numerical modelling almost insoluble.

Conclusions

Evidently, the problem of suitable TNT equivalence will continue to make difficult the applicability of experimentally – and numerically-based results in the future. However, this work should serve to reduce the lack of existing experimental and numerical data in this field, in order to improve the understanding of the TNT equivalent and its use in modelling.

The mesh refinement study is the first step in the verification of numerical models. The presence of shocks, other discontinuities or singularities can difficult grid convergence studies. A priori, the GCI results (if the real result is unknown) would seem more consistent for ProsAir. This is normal because the GCI is designed for CFD. However, the results obtained for a complex finite element program as LS-DYNA are satisfactory.

The peak pressure results obtained using LS-DYNA and compared with field data are better. However, the calculation time used is much longer. The use of one program or the other depends on the available calculation capacity, the user knowledge and the required precision.

Regarding the mesh refinement, the variation in the outcome gets closer to the converged solution for LS-DYNA, while a refinement of the ProsAir model just gives a systematically

higher pressure. The relevance of choosing a correct mesh using LS-DYNA is a key factor, making the difference to provide good results. The results provided here allow us to select the proper air mesh for future or more complex simulations involving, for example, explosives and structures.

Acknowledgements

The participation of the second author has been funded by the Collaboration Grant of the Universidad Politécnica de Madrid, Departments 2018-19.

References

Alañón, A., Cerro-Prada, E., Vázquez-Gallo, M. J., and Santos, A. P. (2018). Mesh size effect on finite-element modeling of blast-loaded reinforced concrete slab. *Engineering with Computers*, *34*(4), 649-658. DOI: 10.1007/s00366-017-0564-4

Anderson, A. E., Ellis, B. J., and Weiss, J.A. (2007) Verification, validation and sensitivity studies in computational biomechanics. *Computer Methods in Biomechanics and Biomedical Engineering*, *10*(3), 171-184. DOI: 10.1080/10255840601160484

Chiquito, M., Castedo, R., López, L. M., Santos, A. P., Mancilla, J. M., and Yenes, J. I. (2019). Blast Wave Characteristics and TNT Equivalent of Improvised Explosive Device at Small scaled Distances. *Defence Science Journal*, *69*(4), 328-335. DOI: 10.14429/dsj.69.13637

Forth, S. (2012). *ProSAir User Guide*. Cranfield, UK: Crandfield University, Applied Mathematics and Scientific Computing Department.

Huang, Y., Willford, M. R., and Schwer, L. E. (2012, June). *Validation of LS-DYNA® MMALE with blast experiments*. Paper presented at the 12th International LS-DYNA Users Conference, Detroit, DYNAmore. https://www.dynalook.com/conferences/12th-international-ls-dyna-conference/blast-impact20-c.pdf/view

Jin, Y. and Shaw, B. D. (2010). Computational modeling of n-heptane droplet combustion in air–diluent environments under reduced-gravity. International *Journal of Heat and Mass Transfer*, *53*(25-26), 5782-5791. DOI: 10.1016/j.ijheatmasstransfer.2010.08.005

Kwaśniewski, L. (2013). Application of grid convergence index in FE computation. *Bulletin of the Polish Academy of Sciences: Technical Sciences*, *61*(1), 123-128. DOI: 10.2478/bpasts-2013-0010

Lapoujade, V., Van Dorsselaer, N., Kevorkian, S., and Cheval, K. (2010, June). *A study of mapping technique for air blast modelling*. Paper presented at the 11th International LS-DYNA Users Conference. Detroit, DYNAmore. https://www.dynalook.com/conferences/international-conf-2010/BlastImpact-1-3.pdf/view

Lee, E., Finger, M., and Collins, W. (1973). *JWL equation of state coefficients for high explosives* [Technical report No. UCID-16189]. Livermore, CA: Lawrence Livermore National Lab (LLNL). DOI: 10.2172/4479737

Liang, Y. and Tao, L. (2017). Interaction of vortex shedding processes on flow over a deep-draft semi-submersible. *Ocean Engineering*, *141*, 427-449. DOI: 10.1016/j.oceaneng.2017.06.056

LSTC (2019). *LS-DYNA Keyword User's Manual* (Volume II: Material Models). Livermore, CA: Livermore Software Technology Corporation. http://ftp.lstc.com/anonymous/outgoing/jday/manuals/LS-DYNA_Manual_Volume_II_R11_Ver2.pdf

Mobaraki, B. and Vaghefi, M. (2015). Numerical study of the depth and cross-sectional shape of tunnel under surface explosion. *Tunnelling and Underground Space Technology*, *47*, 114-122. DOI: 10.1016/j.tust.2015.01.003

Ndebele, B. B. and Skews, B. W. (2019). The interaction of a cylindrical shock wave segment with a converging–diverging duct. *Shock Waves, 29*, 817-831. DOI: 10.1007/s00193-018-00888-7

Rebelo, H. B. and Cismasiu, C. (2017, May). *A Comparison between three air blast simulation techniques in LS-DYNA*. Paper presented at the 11th European LS-DYNA Conference, Salzburg, DYNAmore. https://www.dynalook.com/conferences/11th-european-ls-dyna-conference/air-blast-2/a-comparison-between-three-air-blast-simulation-techniques-in-ls-dyna/view

Rigby, S. E., Tyas, A., Bennett, T., Fay, S. D., Clarke, S. D., and Warren, J. A. (2014). A numerical investigation of blast loading and clearing on small targets. *International Journal of Protective Structures*, *5*(3), 253-274. DOI: 10.1260/2041-4196.5.3.253

Rigby, S. E., Fay, S. D., Tyas, A., Warren, J. A., and Clarke, S. D. (2015). Angle of incidence effects on far-field positive and negative phase blast parameters. *International Journal of Protective Structures*, 6(1), 23-42. DOI: 10.1260%2F2041-4196.6.1.23

Roache, P. J. (1994). Perspective: a method for uniform reporting of grid refinement studies. *Journal of Fluids Engineering*, *116*(3), 405-413. DOI: 10.1115/1.2910291

Rose, T. A. (2001). An approach to the evaluation of blast loads on finite and semi-infinite structures (Ph.D. thesis, Cranfield University). http://hdl.handle.net/1826/4262

Schwer, L. E. (2008). Is your mesh refined enough? Estimating discretization error using GCI. Paper presented at the German LS-DYNA Forum, Bamberg, DYNAmore. https://www.dynamore.de/de/download/papers/forum08/dokumente/I-I-03.pdf

Swisdak, M. M. (1975). *Explosion effects and properties. Part I. Explosion effects in air* [Technical report No. NSWC/WOL/TR-75-116]. White Oak, MD: Naval Surface Weapons Center, White Oak Lab Silver Spring. https://apps.dtic.mil/dtic/tr/fulltext/u2/a018544.pdf

Trajkovski, J., Kunc, R., Perenda, J., and Prebil, I. (2014). Minimum mesh design criteria for blast wave development and structural response-MMALE method. *Latin American Journal of Solids and Structures*, *11*(11), 1999-2017. DOI: 10.1590/S1679-78252014001100006

Ingeniería e Investigación vol. 39 No. 3, December - 2019 (27-33)

DOI: http://dx.doi.org/10.15446/ing.investig.v39n3.74982

Electrodermal activity in relation to diabetes, autonomic neuropathy and aging: a preliminary study

Actividad electrodérmica en relación con la diabetes, neuropatía autonómica y envejecimiento: estudio preliminar

Luis Bolanos[1], Jose María Vicente[2], Oscar Andrés Vivas[3], and José María Sabater-Navarro[4]

ABSTRACT

A reduced electrodermal activity (EDA) may be related to autonomic neuropathy (AN). The aims of this study were to independently study the characteristics of the EDA and its correlation with diabetes and AN. During a self-designed test, mean skin conductance level (M-SCL), mean skin conductance response (M-SCR) to stimuli, and difference in M-SCL between feet (DBF) were obtained through a model-based decomposition based on Bayesian statistics and mathematical convex optimization. A group of 22 subjects were included for the final test. Diabetic patients were stratified based on their clinical history and care habits, dividing them into those out of risk and those at risk of developing AN. Statistical difference was found for the latter regarding M-SCR ($p < 0,01$) and DBF ($p < 0,05$) with respect to the control group. While past research failed to address potential sources of interference with the EDA measurement, namely emotional state, degree of concentration on the task, and body posture, this study proposes a well-defined protocol to stimulate subjects and acquire proper and reliable EDA data.

Keywords: Electrodermal activity, galvanic skin response, autonomic neuropathy, diabetes.

RESUMEN

Una actividad electrodérmica (EDA) reducida puede indicar la presencia de una neuropatıa autonómica (AN) subyacente. El objetivo de este estudio fue investigar las caracterısticas de la EDA y su correlación con la diabetes y la AN. A través de un test desarrollado durante la investigación, el nivel promedio de conductancia de la piel (M-SCL), la respuesta promedio de la conductancia (M-SCR), y la diferencia entre los valores promedio M-SCL de ambos pies fueron calculados utilizando una descomposición paramétrica de la EDA basada en la estadıstica bayesiana y en la optimización matemática convexa. La prueba final incluyó 22 sujetos. Los participantes diabéticos fueron estratificados según su historial clınico y hábitos de cuidado, para obtener un grupo fuera de riesgo y otro en riesgo de desarrollar la AN. Se halló una diferencia estadıstica en las métricas de M-SCR ($p < 0,01$) y DBF ($p < 0,05$) en aquellos pacientes con respecto al grupo de control. Mientras las investigaciones pasadas no incluyeron factores que pueden interferir potencialmente con la medición de la EDA, tales como el estado emocional, el grado de concentración en la tarea, y la postura corporal, el presente estudio define un protocolo para la estimulación de sujetos durante la adquisición de la EDA en una manera confiable.

Palabras clave: Actividad electrodérmica, respuesta galvánica, neuropatıa autonómica, diabetes.

Received: September 19th, 2018
Accepted: October 7th, 2019

Introduction

Autonomic neuropathy (AN) generally describes the affection of the small C nerve fibers, which impairs the autonomic nervous system. In diabetes, its symptoms include either extreme hot or cold sensation across the legs, acute pain, and low sweating capacity or even the absence of it. Furthermore, this set of symptoms usually leads to the so called "diabetic foot". Multiple diagnostic tools are available on the market, such as the monofilament 10g, the quantitative axon reflex test (QSART), the thermoregulatory sweat testing (TST) and the Neuropad (SánzCorbalán et al., 2011, Papanas et al., 2005). Caring strategies have also been exhaustively developed and promoted to improve the life quality and expectancy of those who suffer it. Still, 50% of diabetics will suffer from some type of neuropathy, responsible for 20% of ER visits. It has also been demonstrated that the risk of amputation triples when preceded by an ulceration in diabetics. In addition, foot ulcerations cause 80% of the non-traumatic amputations

[1]Electronics and Telecommunication Engineer, University of Cauca, Colombia. Affiliation: M.Sc. student in Bionics Engineering, School of Advanced Studies Sant'Anna, Italy. E-mail: ldbolanos@unicauca.edu.co
[2]Electronic and Industrial Automation Engineer, Miguel Hernández University of Elche, Spain. M.Sc. in Industrial Engineering, Miguel Hernández University of Elche, Spain. Affiliation: Ph.D. student in Industrial and Telecommunications Technologies, Miguel Hernández University of Elche, Spain. E-mail: jose.vicentes@umh.es
[3]Electronics and Telecommunication Engineer, University of Cauca, Colombia. Ph.D. in Robotics, Université Montpollier II, France. Affiliation: Full Professor, University of Cauca, Colombia. E-mail: avivas@unicauca.edu.co
[4]Industrial Engineer, Universidad Nacional de Colombia, Colombia. Ph.D. in Robotics, Miguel Hernández University of Elche, Spain. Affiliation: Full Professor, Miguel Hernández University of Elche, Spain. E-mail: j.sabater@umh.es

How to cite: Bolanos, L., Vicente, J. M., Vivas, O. A., and Sabater-Navarro, J. M. (2019). Electrodermal activity in relation to diabetes, autonomic neuropathy and aging: a preliminary study. *Ingeniería e Investigación*, *39*(3). DOI: 10.15446/ing.investig.v39n3.74982

worldwide, leaving a life expectancy of 2 to 5 years (Boulton, Cavanagh and Rayman 2007, De Alcalá 2005). The electrical conductance of the skin and its behavior, normally referred to as electrodermal activity (EDA) or as galvanic skin response (GSR) (González-Correa 2018a), is typically divided into low and high frequency components. The former is usually named skin conductance level (SCL) and the latter, skin conductance response (SCR). High frequency responses are also classified depending on whether they are produced by an intended stimulus (event-related SCR) or not (non-specific SCR) (Braithwaite et al., 2013). EDA has been used to measure stress (Najström and Jansson 2007; Reinhardt et at., 2012; Sierra, et al., 2011), modulation during exercise (PosadaQuintero et al., 2018) or to evaluate user experience (Rico-Olarte et al., 2018), just to name a few. For a review in Spanish on the topic, please refer to the study of Mojica-Londono (2017), or in English to Moncada and De la Cruz (2011). Earlier researches have studied the EDA as a method for monitoring diabetes or its correlation with AN in different regions of the body (Khalfallah et al., 2012; Deanfield et al., 1980; ColmenaresGuillén et al., 2015; Li at al., 2004; Nazhel et al., 2002; Rivera Farina et al., 2009; Vlckova et al., 2016; Wang et al., 2008). From the aforementioned studies, only Vlckova, Srotova and Bednarik (2016) found no correlation. More recently, Mohanraj and Narayanan (2016) found a correlation between type 2 diabetes and low GSR in males. Finally, Ionescu-Tirgoviste et al. (2018) found significant differences in the electrical activity of type 2 diabetics in certain regions of the trunk. Colombian contributions relate to the usage of bio-impedance, including EDA, as a clinical diagnostic tool (C. A. González-Correa 2018, C. H. González-Correa 2018) and novel methods to analyse EDA based on frequency-domain features (Posada Quintero et al., 2016). The aims of this study were to independently study the correlation between EDA and AN among diabetic patients, addressing new variables, and to propose a novel low-cost method to diagnose the latter.

Material and Methods

Participants were patients of the diabetic foot care program conducted between September and December 2016 by the medical service of the University of Cauca, in Popayan, Colombia. The study was approved by the Ethics Committee of the same institution. Patients were classified based on the guidelines given by Boulton et al., (2007), De Alcalá (2005), and on the expertise and physical examination of their feet, performed by the head nurse of the program. Clinical data, including gender, age, and time suffering from diabetes, were collected. Therefore 3, groups were formed: the reference group, namely participants without diabetes, diabetics out of risk, and diabetics either at risk of diabetic foot or with already visible complications (ulcerations or toes amputation).

Signal acquisition

A hardware device and its software components, inspired by the circuits contained by the e-Health Arduino shield, CookingHacks (2019) and Zepeda and Mena (2014), were designed as part of the research. Apart from adding desired functionalities, the process of constructing a self-designed device was meant to remove some of the limitations observed when first exploring the e-Health shield, in which noise was the biggest obstacle. As observed, any given electronic device transmitting either wired or wirelessly, and any power outlet or cable nearby the circuit would produce enough noise to completely mask the EDA signal read by the hardware. Modifications to the designs included changing data transmission from Near Field Communication (NFC) to Bluetooth Low Energy (BLE), to allow longer distances between devices. Moreover, the CC2650 Texas Instruments micro controller was used for providing robustness and low energy consumption, in combination with the integrated circuit LM324N. The input was sampled at 4 Hz. The final hardware setup is observed in Figure 1. On the receiving side, a custom software, programmed to handle and plot the data, was written using C♯. The final prototype consisted on an 11 cm * 8 cm printed circuit board, which costed no more than USD 20. The prototype was capable of recording skin conductance for over 100 hours running on a coin battery; sending raw data wirelessly to a PC running Windows; and processing it to calculate mean values. Noise coming from near transmitting devices, power outlets or cables did no longer affect the signal in the self-designed device.

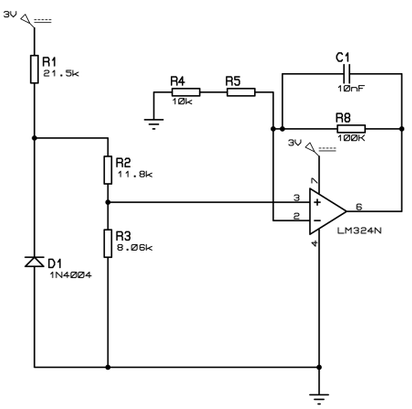

Figure 1. EDA acquisition circuit.
Source: Authors

Experimental protocol

Lack of control concerning experimental variables was found in several projects (Deanfield, Daggett and Harrison 1980, Khalfallah, Ayoub, Calvet, Neveu, Brunswick, Griveau, Lair, Cassir and Bedioui 2012, Rivera Farina, Perez Turiel, Gonzales, Gonzales Sarmiento, Herreros and Higuero 2009, Vlckova et al. 2016, Wang, Jia, Liang, Sun and Huang 2008). Hence, preventive measures were taken on this regard. Multiple protocols and stimuli were designed and put to test to assess them and obtain the best set of guidelines and the most reliable data. Specifically, body posture, relaxation prior to the test, resting between stimulus, placement of electrodes, and state of alertness were assessed.

First, the EDA on the sole of the foot was measured with the participant in three different postures: standing, sitting with the feet on the ground, and sitting with legs raised horizontally. The last posture reported the highest level of conductance, being eight-times the level measured while standing, and 60% higher than while sitting with no elevation of the legs. Both the relief of pressure from the measured surface and the free flow of blood (i.e. when laying horizontally instead of standing) are the reasons for the increase noticed in skin conductance. Furthermore, this applies to any specific region of measurement,thus it was analyzed and verified on the tip of the fingers, the palm of the hands and on the sole of the foot.

Change in posture also signified a reduction in the time needed to obtain a stable EDA. The first measure of 600 seconds was finally reduced to half by releasing weight on the sole of the foot and elevating the leg. With the defined basics, finding an adequate resting time between stimuli was relevant. After applying several stimuli, the time needed to recover the initial SCL was measured. As a result, a spacing of 60 seconds was defined. Concerning human error, a frame to place the electrodes always at the same distance was 3D printed. As the length of the conductor L is inversely proportional to the conductance, manually placing the electrodes would have introduced a source of human error and the recordings would not be comparable among them.

Finally, due to unexpected increases of SCL and appearances of SCRs while the patient intended to relax in a silent room with closed eyes, a method to capture the participant's attention to prevent such phenomenon was developed. After putting to test multiple techniques, such as reading an informative article and watching an emotionally neutral documentary, the most effective method for suppressing non-specific SCRs was the task of following a white dot moving on a black screen. In this way, the researchers could recapture the participant's attention by changing the size and speed of the dot in a non-drastically way. In between the dot frames of the video, 7 stimuli covering different stimulation strategies were inserted to eliminate variance across participants due to susceptibility to one specific kind of stimulus. The final video lasted 7 minutes and 30 seconds and included 3 sudden changes of the screen color simultaneously with loud noises, 2 short 3-seconds-clips of physical injuries, and 2 messages displayed on screen asking to take a deep breath and to cough once. Thus, startle reflexes, and cognitive and physiological stimuli were assessed in this research. In summary, the final protocol started with data collection, followed by electrodes placement and 5 minutes of relaxation, while sitting comfortably on a gurney with the screen at approximately 80 cm. Next, the video was played. After it, the test concluded.

Kim et al. (2018) found that the EDA is affected by the circadian rhythm, showing variations of up to 15% from its mean value, which makes it an important factor to consider when performing multiple recordings. All participants of the present study took part in the test between 10 am and noon, that is, the period along which they were appointed for health controls. In consequence, data presented here should not contain spurious biases because of the circadian rhythm modulation.

Decomposition of the EDA

It has been shown that decomposing the EDA into SCL and SCR is not straightforward. Among the various reasons, one is related to the overlap of SCRs. If the inter stimulus interval is too short (i.e. less that 10-20 s) (Breska, Maoz and Ben-Shakhar 2011). SCRs may overlap making it difficult to discern between them.

Model-based decomposition methods with sound and physiologically inspired constraints have been proven to overcome this issue. The present study used the method proposed by (Greco et al., 2016) based on Bayesian statistics and mathematical convex optimization, while enforcing the sparsity and non-negativity of the reconstructed sudomotor nerve activity. Regarding the post analysis of the data, three values were calculated. First the mean SCL (M-SCL) was the average value between the average of the SCL of each foot. Second, the SCR (M-SCR) was the average value among the average of the SCR of the 7 stimuli of each foot. Finally, the difference between feet (DBF) was the absolute value of the difference between the M-SCL of both feet. Values of 0 μS represented a non-detectable change after the stimulus, or a skin conductance value below the sensitivity of the device at that moment.

Statistical Analysis

All the variables are presented as the mean ± standard deviations. Data was tested for Gaussianity with the Lilliefors test and failed to pass. Comparisons between groups were performed using the Kruskal-Wallis test followed by a *post hoc* test including the Bonferroni correction to reduce the family-wise error rate due to multiple comparisons. A value of $p < 0,05$ was used for statistical significance. Statistical analyses were performed using MATLAB R2019a.

Results

22 subjects participated in the final study: 5 of them were part of the control group (group 1), 6 were classified as out of risk diabetics (group 2) and 11 as at risk (group 3). 3 subjects were excluded from the final analysis due to erroneous data caused by a device failure at the moment of the test. Age correlated well with classification between groups 2 and 3 ($4,4 \pm 4,43$ years vs $11,64 \pm 7,66$ years, $p < 0,05$).

Differences in reaction to stimuli among subjects were found. In Figure 2, a higher response towards loud unexpected noises is evident (stimuli correspondent to vertical dashed lines 1, 2 and 3), followed by lower responses to the other 4 stimuli. In contrast, Figure 3 shows a participant with particularly high sensitivity when deep breathing (sixth dashed line). This heterogeneity was present among all groups.

Patients belonging to group 2 frequently presented an enlarged DBF. In the top graph of Figure 4, notice the

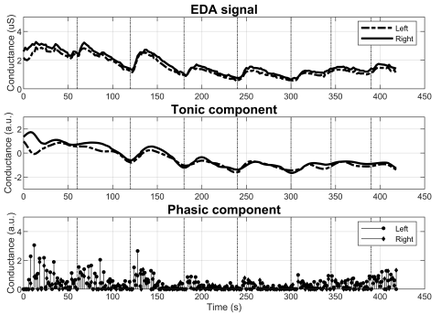

Figure 2. Subject susceptible to external stimuli.
Source: Authors

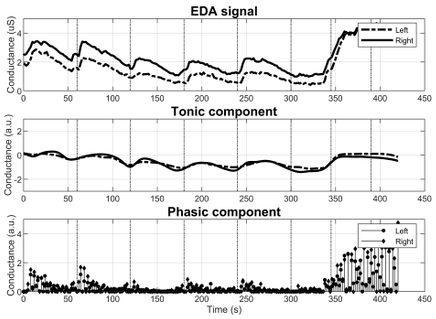

Figure 3. Subject susceptible to internal stimuli.
Source: Authors

gap between the baseline of the feet. This difference is not present in the tonic component (middle graph) as the algorithm receives as input the Z-transform of the EDA signal.

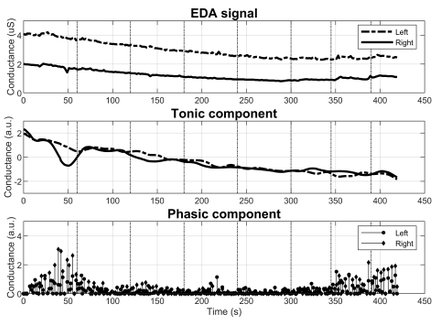

Figure 4. Out-of-risk subject with larger DBF.
Source: Authors

With respect to group 3, the differences in the EDA behavior are noticeable at plain sight. Figure 5 reports a subject with diminished M-SCR, but preserved M-SCL. Figure 6 illustrates abnormality in both metrics. More specifically, the signal starting at 0,7 μS contains no visible SCRs regardless of the 7 stimuli (top graph). Notice as well the estimated phasic component losing its sparsity as a result of the abnormality.

As shown in Table 1, diabetic participants reported both a diminished M-SCL and M-SCR when compared to the

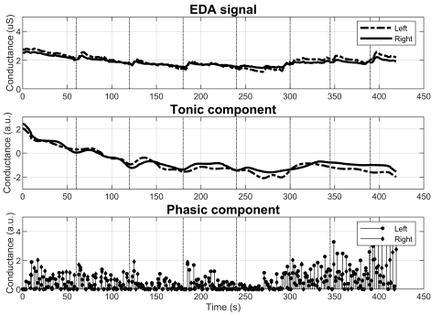

Figure 5. At-risk subject with reduced M-SCR.
Source: Authors

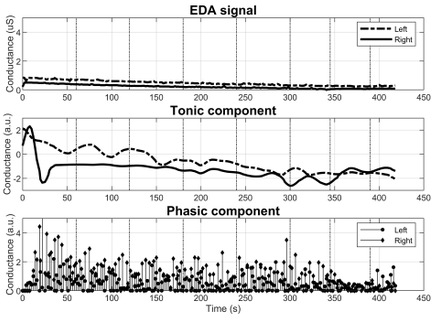

Figure 6. At-risk subject with reduced M-SCL and M-SCR.
Source: Authors

reference group. Numerically, group 2 had in average a 351% lower M-SCL and 55% lower M-SCR to stimuli. Additionally, group 3 presented 236% and 79% lower numeric values for these same two groups of variables.

Table 1. Comparison of the metrics between groups

Characteristics	Reference group (n = 5)	Diabetics out of risk (n = 6)	Diabetics at risk (n = 11)
Age	42,80 ± 18,34	54,33 ± 18,37	63,45 ± 8,72
TWD	0 ± 0	4,40 ± 4,43	11,64 ± 7,66
M-SCL	-0,66 ± 0,55	-2,32 ± 4,74	-1,56 ± 0,74
M-SCR	0,73 ± 0,36	0,33 ± 0,37	0,15 ± 0,08
DBF	0,23 ± 0,32	1,50 ± 3,10	1,66 ± 1,63

Abbreviations: TWD, time with diabetes; M-SCL, mean skin conductance level; M-SCR, mean skin conductance response; DBF, difference between feet. Age and TWD are in years, the rest in arbitrary units.

Source: Authors

Significant difference was found for M-SCR between groups 1 and 3 (0,73 ± 0,36 vs 1,66 ± 1,63, $p < 0,01$). M-SCLs of groups 2 and 3 were significantly different (-2,32 ± 4,74 vs -1,56 ± 0,74, $p < 0,05$). DBF was significantly different between groups 1 and 3 (0,23 ± 0,32 vs 1,66 ± 1,63, $p < 0,05$). No other significant differences were found. Box plots illustrating the distributions for each group of M-SCL, M-SCR and DBF are presented in Figures 7, 8 and 9, respectively.

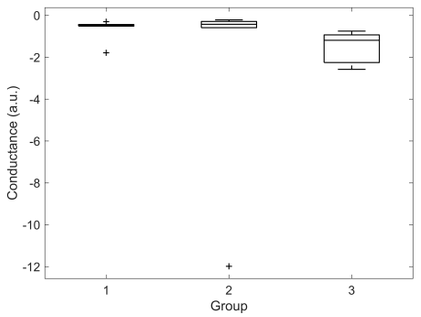

Figure 7. M-SCL distribution among groups.
Source: Authors

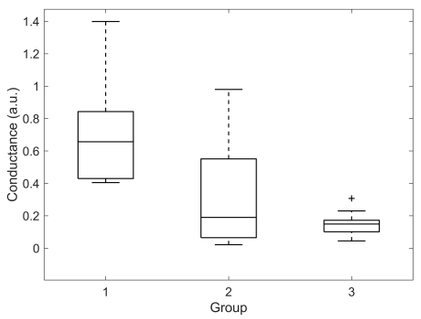

Figure 8. M-SCR distribution among groups.
Source: Authors

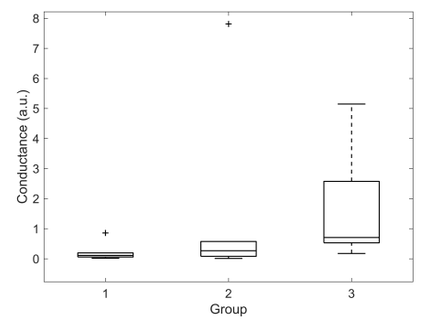

Figure 9. DBF distribution among groups.
Source: Authors

Discussion

Several stimuli techniques have been assessed in scientific literature (Deanfield et al. 1980, Khalfallah et al. 2012, Nazhel, Yetkin, Irkeç and Koçer 2002, Rivera Farina et al. 2009, Vlckova et al. 2016, Wang et al. 2008). Most of them have come to the same conclusion: skin conductance does differ regarding autonomic neuropathy diagnose. For instance, a correlation was found between ulcerations in the feet and the voltage amplitude of the response to startle reflexes (Deanfield et al. 1980). In another research, current through the skin was induced and measured by means of electrochemical reactions (Khalfallah et al. 2012). Their investigation lead to a positive correlation between EDA and AN. In a study by Wang et al. (2008), diabetic patients were associated with higher latency between initiation of the stimulus and waves N and P. However, other study by Vlckova et al. (2016) did not associate lower voltage amplitude nor longer latency with patients diagnosed either with autonomic neuropathy or polyneuropathy.

Although EDA has been extensively studied due to its non-invasive qualities, it only informs about the direct current (DC) response of the body. Its alternating current (AC) counterpart is called bio-impedance analysis (BIA). Phase angles measured at different frequencies using the BIA proved to be useful features when classifying diabetes mellitus in age and sex-matched groups (Jun et al., 2018). For the same group, however, EDA showed marginal results (S. Kim et al., 2019). Compared to this study, measurement protocol of the EDA included both feet and hands, lasted 5 minutes and was repeated 30, 60, 90 and 120 minutes after meal intake. While taking into account glucose variation, subjects were asked to stand still and no intended stimuli were presented during each 5-minutes recording session. As such, the recorded data may be the combination of SCL information and spurious non-specific SCRs, making them highly variable. Mohanraj and Narayanan (2016) studied males with type 2 diabetes during the change from a supine to a standing position. In this study, significantly different EDA was found between diabetics and age and sex-matched controls. In line with our results, studies show that M-SCL by itself is not enough to discriminate between the control group and either of the two other groups ($p > 0,05$) here described. Statistical difference exists only when event-related SCRs are included.

To the best of our knowledge, researches fail to evaluate at once all kinds of stimulation and to assess external variables, since EDA is shaped by multiple other factors such as emotions, alertness and distress. There are several potential reasons for researchers failing to agree on the correlation between EDA, diabetes and autonomic neuropathy. Studies do not take into account the state of alertness, fail to capture the attention of the participant during the whole experiment or do not stimulate the subject at all. Therefore, emotional factors concerning or not the experiment might get involved (e.g. stress due to a possible bad outcome or boredom). Moreover, reasons have been given for one or another type of stimulation. Those in favor of intrinsic ones (e.g. Valsava Maneuver or deep breathing) argue that secondary health issues appear if the stimulus comes from outside, such as deficiencies in the autonomous efferent pathways (Rivera Farina et al. 2009). Thus, it was of paramount priority to conduct a test capable of gathering data regarding all the aforementioned stimuli under a single experiment.

One possible explanation for the variation in the 7 stimuli is the natural consequences of aging. It is well known that diabetes prevails among the elderly, and even though patients were asked to use glasses, and the volume of the computer was adjusted for those with reported hearing loss, decay in reflexes may affect the intended outcome of the stimulus. Similarly, elderly participants might be less prone to be stimulated by videos or crude scenes. While younger participants may become less agitated when asked to take a

deep breath or to cough, and more aroused when disturbed by an unexpected loud noise.

Limitations

The study presented some limitations on its scope. First, even though the average age was similar among groups, the population sample was not big enough to stratify it based on it. Hence, decay in SCL and SCR inherent to aging could not be studied. Second, data regarding blood sugar level, weight, and other factors associated with diabetic foot were not gathered for all the participants. Thus, a more exhaustive correlation analysis could not be made.

Further research should be conducted applying the here exposed diversity of stimuli, in order to study in depth the characteristics and responses provoked by each one, while increasing at the same time the study population to conduct a deeper analysis based on age, sex and diabetes duration. Future clinical tests will serve as well to study the necessary modifications in order to comply with FDA standards.

Conclusion

A portable low-cost custom device for the acquisition of EDA was developed. It was then used to study the behavior of EDA and an experimental protocol accounting for a variety of stimuli was designed. This may allow health centers and clinics to apply an early screening where known but costly tests cannot be afforded, either because they are disposable and thus become costly for large populations, or because they are too expensive for the available budget.

A total of 22 subjects participated in a preliminary study to test the device. Lower M-SCR and higher DBF were associated with patients classified as at risk of AN. Lower M-SCL may not be directly associated with AN, although it could be taken into account when analyzed by a doctor. Finally, the abnormal state of only one of the above variables might indicate the beginning of AN.

Acknowledgements

This study was possible thanks to the help and funding provided by the Miguel Hernández University of Elche, Spain and the University of Cauca in Popayán, Colombia.

References

Boulton, A. J., Cavanagh, P. R. and Rayman, G. (2007). *Pie diabético* (4 ed.). México D.F.: El Manual Moderno.

Braithwaite, J. J., Watson, D. G., Jones, R. and Rowe, M. (2013). *A Guide for Analysing Electrodermal Activity (EDA) and Skin Conductance Responses (SCRs) for Psychological Experiments*, Technical report, University of Birmingham, Birmingham.

Breska, A., Maoz, K. and Ben-Shakhar, G. (2011). Interstimulus intervals for skin conductance response measurement, *Psychophysiology 48*(4), 437-440. DOI: 10.1111/j.1469-8986.2010.01084.x

Colmenares-Guillén, L. E., Ruíz, M. C. and Niño, E. H. (2015). Aplicación de cómputo móvil y pervasivo para el monitoreo no invasivo de la diabetes en tiempo real, *European Scientific Journal, ESJ 11*(33), 130-147. Retrieved from: http://eujournal.org/index.php/esj/article/view/6641/6378

CookingHacks (2019). *e-Health Sensor Platform V2.0 for Arduino and Raspberry Pi [Biometric/Medical Applications]*. Retrieved from https://www.cooking-hacks.com/documentation/tutorials/ehealth-biometric-sensor-platform-arduino-raspberry-pi-medical

De Alcalá, D. (2005). *Cuidados del pie diabetico* (2 edn). Madrid: Editorial Arán.

De Santos Sierra, A., Sánchez-Ávila, C., Guerra-Casanova, J. and Bailador, G. (2011). Real-Time Stress Detection by Means of Physiological Signals, *in* J. Yang and N. Poh (eds), *Recent Application in Biometrics*, InTech, London, pp. 23-44. DOI: https://doi.org/10.5772/18246

Deanfield, J., Daggett, P. and Harrison, M. (1980). The Role of Autonomic Neuropathy in Diabetic Foot Ulceration, *Journal of the Neurological Sciences 47*(2), 203-210. DOI: 10.1016/0022-510X(80)90004-0

González-Correa, C. A. (2018). Clinical Applications of Electrical Impedance Spectroscopy. In: Simini F., Bertemes-Filho P. (eds). *Bioimpedance in Biomedical Applications and Research*, New York: Springer, Cham, pp. 187-218. DOI: 10.1007/978-3-319-74388-2_10

González-Correa, C. H. (2018). Body Composition by Bioelectrical Impedance Analysis. In: Simini F., Bertemes-Filho P. (eds). *Bioimpedance in Biomedical Applications and Research*, New York: Springer, Cham, pp. 219-241. Springer. DOI: 10.1007/978-3-319-74388-2_11

Greco, A., Valenza, G., Lanata, A., Scilingo, E. and Citi, L. (2016). cvxEDA: a Convex Optimization Approach to Electrodermal Activity Processing, *IEEE Transactions on Biomedical Engineering 63*(4), 797-804. DOI: 10.1109/TBME.2015.2474131

Ionescu-Tirgoviste, C., Gagniuc, P. A., and Gagniuc, E. (2018). The electrical activity map of the human skin indicates strong differences between normal and diabetic individuals: A gateway to onset prevention. *Biosensors and Bioelectronics, 120*: 188-194. DOI: 10.1016/J.BIOS.2018.08.057

Jun, M.-H., Kim, S., Ku, B., Cho, J., Kim, K., Yoo, H.-R. and Kim, J. U. (2018). Glucose-independent segmental phase angles from multi-frequency bioimpedance analysis to discriminate diabetes mellitus, *Scientific Reports 8*(1), 648. DOI: 10.1038/s41598-017-18913-7

Khalfallah, K., Ayoub, H., Calvet, J. H., Neveu, X., Brunswick, P., Griveau, S., Lair, V., Cassir, M. and Bedioui, F. (2012). Noninvasive Galvanic Skin Sensor for Early Diagnosis of Sudomotor Dysfuntion: Application to Diabetes, *IEEE Sensors Journal 12*(3), 456-463. DOI: 10.1109/JSEN.2010.2103308

Kim, J., Ku, B., Bae, J.-H., Han, G.-C., and Kim, J. U. (2018). Contrast in the circadian behaviors of an electrodermal activity and bioimpedance spectroscopy. *Chronobiology International, 35* (10), 1413-1422. DOI: 10.1080/07420528.2018.1486852

Kim, S., Cho, J., Ku, B., Jun, M., Kim, G., Yoo, H., Park, S. and Kim, J. U. (2019). Variability of electrochemical skin conductance for screening diabetes mellitus, *Biomedical Engineering Letters 9*(2), 267-274. DOI: 10.1007/s13534-019-00111-1

Li, Y.-q., Wang, S.-j., Gao, F. and Deng, Q.-k. (2004). Value of galvanic skin response in assessment of diabetic autonomic neuropathy, *Academic journal of the first medical college of PLA 24*(10), 1140-2, 1146. DOI: 10.18410/jebmh/2016/560

Mojica-Londoño, A. G. (2017). Actividad electrodérmica aplicada a la psicología: análisis bibliométrico. *Revista Mexicana de Neurociencia, 18*(4), 46-56. https://www.medigraphic.com/pdfs/revmexneu/rmn-2017/rmn174f.pdf

Moncada, M. E., and De la Cruz, J. (2011). La actividad electrodérmica -Revisión. *Ingeniería e Investigación, 31*(2), 143-151. Retrieved from https://revistas.unal.edu.co/index.php/ingeinv/article/view/23473/33764

Mohanraj, S. and Narayanan, K. (2016). Sympathetic Skin Response and Galvanic Skin Resistance in Males with Type 2 Diabetes Mellitus. *Journal of Evidence Based Medicine and Healthcare, 3* (50), 2544-2549. DOI: 10.18410/jebmh/2016/560

Najström, M. and Jansson, B. (2007). Skin conductance responses as predictor of emotional responses to stressful life events. *Behaviour research and therapy 45*(10), 2456-2463. DOI: 10.1016/j.brat.2007.03 .001

Nazhel, B., Yetkin, I., Irkeç, C. and Koçer, B. (2002). Sympathetic skin response in diabetic neuropathy, *Electromyography and clinical neurophysiology 42*(3), 181-185.

Papanas, N., Papatheodorou, K., Christakidis, D., Papazoglou, D., Giassakis, G., Piperidou, H., Monastiriotis, C. and Maltezos, E. (2005). Evaluation of a New Indicator Test for Sudomotor Function (Neuropad) in the Diagnosis of Peripheral Neuropathy in Type 2 Diabetic Patients, *Experimental and Clinical Endocrinology and Diabetes 113*(04), 195-198. DOI: 10.1055/s-2005-837735

Posada-Quintero, H. F., Florian, J. P., Orjuela-Cañón, A. D., Aljama-Corrales, T., Charleston-Villalobos, S. and Chon, K. H. (2016). Power Spectral Density Analysis of Electrodermal Activity for Sympathetic Function Assessment, *Annals of Biomedical Engineering 44*(10), 3124-3135. DOI: 10.1007/s10439-016-1606-6

Posada-Quintero, H. F., Reljin, N., Mills, C., Mills, I., Florian, J. P., VanHeest, J. L. and Chon, K. H. (2018). Time-varying analysis of electrodermal activity during exercise, *PLOS ONE 13*(6). DOI: 10.1371/journal.pone.0198328

Reinhardt, T., Schmahl, C., Wüst, S. and Bohus, M. (2012). Salivary cortisol, heart rate, electrodermal activity and subjective stress responses to the Mannheim Multicomponent Stress Test (MMST), *Psychiatry Research 198*(1), 106-111. DOI: 10.1016/j.psychres.2011.12.009

Rico-Olarte, C., López, D. M. and Kepplinger, S. (2018). Towards a Conceptual Framework for the Objective Evaluation of User Experience. In: Marcus A., Wang W. (eds) Design, User Experience, and Usability: Theory and Practice. Lecture Notes in Computer Science (vol 10918). New York: Springer, Cham, pp. 546-559. DOI: 10.1007/978-3-319-91797-9_39

Rivera Farina, P., Perez Turiel, J., Gonzales, L., Gonzales Sarmiento, E., Herreros, A. and Higuero, S. (2009). Neural network application to the development of a novel diabetic neuropathy diagnosis tool using the Valsava Index and the SCR. Paper presented at the *9th International Conference on Information Technology and Applications in Biomedicine* (*ITAB*), IEEE, Larnaca, Cyprus, pp. 1-4. DOI: 10.1109/ITAB.2009.5394431

SánzCorbalán, I., Lázaro, J. L. and García Morales, E. (2011). Eficacia del Neuropad como prueba diagnóstica clínica de la neuropatía diabética, *Reduca 3*(2), 575-600. http://revistareduca.es/index.php/reduca-enfermeria/article/view/767/783

Vlckova, E., Srotova, I. and Bednarik, J. (2016). Sympathetic Skin Response in the Diagnosis of Small Fibre Neuropathy, *Ceska a Slovenska Neurologie a Neurochirugie 112*(1), 52-60.

Wang, H., Jia, Z., Liang, W., Sun, X. and Huang, Y. (2008). Significance of sympathetic skin response in diagnosis diabetic small fiber neuropathy, *Zhonghua Yi Xue Za Zhi 88*(25), 1753-1755.

Zepeda, R. and Mena, R. (2014). Design of an NFC enabled bio-patch solution. Paper presented at the *57th international midwest symposium on circuits and systems* (pp. 322-325). College Station: IEEE. DOI: 10.1109/MWSCAS.2014.6908417

Ingeniería e Investigación vol. 39 No. 3, December - 2019 (34-43)

DOI: http://dx.doi.org/10.15446/ing.investig.v39n3.70221

Compatibility of objective functions with simplex algorithm for controller tuning of HVDC system

Compatibilidad de funciones objetivas con algoritmo simplex para el ajuste del controlador del sistema HVDC

Haaris Rasool[1], Aazim Rasool[2], Ataul Aziz Ikram[3], Urfa Rasool[4], Mohsin Jamil[5], and Haaziq Rasool[6]

ABSTRACT

This work aims to tune multiple controllers at the same time for a HVDC system by using a self-generated (SG) simulation-based optimization technique. Online optimization is a powerful tool to improve performance of the system. Proportion integral (PI) controllers of Multi-infeed HVDC systems are optimized by the evaluation of objective functions in time simulation design (TSD). Model based simulation setup is applied for rapid selection of optimal PI control parameters, designed in PSCAD software. A multiple objective function (OF), i.e. Integral absolute error (IAE), integral square error (ISE), integral time absolute error (ITAE), integral time square error (ITSE), and integral square time error (ISTE), is assembled for testing the compatibility of OFs with nonlinear self-generated simplex algorithm (SS-SA). Improved control parameters are achieved after multiple iterations. All OFs generate optimum responses and their results are compared with each other by their minimized numerical values. Disturbance rejection criteria are also proposed to assess the designed controller performance along with robustness of system. Results are displayed in form of graphs and tables in this paper.

Keywords: HVDC, simplex optimization, proportional integral (PI) controller, PSCAD, objective function, IAE, ISE, ITAE, ITSE, ISTE.

RESUMEN

Este trabajo tiene como objetivo la sintonización de múltiples controladores al mismo tiempo para el sistema HVDC utilizando la técnica de optimización basada en la simulación autogenerada (SG). La optimización en línea es una herramienta poderosa para mejorar el rendimiento del sistema. El control integral de proporciones (PI) del sistema HVDC de alimentación múltiple se optimiza mediante la evaluación de la función objetivo en el diseño de simulación en tiempo (TSD). La configuración de simulación basada en el modelo se aplicó para la selección rápida de los parámetros de control PI óptimos, diseñados en el software PSCAD. La función de objetivo múltiple (OF), es decir, error absoluto integral (IAE), error cuadrado integral (ISE), error absoluto de tiempo integral (ITAE), error de cuadrado de tiempo integral (ITSE) y error de tiempo cuadrado integral (ISTE), se ensambla para probar la compatibilidad de OFs con algoritmo simplex autogenerado no lineal (SS-SA). Se logran parámetros de control mejorados después de múltiples iteraciones. Todos los OF generan respuestas óptimas y sus resultados se comparan entre sı por sus valores numéricos minimizados. Los criterios de rechazo de perturbaciones también se proponen para evaluar el rendimiento del controlador diseñado junto con la solidez del sistema. Los resultados se muestran en forma de gráficos y tablas en este documento.

Palabras clave: HVDC, optimización simplex, controlador integral proporcional (PI), PSCAD, función objetivo, IAE, ISE, ITAE, ITSE, ISTE.

Received: February 5th, 2018
Accepted: December 3rd, 2019

Introduction

The AC/DC system stability is a significant performance evaluator of HVDC systems (Anbarasi and Muralidharan, 2016). The performance of a system relies on its stability and dynamic performance. The efficiency of a control system is estimated by exposing the system to fault or disturbance and observing its reaction under these abnormal conditions (Tan et al., 2006). The HVDC control system based on line commutation converters is influenced by the number of

[1]M.Sc. in Electrical Engineering, National University of Computer and Emerging Sciences - FAST, Pakistan. Affiliation: Ph.D. researcher in Electrical Engineering and Energy Technology, Vrije Universiteit Brussel, Belgium.
E-mail: haaris.rasool@vub.be
[2]M.Sc. in Electrical Engineering, North China Electric Power University, China. Affiliation: Ph.D. student, North China Electric Power University, Beijing, China. E-mail: a.rasool@ncepu.edu.cn
[3]Ph.D. in Electrical Engineering, City College of New York, USA. Affiliation: Professor, National University of Computer and Emerging Sciences - FAST, Pakistan. E-mail: ata.ikram@nu.edu.pk
[4]M.Sc. in Mechanical Engineering, National University of Sciences & Technology, Pakistan. Affiliation: Ph.D. in Nuclear Engineering, North China Electric Power University, China. E-mail: urfarasool@ncepu.edu.cn
[5]Ph.D. in Electrical Engineering, University of Southampton, United Kingdom. Affiliation: Assistant Professor, Memorial University of Newfoundland, Canada. Email: mjamil@mun.ca
[6]B.Sc. in Electrical Engineering, Affiliation: Student, Ghulam Ishaq Khan Institute of Engineering Sciences and Technology, Pakistan.
E-mail: haaziq.1998@gmail.com

How to cite: Haaris R., Aazim R., Aziz I., Urfa R., Mohsin J., and Haaziq, R. (2019). Compatibility of objective functions with simplex algorithm for controller tuning of HVDC system. *Ingeniería e Investigación*, *39*(3).
DOI: 10.15446/ing.investig.v39n3.70221

factors (Sellick and Åkerberg, 2012), but the PI controller is considered the most influential control among all. The overall system stability depends on it because the response of the current controller is directly affected by the PI controller (Jing et al., 2002).

Tuning has always been essential for controllers. Control engineers are very serious to make the system more robust, so constructing a proper tuning algorithm for control parameters is in vogue (Srinivas et al., 2014; Yang et al., 2006). Previously, engineers used Ziegler Nichols method for tuning purposes (Ho et al.e, 1995; Ziegler and Nichols, 1993), but now researchers make their efforts to adopt a fast and efficient technique of tuning. Therefore, modification in procedures are shifting toward the soft computing method. There are a lot of soft computing techniques used to tune the gains and time constant of the PI or PID controller (Stojic et al., 2017). Some examples are simplex algorithm (Gole et al., 2003; Zhao et al., 2007), linear programing based tuning (Oliveira et al., 2014), Modified Genetic Algorithm (Y. P. Wang et al., 2002), offline tuning of discrete-time fractional-order to minimize the cost function (Merrikh-Bayat et al., 2015), Hybrid PID-Artificial Neural Network (ANN) controller to control PWM signal for DC to DC conversion (Muruganandam and Madheswaran, 2013), fuzzy logic algorithm (Sahin and Altas, 2017; Ilyas et al., 2013; Kassem, 2013), State Transition Algorithm (STA) (Saravanakumar et al., 2015), Particle Swarm Optimization (PSO) (Aazim et al., 2017; Rajagopal and Ponnusamy, 2014), etc. With the help of these techniques, it became easy to select parameters intelligently and give optimal results in a very short time compared with the arbitrary or logarithmic searches. Offline tuning methods have also been considered to calculate cost functions by solving the equations (Merrikh-Bayat et al., 2015; M. Wang et al., 2016) or linear models (Oliveira et al., 2014), which is proficient but too complicated.

In this paper, the technique consists in constructing current error in a simulation for the objective function, instead of solving equations and designing a system model or transfer function through system identification (Eriksson, 2011) using MATLAB (Ho et al., 1995; Xu, 2013). This technique is fine, but it is difficult with lack of perfections and does not give precise and flawless results compared with the system. Optimizations are based on time simulation of a HVDC system (Filizadeh and Gole, 2005; Gole et al., 2005). The simulation gives accurate results. Further convergence of the fitness value appearing from every objective function (Jing et al., 2002; Saravanakumar et al., 2015) is performed through simplex algorithm in PSCAD (Zhao et al., 2007). This control design optimization methodology can also be applicable in future HVDC projects in Colombia, which has a rating of 2 000 MW/500 kV DC and project of Colombia-Panama, which has a rating of 400 MW/300 kV DC. It is expected to be in operation in 2025.

Stability issues of this system have also been resolved by simulated self-generated (SSG) PSO (Aazim et al., 2017), but the question arose for the selection of compatible OF with PSO in the process of research and implementation. For this purpose, ISE-OF was selected after survey. The team agreed on a single point and concluded it might be possible that another OF can behave well. In this paper, SG-SA has been used for the optimal selection of PI control parameters for multiple controllers of a HVDC system, and of the best suitable objective functions among all on the basis of the logged data results through a comparison chart. The design process of this method is difficult, but its operation is easy and produces precise control parameters. However, for this kind of optimization process, the resources and time required for computing are considerably higher.

Optimization techniques

In this technique, the optimized PI control parameters are obtained through time simulation results of a system. PSCAD-based simulation makes the HVDC system robust through PI control parameters. It is done after the evaluation of the best objective function for the simplex algorithm. Five different types of objective functions (Filizadeh et al., 2007; Saravanakumar et al., 2015) are taken into account to optimize the initial PI control parameters of a bipolar HVDC system.

Simplex Algorithm

The nonlinear-simplex method was introduced by Nelder and Mead for heuristic optimization (Grešovnik, 2007; Rana et al., 2016), which is based on geometric consideration. Vertices of simplex are set of the $n+1$ point and geometric object is formed in a set of n-dimensional space. An algorithm is initiated by initial simplex parameters $x_1^{(1)}, \ldots, x_{n+1}^{(1)}$ with $n+1$ vertices. The function at vertices is estimated after the generation of the initial parameter. Points are moved steadily in a single iteration according to a strategy that makes the function minimum (Gole et al., 2003).

The simplex algorithm minimizes the fitness value by generating the new vertices through order, reflection, expansion, contraction, shrink and finally, convergence status checked in multiple iterations.

An algorithm is formed as follows:

Choose the initial simplex parameters and then evaluate the function in its vertices.

$$f_i^{(1)} = f\left(\boldsymbol{x}_i^{(1)}\right) \qquad i = 1, \ldots, n+1$$

The number of iterations is obtained in terms of k.

In **ordering**, the vertices are recorded and their functions are the following:

$$f_1^k \leq f_2^k \leq \cdots \leq f_{n+1}^k$$

$$f_i^k = f(\boldsymbol{x}_i^k)$$

Reflection is the worst vertex reflected between the superlative n vertices center point

$$x'^k = \frac{1}{n}\sum_{i=1}^{n} x_i{}^k \tag{1}$$

Reflected point $x_r{}^k$ are calculated as follows:

$$x_r^k = x^k + \left(x'^k - x_{n+1}^k\right) \tag{2}$$

Then, evaluate their function $f_r^k = f(\boldsymbol{x}_r^k)$.

If condition $f_1^k \leq f_r^k < f_n^r$ is satisfied, take x_r^k and move toward the convergence check.

Expansion takes place if $f_r^k < f_1^k$, then, calculate x_e^k

$$x_e{}^k = x'^k + 2(x_r^k - x'^k) \tag{3}$$

Next, evaluate their function $f_e^k = f(\boldsymbol{x}_e^k)$.

If condition $f_e^k = f(\boldsymbol{x}_e^k)$ is satisfied, then take x_e^k, otherwise, take $x_r{}^k$ and move toward the convergence check.

Outside and inside **contraction** is performed if $f_r^k \geq f_n^k$.

If $f_r^k < f_{n+1}^k$, it is named as outside contraction, then, calculate x_c^k

$$x_c^k = x'^k + \frac{1}{2}(x_r^k - x'^k) \tag{4}$$

and evaluate function $f_c^k = f(\boldsymbol{x}_c^k)$.

If expression $f_c^k \leq f_r^k$ is satisfied, then, take x_c^k and move toward the convergence check.

If $f_r^k \geq f_{n+1}^k$, it is named as inside contraction, thus find x_c^k

$$x_c^k = x'^k - \frac{1}{2}(x'^k - x_{n+1}^k) \tag{5}$$

Next, evaluate function $f_c^k = f(\boldsymbol{x}_c^k)$.

If expression $f_c^k < f_{n+1}^k$ is satisfied, then, take x_c^k and move toward the convergence check.

Shrink pass all vertices except the best one.

$$x_c{}^k v_i{}^k = x_1{}^k + \frac{1}{2}(x_i{}^k - x_1{}^k) \tag{6}$$

Then, evaluate function $f_i'^k = f(\boldsymbol{v}_i^k)$, $i = 2, \ldots, n+1$ and take v_i^k as fresh vertices.

If **convergence** is satisfied, then, the iterations end, otherwise initiate the next iteration.

This process repeats again and again with a number of iterations to reduce the fitness value of the function sluggishly until it reaches in the optimum point vicinity.

The simplex algorithm is one of the convergence algorithms to obtain optimized control values, in order to produce the smallest fitness value of an objective function through a soft computing optimization technique. This technique is used in this work to get the optimal values of multiple PI (Aazim et al., 2017) controller parameters (Saravanakumar et al., 2015). Several runs are executed to minimize the fitness value of an objective function (Filizadeh and Gole, 2005), as shown in Figure 1.

In the simulation, the previously defined PI control parameters, k_p and k_i, of a system are set as the initial values to the simplex algorithm, and the tolerance is set to 0,0001.

The selection of control parameters of a system is a very sensitive task to make the system dynamically stable and robust (Muruganandam and Madheswaran, 2013). In

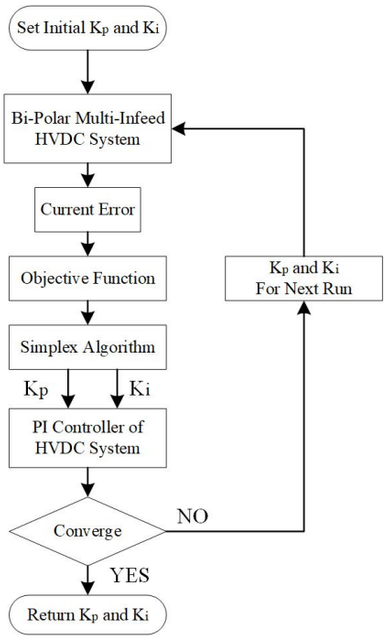

Figure 1. Flow Chart of Simplex Optimization.
Source: Authors

case of simplex algorithm, it is essential to set the initial control parameters, because upcoming runs depend on them. Usually, the previous control parameters are deliberated as initial value (Jing et al., 2002).

The first step is to set the initial control parameters of the HVDC bipolar system and to generate a current error, which is sent to the objective function to integrate the whole error effect and obtain the fitness value. This process evaluates the best objective function through multiple runs of simulation for selecting optimal control parameters by using a simplex algorithm (Gole et al., 2003; Zhao et al., 2007).

The pre-arranged procedure can improve overshoot, rise time and settling time of response. In the case of the HVDC inverter and rectifier, current error is considered, because little variation in current can affect the whole network. Our main focus is to stabilize the current that in turn improves the system.

Objective function

This paper describes the idea for the selection of an objective function in the simulation environment. By using this idea, the objective function of a problem can be designed easily in simulation programming. Five objective functions (IAE, ITAE, ISE, ITSE, and ISTE) are compared for tuning purposes. These objective functions are individually used to find the fitness value that is further fed into simplex algorithm to obtain optimization parameters of multiple PI controllers. The difference of reference current (Iord) and measured current (Im) is error current (CERRR) (Aazim et al., 2017; Saravanakumar et al., 2015).

$$CERRR = I = Iord - Im \tag{7}$$

CERRR is calculated in the simulation environment of PSCAD. Error current for the aforementioned objective functions is shown in Figure 2. The fitness value is found by taking current error from simulation of the HVDC system and forwarding it to the objective functions. It can be handled effortlessly for the selection of optimum gains (k_p and k_i) of PI controllers. Their results would be more precise than the offline tuning technique. Through this technique it is not essential to solve an equation or computing transfer function for the construction of current error as in the conventional approach.

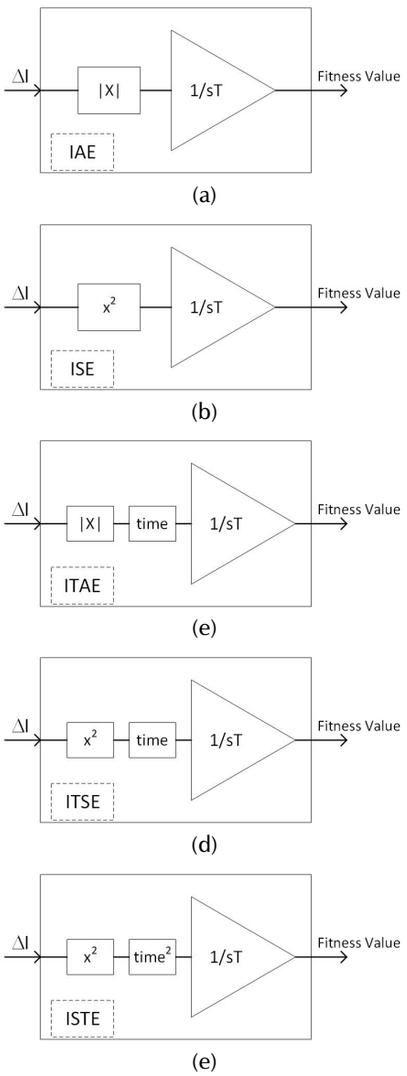

Figure 2. Block Diagram of objective functions: (a) IAE, (b) ISE, (c) ITAE, (d) ITSE, and (e) ISTE.
Source: Aazim et al. (2017)

These five different types of objective functions designed in a simulation environment of PSCAD are used with simplex algorithm.

The five objective functions are the following:

$$\text{Integral Absolute Error } IAE = \int |e|dt \tag{8}$$

$$\text{Integral Square Error } ISE = \int e^2 dt \tag{9}$$

$$\text{Integral Time Absolute Error } ITAE = \int t|e|dt \tag{10}$$

$$\text{Integral Time Square Error } ITSE = \int te^2 dt \tag{11}$$

$$\text{Integral Square Time Error } ISTE = \int t^2 e^2 dt \tag{12}$$

The fitness value of these functions is converged through simplex algorithm to attain the stability in a system by PI control parameters.

The convergence graphs of objective functions are shown in Figure 3. It can be concluded from graphs that the fitness value is reducing in all cases. It is observed that some objective functions attain tolerance range in a smaller number of simulation runs, whereas others attain it in a larger number of simulation runs.

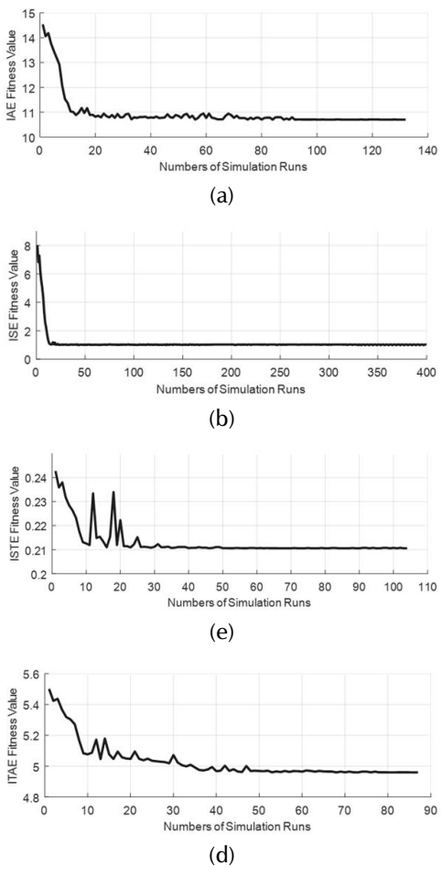

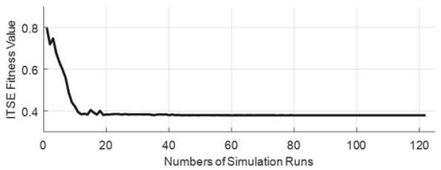

(e)

Figure 3. Convergence graphs of simulation-based objective function using simplex algorithm: (a) IAE, (b) ISE, (c) ITAE, (d) ITSE, and (e) ISTE.
Source: Authors

Tuning of control parameters through the simplex algorithm in time simulation route is represented by a dotted line in Figure 4. Each objective function (IAE, ISE, ITAE, ITSE, and ISTE) operates individually. The simplex algorithm generates new parameters in each run of simulation by considering the fitness value of the objective function.

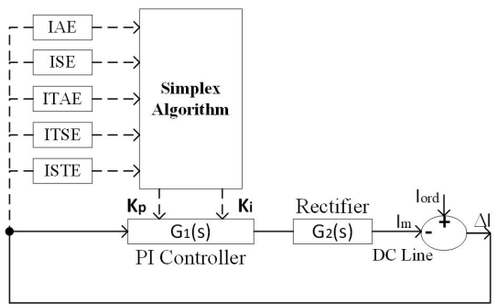

Figure 4. Feedback control loop of bipolar HVDC rectifier side. PI control parameter tuning through IAE, ISE, ITAE, ITSE, and ISTE objective functions.
Source: Authors

HVDC network under consideration

The model of multi-infeed HVDC systems interconnecting Central and East China power systems is shown in Figure 5 and it is used as a test network. PI control parameters are optimized for one of three lines, i.e. three Gorges-Changzhou ± 500 KV HVDC (Jing et al., 2002). These optimized control parameters are also implemented in other two HVDC lines. The results are produced after multi-runs of the optimization process and presented in graphs and tables.

Three 940 Km long HVDC lines of rated voltage ± 500 KV are interconnected with the help of bipolar configuration, as shown in Figure 6. Power capacities of the three lines are 3 000 MW, 3 000 MW and 1 200 MW for line-1, line-2 and line-3, respectively. Line with 3 000 MW HVDC capacity comprises the upper and lower side of the bipolar system 2 x 1500 MW (Jing et al., 2002).

The simulation of HVDC contains AC-DC (Rectifier) and DC-AC (Inverter), as shown in Figure 5. The AOI-11, 12 and AOR-11, 12 are the firing angles of the bipolar inverter and rectifier. The rectifier is considered for the active and reactive power of the system under examination.

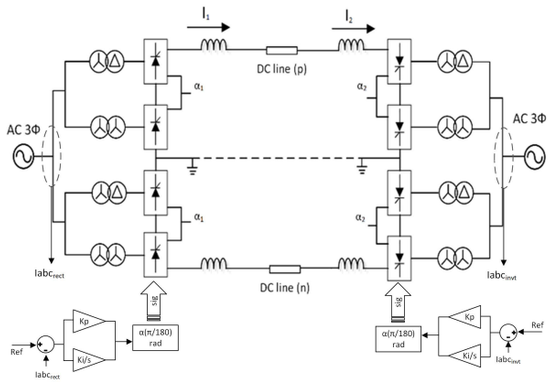

Figure 5. Bipolar Connection of HVDC transmission line with closed-loop control. Source: Jing et al. (2002).
Source: Authors

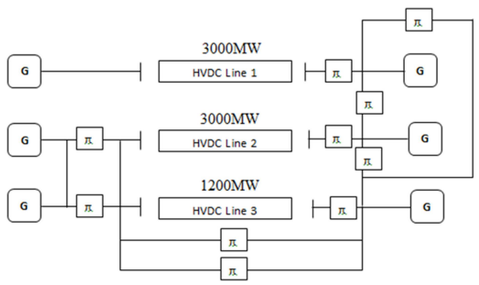

Figure 6. Three HVDC lines connecting Central China and Eastern China power system.
Source: Jing et al. (2002)

This is the closed-loop control system of HVDC, and the PI controllers are used for controlling power in the operation of conversion. Two independent PI controllers are used to control the firing pulse of the upper and lower bridge of the converter. The input of the controller is the current error, whereas the output is the firing angle of thyristor bridge. Block diagram of closed-loop control is shown in Figure 4 and Figure 5. However, the Kp and Ki have a huge contribution to online optimization. Algorithmic based automatic tuning of the aforementioned gains of PI controller is presented in this paper.

The procedure applies to divide the tasks into two cases, i.e. Case I and Case II for finding optimized parameters of PI controllers. Case I shows the system performance on all control parameters related to objective functions. Case II describes the disturbance analysis of control functions related to the best selected objective functions.

CASE-I

The initial parameters of the existing PI controller of San-Chang network of multi-infeed HVDC systems are k_p = 2,8 and k_i = 23 for both rectifier and inverter sides.

To implement the optimization technique, previous values of control parameters are used as initial parameters in the

simplex algorithm. The initialization of the simplex algorithm for optimization through these parameters can reduce the overshoots, undershoots, rise time and settling time with the help of the fitness value of an objective function. Plots of first polar and second polar DC voltages and DC currents of bipolar configuration of HVDC are voltage_11, voltage_12, current_11 and current_12, as shown in Figure 7.

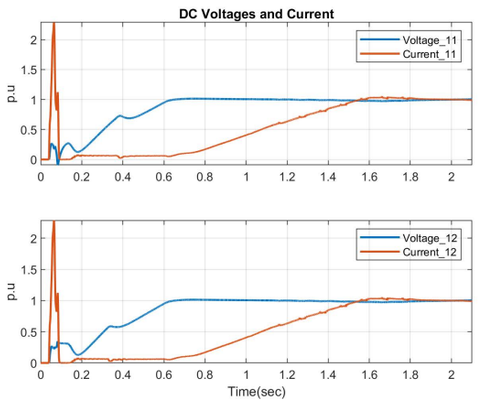

Figure 7. DC voltage and current waveforms of the rectifier of initial PI control parameters.
Source: Authors

Tuning Through IAE, ISE and ITSE Objective Function

IAE, ISE and ITSE with simplex produces the proportional and integral gains of 24,576228 and 32,012679 in 132 runs with IAE, 37,749841 and 35,193554 in 330 runs with ISE, and 11,129470 and 25,599420 in 104 runs of simulation with ITSE. With these control parameters, voltage and current graphs are compared with initial gains. Graphs are shown in Figure 7 and 8. Starting overshoot in DC voltages and current at both poles of the HVDC system has improved but unstable behavior of the system was observed from 0,2 to 0,6 sec and after 1,4 sec in the response of current. This is shown in Figure 8a, whose zoom portion of upper side is in Figure 8b. In these figures, performance trends with these objective functions are nearly same.

Tuning Through ITAE Objective Function

ITAE with simplex produces the proportional and integral gains (k_p and k_i) of 7,910455 and 33,939345 after 87 multiple runs of simulation. Using these control parameters, voltage and current graphs are compared with the initial gain graphs shown in Figure 7 and Figure 9. With these parameters, the system generates stable results and starting overshoot in DC voltages and current at both poles of the HVDC system has improved.

Plots of the first polar and second polar DC voltages and DC currents of a bipolar configuration of HVDC are voltage_11, voltage_12, current_11 and current_12, as shown in Figure 9.

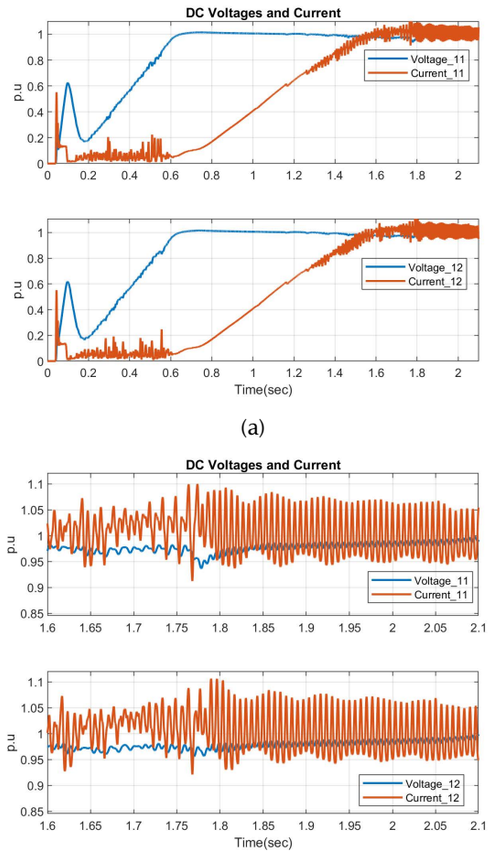

Figure 8. DC voltage and current waveforms with (a) IAE, ISE and ITSE parameters and (b) zoomed portion of upper Figure 8a.
Source: Authors

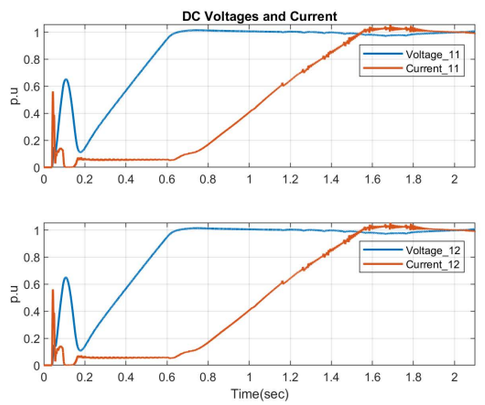

Figure 9. DC voltage and current waveforms of Rectifier with ITAE parameters: (a) upper side and.
Source: Authors

Tuning Through ISTE Objective Function

The simplex algorithm produces the proportional and integral gains (k_p and k_i) of 11,129470 and 25,599420 in 104 runs of simulation with ISTE. Using these control parameters, voltage and current graphs are compared with initial gains. Graphs are shown in Figure 7 and 10. With these parameters, the system generates stable results similar to those of ITAE parameters.

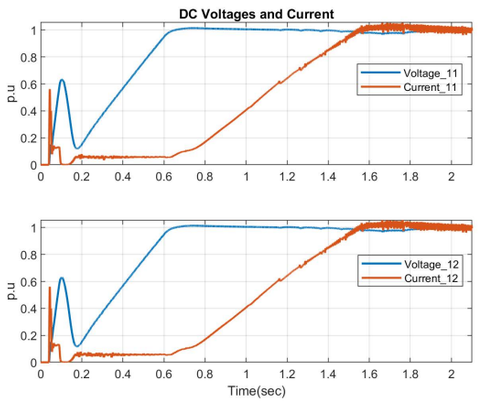

Figure 10. DC voltage and current waveforms of Rectifier with ISTE parameters.
Source: Authors

CASE-II

Table 1 and plots shown in the above figures indicate that the objective function ITAE seems to be the best among all. Disturbance analysis of multi-infeed HVDC system is required to study the performance of ITAE control parameters. Case-2 illustrates the system performance. The procedure is applied to insert three phases to ground fault at the rectifier side of the second line in time simulation for a finite interval of 0,04 sec, i.e. from 2,6 to 2,64 sec. Figure 11, 12, 13 and 14 show the PSCAD simulation results of the three lines active-reactive power comparison between initial and optimized control parameters of HVDC. The legend shown in figures of active_1, 2, 3 and reactive_1, 2, 3 are the active-reactive powers of the HVDC line-1, line-2 and line-3.

Table 1. Comparison of control parameters with different objective functions

	OFs with Simplex	Kp	Ki	Runs	IAE	ISE	ITAE	ITSE	ISTE
Initial		2,8	23	1	14,5479	8,02399	5,52078	0,793956	0,240609
Optimized	IAE	24,5762	32,0127	132	10,3568	0,909036	6,4258	0,386627	0,287227
	ISE	37,7498	35,1936	330	11,396	0,984307	8,55782	0,535229	0,557922
	ITAE	7,9104	33,9393	87	9,63269	0,908641	4,93553	0,341739	0,207539
	ITSE	18,6188	27,5130	122	10,2941	0,939524	6,01125	0,364564	0,249586
	ISTE	11,1295	25,5994	104	9,64781	0,934593	4,85306	0,339563	0,204088

Source: Authors

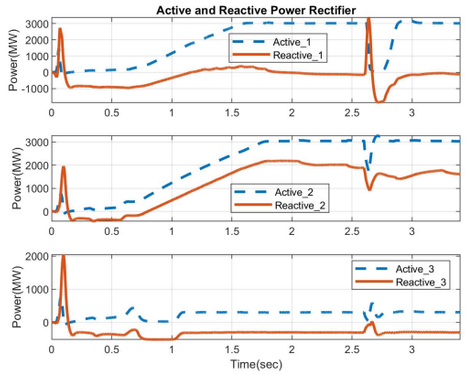

Figure 11. Active-reactive power three-line waveforms HVDC Rectifier with initial parameters.
Source: Authors

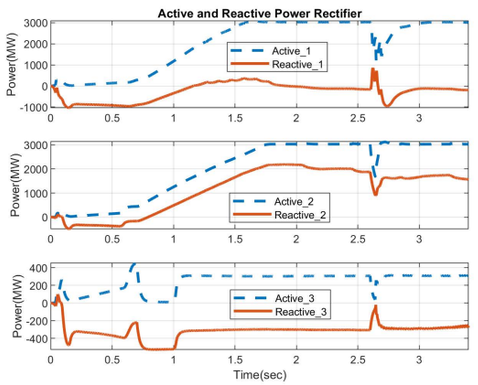

Figure 12. Active-reactive power three-line waveforms of HVDC Rectifier with ITAE parameters.
Source: Authors

Results collected after using optimized control parameters are shown in Figure 13 and 14.

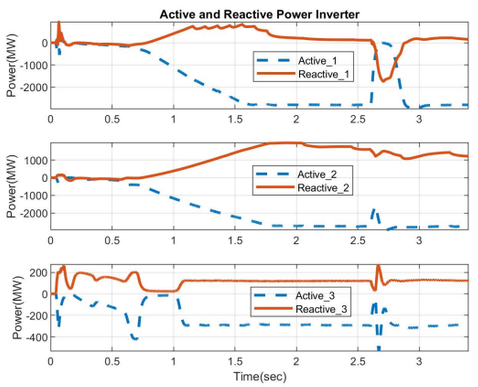

Figure 13. Active-reactive power three-line waveforms of HVDC Inverter with initial parameters.
Source: Authors

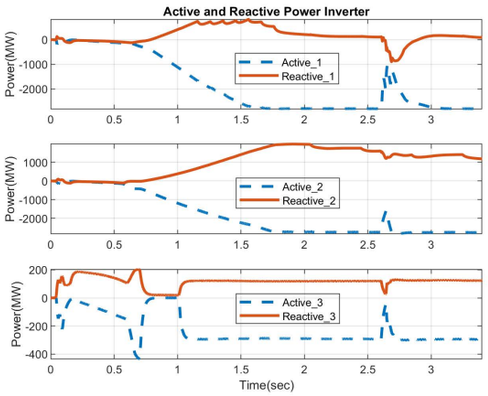

Figure 14. Active-reactive power three-line waveforms of HVDC Inverter with ITAE parameters.
Source: Authors

Simulation Results

Enhancements in the system parameters are shown in Table 1 and Table 2. Two cases are considered in this paper. Case-1 describes results of different types of objective functions and their control parameters and case-2 describes results of the best objective function and their control parameters in a situation of disturbance. The objective function has two purposes. One purpose is the optimization of parameters with simplex algorithm and the other purpose is judgment of the system robustness through the minimum value of the objective function. In Table 1, vertical objective functions merged with simplex algorithm and their control parameters are obtained after a number of simulation runs. The horizontal objective functions and their minimum value clarify the system robustness. The horizontal objective function and their numerical values in Table 1 are achieved by setting 2,1 sec simulation run time for no disturbance. Table 2 shows the result of control parameters of the best compatible objective function ITAE from simplex algorithm. Horizontal objective function numerical values in Table 2 are obtained by setting a 3,7 sec simulation run time for disturbance from 2,6 to 2,64 sec. It is observed that optimized control parameters improved settling time, overshoot, numerical value of objective function and variation in power drop with or without fault condition. This shows the robustness of the system.

Table 2. Disturbance analysis of ITAE control parameters

	OFs with Simplex	Kp	Ki	Runs	IAE	ISE	ITAE	ITSE	ISTE
Initial	– – –	2,8	23	1	23,3553	13,2036	29,57	14,6419	37,0709
Optimized	ITAE	7,9104	33,9393	87	13,2665	1,24908	15,3951	1,27671	2,78932

Source: Authors

Conclusion

In this paper, time simulation design of multi-infeed HVDC bipolar configuration is presented. Primarily, multiple PI controllers of the HVDC system are considered and it was concluded that the system can be robust by tuning their control parameters. Five objective functions (IAE, ISE, ITAE, ITSE and ISTE) are used with SG-SA in PSCAD software, and their results are compared with each other using values of voltage, current and active-reactive power for rectifier and inverter. It is observed that ITAE is the best option with SA tuner because it gives the best overall responses than other OFs in minimum runs of 87. Finally, their results are matched with initial control parameters results. In all cases, responses like overshoot-undershoot, rise time and settling time are improved, but some issues were observed at the end of current response with objective functions of IAE, ISE and ITSE. This indicates the unstable behavior of the system due to fast asymmetric variations of these functions. ITAE-OF with SA tuner produced robust and optimized responses. Finally, it is suggested that all objective functions with soft computing techniques (SA or PSO) can be used for tuning purposes of controller, but selection of one OF is necessary. When comparing the optimized results of active-reactive powers of SSG-PSO (Aazim et al., 2017) and SG-SA parameters, responses of ISE-PSO are slightly better than ITAE-SA. From all these performances of system, it might be possible that PSO with ITAE-OF can produce surprising results.

Acknowledgements

The authors thank Professor and Assistant Professors of the National University of Computer and Emerging Sciences FAST, Islamabad, Pakistan for their valuable suggestions, encouragement, and guidance. They also provided us with the essential support and facilities to develop this work.

References

Aazim, R., Liu, C., Haaris, R., and Mansoor, A. (2017). Rapid generation of control parameters of Multi-Infeed system through online simulation. *Ingeniería E Investigación*, *37*(2), 67-73. DOI: 10.15446/ing.investig.v37n2.61822

Anbarasi, S. and Muralidharan, S. (2016). Enhancing the Transient Performances and Stability of AVR System with BFOA Tuned PID Controller. *Journal of Control Engineering and Applied Informatics*, *18*(1), 20-29. Retrieved from: http://www.ceai.srait.ro/index.php?journal=ceai&page=article&op=view&path%5B%5D=2515&path%5B%5D=1377

Eriksson, R. (2011). *Coordinated control of HVDC links in transmission systems*. (Ph.D. thesis, KTH Royal Institute of Technology). Retrieved from: http://www.diva-portal.org/smash/get/diva2:401164/FULLTEXT01.pdf

Filizadeh, S., and Gole, A. M. (2005). A gradient-based approach for power system design using electromagnetic transient simulation programs. In *Proc. International Conference on Power System Transients* (*IPST*), Montreal, Canadá,

05IPST058-15b. Retrieved from: http://www.ipstconf.org/papers/Proc_IPST2005/05IPST058.pdf

Filizadeh, S., Gole, A. M., Woodford, D. A., and Irwin, G. D. (2007). An optimization-enabled electromagnetic transient simulation-based methodology for HVDC controller design. *IEEE Transactions on Power Delivery*, *22*(14), 2559-2566. DOI: 10.1109/TPWRD.2007.905856

Gole, A. M., Filizadeh, S., Menzies, R. W., and Wilson, P. L. (2003). Electromagnetic transients simulation as an objective function evaluator for optimization of power system performance. In *Proceedings of the International Conference on Power System Transients* (*IPST*), *New Orleans, USA, 03IPST01-02*. Retrieved from: http://ipstconf.org/papers/Proc_IPST2003/03IPST01-02.pdf

Gole, A. M., Filizadeh, S., Menzies, R. W., and Wilson, P. L. (2005). Optimization-enabled electromagnetic transient simulation. *IEEE Transactions on Power Delivery*, *20*(1), 512-518. DOI: 10.1109/TPWRD.2004.835385

Grešovnik, I. (2007). *Simplex algorithms for nonlinear constraint optimization problems*. [Technical report] Retrieved from: http://www2.arnes.si/~ljc3m2/igor/doc/rep/optalgsimplex.pdf

Ho, W. K., Hang, C. C., and Zhou, J. H. (1995). Performance and gain and phase margins of well-known PI tuning formulas. *IEEE Transactions on Control Systems Technology*, *3*(2), 245-248. DOI: 10.1109/87.388135

Ilyas, A., Jahan, S., and Ayyub, M. (2013). Tuning of conventional PID and fuzzy logic controller using different defuzzification techniques. *International Journal of Scientific and Technology Research*, *2*(1), 138-142. Retrieved from: http://www.ijstr.org/final-print/jan2013/Tuning-Of-Conventional-Pid-And-Fuzzy-Logic-Controller-Using-Different-Defuzzification-Techniques.pdf

Jing, Y., Ren, Z., Ou, K., and Yu, J. (2002). Parameter estimation of regulators in Tian-Guang HVDC transmission system based on PSCAD/EMTDC. In *Proceedings of the International Conference on Power System Technology*, Kunming, China. DOI: 10.1109/ICPST.2002.1053600

Kassem, A. M. (2013). Fuzzy-logic based self-tuning PI controller for high-performance vector controlled induction motor fed by PV-generator. *WSEAS Trans. Syst*, *12*(1), 22-31. Retrieved from: http://www.wseas.org/multimedia/journals/systems/2013/55-509.pdf

Merrikh-Bayat, F., Mirebrahimi, N., and Khalili, M. R. (2015). Discrete-time fractional-order PID controller: Definition, tuning, digital realization and some applications. *International Journal of Control, Automation, and Systems*, *13*(1), 81-90. DOI: 10.1007/s12555-013-0335-y

Muruganandam, M., and Madheswaran, M. (2013). Stability analysis and implementation of chopper fed DC series motor with hybrid PID-ANN controller. *International Journal of Control, Automation and Systems*, *11*(5), 966-975. DOI: 10.1007/s12555-012-9209-y

Oliveira, E. J., Honorio, L. M., Anzai, A. H., and Soares, T. X. (2014). Linear Programming for Optimum PID Controller Tuning. *Applied Mathematics*, *5*(6), 886-897. DOI: 10.4236/am.2014.56084

Rajagopal, K., and Ponnusamy, L. (2014). Biogeography-based optimization of PID tuning parameters for the vibration control of active suspension system. *Journal of Control Engineering and Applied Informatics*, *16*(1), 31-39. http://www.ceai.srait.ro/index.php?journal=ceai&page=article&op=view&path%5B%5D=1745&path%5B%5D=1278

Rana, K. P. S., Kumar, V., Garg, Y., and Nair, S. S. (2016). Efficient Design of Discrete Fractional-Order Differentiators Using Nelder-Mead Simplex Algorithm. *Circuits, Systems, and Signal Processing*, *35*(6), 2155-2188. DOI: 10.1007/s00034-015-0149-7

Sahin, E., and Altas, I. H. (2017). FPA Tuned Fuzzy Logic Controlled Synchronous Buck Converter for a Wave/SC Energy System. *Advances in Electrical and Computer Engineering*, *17*(1), 39-48. DOI: 10.4316/AECE.2017.01006

Saravanakumar, G., Valarmathi, K., Rajasekaran, M. P., Srinivasan, S., Iruthayarajan, M. W., and Balas, V. E. (2015). Tuning Multivariable Decentralized PID Controller Using State Transition Algorithm. *Studies in Informatics and Control*, *24*(14), 367-378. DOI: 10.24846/v24i4y201501

Sellick, R. L., and Åkerberg, M. (2012). *Comparison of HVDC Light* (*VSC*) *and HVDC Classic* (*LCC*) *site aspects, for a 500 MW 400 kV HVDC transmission scheme*. Paper presented at the 10th IET International Conference on AC and DC Power Transmission, Birmingham, Institution of Engineering and Technology. DOI: 10.1049/cp.2012.1945

Srinivas, P., Lakshmi, K. V., and Kumar, V. N. (2014). A Comparison of PID Controller tuning methods for three tank level process. *International Journal of Advanced Research in Electrical, Electronics and Instrumentation Engineering*, *3*(1), 6810-6820. Retrieved from: https://www.ijareeie.com/upload/2014/january/26_A%20Comparison.pdf

Stojic, D., Tarczewski, T., and Klasnic, I. (2017). Proportional-Integral-Resonant AC Current Controller. *Advances in Electrical and Computer Engineering*, *17*(1), 81-88. DOI: 10.4316/AECE.2017.01012

Tan, W., Liu, J., Chen, T., and Marquez, H. J. (2006). Comparison of some well-known PID tuning formulas. *Computers and Chemical Engineering*, *30*(9), 1416-1423. DOI: 10.1016/j.compchemeng.2006.04.001

Wang, M., Zhang, Z., and Liu, Y. (2016). Adaptive backstepping control that is equivalent to tuning functions design. *International Journal of Control, Automation, and Systems*, *14*(1), 90-98. DOI: 10.1007/s12555-014-0515-4

Wang, Y. P., Watson, N. R., and Chong, H. H. (2002). Modified genetic algorithm approach to design of an optimal PID controller for AC-DC transmission systems. *International Journal of Electrical Power and Energy Systems*, *24*(1), 59-69. DOI: 10.1016/S0142-0615(01)00006-0

Xu, L. (2013). *Modeling, analysis and control of voltage-source converter in microgrids and HVDC* (Ph.D. thesis, University of South Florida). Retrieved from: https://scholarcommons.usf.edu/etd/4967

Yang, F., Xu, Z., and Zhang, J. (2006). Study on parameter optimization of HVDC PI controllers. *Power System Technology*, *30*(11), 15-20. Retrieved from: http://en.cnki.com.cn/Article_en/CJFDTotal-DWJS200611007.htm

Zhao, C., Lu, X. and Li, G. (2007). *Parameters optimization of VSC-HVDC control system based on simplex algorithm*. Paper presented at the Power Engineering Society General Meeting, Tampa, IEE*E*. DOI: 10.1109/PES.2007.386085

Ziegler, J. G. and Nichols, N. B. (1993). Optimum settings for automatic controllers. *Journal of Dynamic Systems, Measurement, and Control*, *115*(2B), 220-222. DOI: 10.1115/1.2899060

Ingeniería e Investigación vol. 39 No. 3, December - 2019 (44-49)

DOI: http://dx.doi.org/10.15446/ing.investig.v39n3.81161

Performance measurement of a solution for the travelling salesman problem for routing through the incorporation of service time variability

Medición del desempeño de una solución del problema de agente viajero para ruteo a través de la incorporación de la variabilidad de los tiempos de servicio

Dafne Lagos[1], Rodrigo Mancilla[2], Paola Leal[3], and Franco Fox[4]

ABSTRACT

This work assessed the performance of a solution to the problem of assigning service squads, incorporating the variability of service times. The initial problem was modelled as a Travelling Salesman Problem (TSP), whose solution was obtained by the ant colony algorithm, showing the efficient route to be followed by the squad. Assessment of the performance of the solution by discrete event simulation (DES) included the travel time and added the service time. The TSP solution indicated that up to six customer visits could be carried out in an 8-hour working day. Validation by DES presented a stable behavior of the variance, regardless of the number of visit sites assigned along the route.

Keywords: Traveling salesmen problem (TSP), performance, discrete event simulation (DES), service time.

RESUMEN

En este trabajo, se evaluó el desempeño de una solución del problema de asignación de brigadas al incorporar la variabilidad de los tiempos de servicio. La problemática inicial se modeló como un problema de agente viajero (TSP), cuya solución se obtuvo por medio del algoritmo colonia de hormigas y mostró la ruta eficiente que debe seguir una brigada. La evaluación del desempeño de la solución, a través de simulación de eventos discretos (DES), consideró el tiempo de recorrido y agregó el tiempo del servicio. La evaluación de desempeño de la solución del modelo TSP indicó que se pueden visitar hasta seis clientes en una jornada laboral diaria de 8 horas. El modelo de validación mediante DES presentó un comportamiento estable de la varianza, independientemente de la cantidad de puntos asignados a visitar dentro de la ruta.

Palabras clave: Problema del agente viajero (TSP), desempeño, simulación de eventos discretos (DES), tiempo de servicio.

Received: July 19th, 2019
Accepted: October 23rd, 2019

Introduction

In the Chilean electricity market, distribution companies are responsible for delivering electricity to the final users. Due to the importance of this task, national legislation obliges these companies to pay compensation for failures to deliver service to customers in a timely manner. Consequently, the distribution companies seek to guarantee constant supply. One distribution company in particular has service squads available (work teams composed of two operators) which are sent to carry out maintenance and/or repairs to electricity grid cables in response to customer requests. The route taken by each squad is determined by a central operator without any tools, who provides information to support efficient decision-making. Therefore, a travelling salesman model is proposed to establish route assignment for the squads and minimize their total distance travelled. The mathematical model is solved by the heuristic ant colony algorithm, and then the performance of the solution obtained is evaluated by discrete event simulation. The aim of the simulation is to measure the efficiency obtained by the route, considering in addition the service times needed on the ground to solve the customers' requirements. This is done using probability distribution functions to define the service times.

[1]Industrial Civil Engineer, Universidad de La Frontera, Chile. Sc.D. with a major in Industrial Engineering, United States of America. Affiliation: Professor, Universidad Católica de Temuco, Chile. E-mail: dlagos@uct.cl
[2]Industrial Civil Engineer, Universidad Católica de Temuco, Chile. Bachelor of Engineering Sciences, Universidad Católica de Temuco, Chile. Affiliation: Professor, Universidad Católica de Temuco, Chile. E-mail: rmancilla@uct.cl
[3]Industrial Civil Engineer, Universidad de La Frontera, Chile. M.Sc. in Higher Education and University Pedagogy, Universidad Mayor, Chile. Affiliation: Vice-dean of the School of Engineering, Universidad Católica de Temuco, Chile.
E-mail: pleal@uct.cl
[4]Industrial Civil Engineer, Universidad Católica de Temuco, Chile. Bachelor of Engineering Sciences, Universidad Católica de Temuco, Chile.
E-mail: francofox1994@gmail.com

How to cite: Lagos, D., Mancilla, R., Leal, P., and Fox, F. (2019). Performance measurement of a solution for the travelling salesman problem for routing through the incorporation of service time variability. *Ingeniería e Investigación*, *39*(3). DOI: 10.15446/ing.investig.v39n3.81161

The Travelling Salesman Problem (TSP) reflects the routing decisions that a salesman has to take. It involves travelling around a set of customers in order to visit each one. Furthermore, salesmans must start and end their route at the same point, while seeking to minimize the total distance travelled. The answer to the problem generates the ideal route with a visit to each customer and the minimum total distance travelled. The TSP is considered to be a NP-Hard problem. In 1954, Dantzig, Fulker-son and Johnson presented the first efficient algorithm for solving relatively big problems (Wang et al., 2015). Technological progress has developed new tools for solving this problem, including non-linear programming, ant colony, genetic algorithms, neural networks, etc.

Variations of the TSP have been introduced over time. Alkaya and Duman (2010) say that the addition of new restrictions produces different generalizations of the problem, and each new generalization constitutes the starting point for a new area of research. They therefore defined and formulated the Sequence Dependent Travelling Salesman Problem (SDTSP). In the SDTSP, the cost of travelling between two points does not depend only on the distance between them but also on the characteristics of a quantity of points to be visited subsequently. Other variations of the TSP found in the literature are: the Multiple Travelling Salesmen Problem (mTSP) (Chen, 2015), to find efficient routes for all the salesmen; the Travelling Salesman Problem with Draft Limits (TSPDL) (Todosijevic et al., 2017), which includes limitations on travel characteristics or conditions; the Travelling Salesman Problem with Pickups and Deliveries, Time Windows and Draft Limits (TSPPD-TWDL), which involves guaranteeing visits within defined time windows (Arnesen et al., 2017); and the Family Travelling Salesman Problem (FTSP), where the set of nodes on the graph are divided into various subsets, called families, and the objective is to visit a predefined number of nodes in each family at a minimum cost (Bernardino and Paias, 2018).

In another context, the TSP is the basis for the Vehicle Routing Problem (VRP), which seeks to establish a route involving the lowest cost (or distance) to visit the different customers, while also complying with the capacity of each vehicle and the demand requirements of each customer. Like the TSP, the VRP presents variations.

The aim of the present work is to verify whether the result of the travelling salesman model, obtained by ant colony, is able to provide a solution to the problem of assigning squads so as to ensure a working day of up to 8 hours, while incorporating the variability of service times. At the same time, an additional contribution of the document, within the distribution of electricity in Chile, is the field of study particularly focused on the operation of the allocation of service squads. The article is therefore organized as follows: Section 2 offers a general description of previous studies relating to the use of the TSP in related problems, and tools for solution. Section 3 describes the methodology and the assumptions made. In Section 4 the results obtained are presented and analyzed. Finally, Section 5 presents the conclusions.

Related works

Vartdal et al. (2019) indicate that the electricity cables in tidal turbine farms generate high capital expenditure. They therefore aimed to find the cheapest configuration for routing the electrical supply cables, which connect the turbines to the collection center. They used TSP and mTSP models to solve the ideal route, obtaining the cheapest route for three concentrators, and an improvement in models for one or two concentrators.

Tinarut and Leksakul (2019) proposed the Self-Organizing Map (SOM) algorithm, which is used to solve the TSP, but does not give the shortest route or the optimum solution. In consequence, they developed a solution based on SOM together with the local search algorithm to find a better solution. Evaluation of their results indicates that the proposed solution for the algorithm improves the processing time over the results of other researches, but the quality of the solution obtained is not better than that of other studies.

Through the incorporation of service time variability, Lynskey (2019) proposed an algorithm for the best way of finding drone ports, seeking to minimize the average journey distance from the ports to the tasks generated in a given area. In their proposal, they apply various travelling salesman algorithms to determine the shortest route to be travelled by the drone to visit all the tasks. The combination of approach algorithms guarantees that the group of tasks belonging to each drone port is within its range and that the drone can carry out the maximum number of tasks before returning to port to recharge.

Dong et al. (2019) propose an artificial bee colony algorithm (ABC) to solve a combined optimization problem modelled as a colored traveling salesman problem (CTSP) applied to real-world planning problems, specifically a Multi-Machine Engineering System (MES).

Zhou et al. (2019) indicate that the TSP belongs to the NP-hard type. Given its complexity, they propose a new algorithm based on Simulated Annealing (SA) and Gene Expression Programming (GEP) to find the best solution to the problem. The simulated annealing algorithm is used to increase the diversity of the Gene Expression Programming (GEP) population and improve its global search capacity. The results of their experiments show that the proposed algorithm outperforms other heuristic algorithms in terms of the best solution, the worst solution, algorithm execution time, velocity of convergence, and rate of difference between the best solution and the optimum known solution.

Ko et al. (2018) suggest price policies and collaboration models to increase the competitiveness of urgent delivery companies, based on the time market density model. In the price model, they introduce a procedure for finding an optimum price, thus expanding the market for delivery services. They also derive a last mile delivery time function (LMF) of market density with the results of the TSP determined by a genetic algorithm (GA) and simulated with randomly generated customers. Furthermore, they propose a collaboration model as an alternative strategy to

mediate in the service price in a difficult market situation. The applicability and efficiency of the two proposed models are shown in a numerical example. They also indicate that it is beneficial to carry out case studies with real data compiled from companies providing urgent delivery services.

Zhang et al. (2018) propose a new test scheme for data compression for circular exploration. To do this, the previous test vector is used as the template of the next test vector, and only the bits in conflict between the previous response and the next vector need to be updated. To reduce the volume of test data and the application time of the test, the problem addressed seeks to minimize the number of bits in conflict by an optimum re-ordering of the test vectors. The problem is solved using the TSP: each vector represents a city and the number of bits in conflict between two test vectors is considered as the distance between them. The genetic algorithm is used to solve the TSP. The results of the experiment show that the proposed scheme could reduce the volume of test data efficiently with no additional hardware costs.

Chládek and Smetanová (2018) study the TSP in terms of shipping companies and Black Sea ports. They use algorithms based on graph theory to find the most economical route. The start and end of the route are in Prague, since the Czech companies currently operating in the Black Sea have their head offices there.

Li et al. (2018) present a case study of a large triple bridge waterjet cutting system that is modelled as a serial-colored traveling salesman problem. To solve it, a greedy algorithm that selects a neighboring city satisfying proximity is developed. The algorithm allows a salesman to select randomly its shared cities and runs accordingly many times. It can thus be used to solve job scheduling problems with Multi-bridge machining systems.

Meng et al. (2017) present a more common CTSP, in which city colors are diverse. They use a variable neighborhood search (VNS) approach to solve it, instead of computationally intractable exact solutions. Their results show that the proposed VNS is efficient heuristics to solve.

Anaya Fuentes et al. (2016) explain some methodologies for solving the TSP, which are also used for solving the VRP by coding it as a TSP. The solution tool applied is the genetic algorithm (GA), and they conclude that VRPs occurring in the industry can be solved fast enough by fitting the task times to a TSP. When this is solved by a metaheuristic method like GA, it produces results close to the optimum.

Osorio Gómez et al. (2008) solve a flexible job shop problem with interruptions and sequence dependent preparation times. For this purpose, they consider that the preparation times are sequence dependent and that preemptions are allowed. Thus, the problem of assignment to each center consists in determining which machine will be used for processing the sections or parts into which the operations that comprise a job can be divided. To assign the sections, they reduce the problem of each work center to one in which there is only one resource (single machine scheduling problem - SMSP), and then transform and solve these problems by a TSP solution.

González and González (2007) present vehicle routing mechanisms. One way of solving the routing problem is by application of a genetic algorithm. The second way analyzed starts by clustering the customers to be visited and then solving the TSP to determine the best route. The TSP is solved by a local search heuristic.

Methodology

Mathematical model. Obtaining an efficient route requires the construction of a mathematical model allowing the available options to be recognized and evaluated. The mathematical structure used was that of the TSP.

Decision variables. X_{ij} = Binary variable indicating whether (or not) the route between customer i and customer j has been assigned (1: assigned, 0: not assigned).

Parameters. S = number of service orders and/or requirements for assignment to a particular squad. D_{ij} = travel distance in kilometers between the locations of customer i and customer j. The travel distance between the base (initial point) and the first customer, and between the last customer and the base.

Object function: The object function of the model minimize the total distance travelled by the planned assignment of squads. Equation (1) defines the object function.

$$\min = \sum_{i=1} \sum_{j=1} D_{ij} X_{ij} \tag{1}$$

Restrictions. The restrictions considered in the model are:

$$\sum_{j=1}^{S} X_{ij} = 1 \qquad \forall\, i \in [1, S] \tag{2}$$

$$\sum_{i=1}^{S} X_{ij} = 1 \qquad \forall\, j \in [1, S] \tag{3}$$

$$X_{ij} + X_{ji} \leq 1 \qquad \forall\, i, j \tag{4}$$

$$X_{ij} = 0 \qquad \forall\, i = j \tag{5}$$

Restrictions (2) and (3) guarantee the existence of a route assignment to visit the customers. Restriction (4) seeks to avoid the repeated travel and return routes (i.e. avoid creating a route that passes the same customer twice). Restriction (5) eliminates the choice of a variable with the same origin and destination.

Ant colony algorithm. The model is solved by the ant colony optimization algorithm (ACO). This algorithm replicates the efficient behavior of ants looking for the shortest way from their nest to a food source. The route is marked by a pheromone trail which intensifies as the route is more frequently used, which is what occurs with the shortest route.

According to Arias-Rojas et al. (2012), the algorithm starts considering a set of ants (or agents). Each ant (agent) constructs a viable solution to the problem by iterative application of a movement rule that includes information about which decisions are the best in the short term (through a heuristic or greedy rule), and which are the best in the long term (given by the knowledge stored in the pheromone trail). To create a solution, each agent updates a pheromone trail that leads other ants to construct their own solutions. Thus, the ACO algorithm guides the ants to find good solutions in a relatively short time.

According to Zhang and Zhang (2018), ant k which is at location i, at moment t, moves to j according to a certain probability of movement $P_{ij}^{k}(t)$ given by equation (6):

$$P_{ij}^{k}(t) = \begin{cases} \frac{\tau_{ij}^{\alpha}(t)\,\eta_{ij}^{\beta}(t)}{\sum_{s \in nallowed_k} \tau_{is}^{\alpha}(t)\,\eta_{is}^{\beta}(t)} & j \in nallowed_k \\ 0 & otherwise \end{cases} \quad (6)$$

where: τ_{ij} represents the quantity of pheromones present in arc i, j of the route at moment t; η_{ij} is the visible coefficient from location i to j; α denotes the importance of the pheromones for the ant in selecting its direction of travel, and β denotes the importance of the heuristic information; the *nallowed* set represents the following position, in which ant k is allowed to travel from position i, being a subset of the nodes of the network.

The visible coefficient η_{ij} shows how desirable it is to move from i to j, and according to Xu et al. (2018) this coefficient can be expressed as the inverse of the distance between position i and position j. The shorter the distance, the more visible (or desirable) is the route.

Yen and Cheng (2018) indicate that the ants will deposit pheromones on the routes that they travel. When a route is completed, it is compared with the shortest existing route in order to establish the best current route. The best route is updated by adjusting the quantity of pheromone available on the route. According to Rubaiee and Yildirim (2019), this is done using equation (7):

$$\tau_{(a,b)} = (1 - \rho_i)\,\tau_{(a,b)} + \rho_i\,\tau_0 \quad (7)$$

where τ_0 is the initial level of pheromone and ρ_i $(0 < \rho_i < 1)$ is the evaporation parameter of local pheromone.

After all the ants have completed their routes, pheromone evaporation begins in all arcs. Each ant k deposits a quantity of pheromone $\Delta(t)$ in each arc, according to the following rule presented in equation (8):

$$\Delta\tau_{ij}^{k}(t) = \begin{cases} \frac{1}{L^{k}(t)} & if\ (i,j) \in T^{k}(t) \\ 0 & otherwise \end{cases} \quad (8)$$

where $T^{k}(t)$ is the route completed by an ant k in iteration t, and $L(t)$ is its length. The advantage of evaporation is that it provokes delays and avoids convergence on a solution which is optimal at the local level. This means that the algorithm can explore different routes during the search process (Sabbani et al., 2019).

Evaluation of performance by simulation. Using an interaction of optimization and simulation tools for routing problems, as proposed by Niu and Liu (2005) and Krushel et al. (2014), the performance of the solutions obtained by the optimization heuristic (ant colony) was evaluated, to include the effect of the variability of the squads service times. For this purpose, a discrete event simulation model was constructed, representing the working day of each squad, including travel times between customers (previously established) and the service carried out for each one. A gamma probability distribution function was used to represent service time (Garg, 2018). The aim of the application was to measure the effectiveness of the route defined by the optimization mechanism, by analyzing the completion of work orders defined by the time of a working day.

Results

To determine the best movement route of service squads, the TSP model was applied and solved using the ant colony algorithm. Real data were considered when determining the routes, allowing a preliminary evaluation of the efficiency of the model. The information used was taken from a day with high demand for service. Under the modus operandi of the company, the service requirements are received in a telephone exchange, which processes them and issues the assignment orders and routes of the squads for the following day. This information means that the geographical location of the service is known in advance.

The test data included the distances from the origin to the different service locations that each squad must visit. The solution of the model using the ant colony algorithm considered $\alpha = 1$, $\beta = 2$, $\rho = 0{,}5$, and number of ants = 6. Table 1 shows the results of the distance travelled according to the assignment by the ant colony algorithm and compared with the manual method (without optimization and based on the operators' experience).

When comparing the total distances travelled presented in Table 1, a reduction of approximately 20% is found with solution of the TSP model by ant colony, as compared to the manual assignment method.

To evaluate the time of assignment established with the ant colony algorithm, a distance-time conversion factor of 45 km/h was used, which is the average travel speed in non-urban areas with gravel roads. To add the effect of the service time for each customer, a gamma probability distribution was used with parameters $\alpha = 1{,}698$ and $\beta = 30{,}90$. A total of 385 replicas were simulated for each scenario (service squad) with a confidence level of 95%. Table 2 shows the results of the discrete event simulation routine associated with the total time implied in travel and service times.

Results of Table 2 show that in a working day of 8 hours, it is feasible to visit up to six customers. The variances tend to stabilize, and to be constant, when the same number of

points assigned is considered. This is due to the number of replications simulated and the use of the same probability distribution for the customer service time.

Table 1. Results of the distance travelled with assignment by ant colony and by the manual method

Name of service squad	Number of points assigned	Total distance travelled (km) with manual method	Total distance travelled (km) with ant colony
Squad A	3	101,9	70,7
Squad B	4	87,6	75,6
Squad C	4	108,5	97,1
Squad D	4	56,8	55,1
Squad E	4	192,9	180,1
Squad F	4	128,7	91,6
Squad G	5	158,7	96,3
Squad H	6	220,74	140,3
Squad I	7	252,9	194,8
Squad J	7	185,07	147
Squad K	7	141,51	149
Squad L	7	155,2	123
Squad M	8	173	169,5
Squad N	8	259,8	177,4
Total distance travelled		2 223,3 km	1 767,5 km

Source: Authors

Table 2. Results of the simulation of the routes assigned and the service time

Name of service squad	Number of points assigned	Mean total time (h) of travel and service	Standard deviation of the total time (h)
Squad A	3	4,14	1,14
Squad B	4	5,20	1,39
Squad C	4	5,68	1,39
Squad D	4	4,74	1,39
Squad E	4	7,52	1,39
Squad F	4	5,56	1,39
Squad G	5	6,55	1,53
Squad H	6	8,37	1,63
Squad I	7	10,47	1,81
Squad J	7	9,41	1,81
Squad K	7	9,46	1,81
Squad L	7	8,88	1,81
Squad M	8	10,79	1,88
Squad N	8	10,96	1,88

Source: Authors

Conclusions

The travelling salesman model was solved using the ant colony algorithm, produced more efficient squad movement routes than the manual method, with a reduction of up to 20% in the distance travelled by each service squad.

The valuation of the performance of the solution obtained by discrete event simulation, incorporating the service time required to attend to each customer visited on the route, showed that the result of the assignment allowed up to 6 customers to be visited within a maximum working day of 8 hours.

Validation by discrete event simulation presented a stable behavior of the variance, independently of the number of visit points assigned in the route. However, the specific value of the variance was identical, depending on the number of customers visited. Based on the results obtained, it is proposed that the TSP model needs to be adapted if visits to more than 6 customers are to be included, adding the service time as an additional restriction in order to ensure compliance with a defined working day.

Current research evaluates the efficiency of a solution, through a criterion that involves variable attention times, without incorporating this factor in the determination of the result. According to this, a line for future research could be the study of the effect that the incorporation of service time variability would have as part of the model that generates the solution.

References

Alkaya, A. F. and Duman, E. (2010). A new generalization of the traveling salesman problem. *Applied and Computational Mathematics*, *9*(2), 162-175. Retrieved from: https://hdl.handle.net/11376/1317

Anaya Fuentes, G. E., Hernández Gress, E. S., Seck Tuoh Mora, J. C., and Medina Marín, J. (2016). Solution of the job-shop scheduling problem through the traveling salesman problem. *RIAI - Revista Iberoamericana de Automática e Informática Industrial*, *13*(4), 430-437. DOI: 10.1016/j.riai.2016.07.003

Arias-Rojas, J. S., Jiménez, J. F., and Montoya-Torres. J. R. (2012). Solving of school bus routing problem by ant colony optimization. *Revista EIA*, (17), 193-208. Retrieved from: http://www.scielo.org.co/scielo.php?script=sci_arttext&pid=S1794-12372012000100015&lang=es

Arnesen, M. J., Gjestvang, M., Wang, X., Fagerholt, K., Thun, K., and Rakke, J. G. (2017). A traveling salesman problem with pickups and deliveries, time windows and draft limits: Case study from chemical shipping. *Computers and Operation Research*, *77*, 20-31. DOI: 10.1016/j.cor.2016.07.017

Bernardino, R. and Paias, A. (2018). Solving the family traveling salesman problem. *European Journal of Operational Research*, *267*(2), 453-466. DOI: 10.1016/j.ejor.2017.11.063

Chen, S. H. (2015). Minimization of the total traveling distance and maximum distance by using a transformed-based encoding eda to solve the multiple traveling salesmen problem. *Mathematical Problems in Engineering*. DOI: 10.1155/2015/640231

Chládek, P. and Smetanová, D. (2018). Travelling Salesman Problem Applied to Black Sea Ports Used By Czech Ocean Shipping Companies. *Nase More*, *65*(3), 141-145. DOI: 10.17818/NM/2018/3.2

Dong, X., Lin, Q., Xu, M., and Cai, Y. (2019). Artificial bee colony algorithm with generating neighbourhood solution for large scale coloured traveling salesman problem. *IET Intelligent Transport Systems, 13*(10), 1483-1491. DOI: 10.1049/iet-its.2018.5359

Garg, H. (2018). Analysis of an industrial system under uncertain environment by using different types of fuzzy numbers. *International Journal of Systems Assurance Engineering and Management*, *9*(2), 525-538. DOI: 10.1007/s13198-018-0699-8

González, G., and González, F. (2007). Metaheurísticas aplicadas al ruteo de vehículos. Un caso de estudio. Parte 2: algoritmo genético, comparación con una solución heurística. *Ingeniería e Investigación*, *27*(1), 149-157. Retrieved from: https://revistas.unal.edu.co/index.php/ingeinv/article/view/14795

Ko, S. Y., Cho, S. W., and Lee, C. (2018). Pricing and collaboration in last mile delivery services. *Sustainability*, *10*(12), 4560. DOI: 10.3390/su10124560

Krushel, E. G., Stepanchenko, I. V., Panfilov, A. E., and Berisheva, E. D. (2014, September). An experience of optimization approach application to improve the urban passenger transport structure. In: Kravets A., Shcherbakov M., Kultsova M., Iijima T. (Eds.) *Knowledge-Based Software Engineering*. JKBSE 2014. Springer, Cham. DOI: 10.1007/978-3-319-11854-3_3

Li, J., Meng, X., and Dai, X. (2018). Collision-free scheduling of multi-bridge machining systems: A colored traveling salesman problem-based approach. *IEEE/CAA Journal of Automatica Sinica*, *5*(1), 139-147. DOI: 10.1109/JAS.2017.7510415

Lynskey, J., Thar, K., O, T. Z., and Hong, C. S. (2019). Facility location problem approach for distributed drones. *Symmetry*, *11*(1), 118. DOI: 10.3390/sym11010118

Meng, X., Li, J., Dai, X., and Dou, J. (2017). Variable neighborhood search for a colored traveling salesman problem. *IEEE Transactions on Intelligent Transportation Systems, 19*(4), 1018-1026. DOI: 10.1109/TITS.2017.2706720

Niu, Y. and Liu, Y. (2005). Performance optimization and simulation analysis of the railway communication network route search. *Xitong Fangzhen Xuebao / Journal of System Simulation*, *17*(2), 468-471. http://en.cnki.com.cn/Article_en/CJFDTOTAL-XTFZ20050201K.htm

Osorio Gómez, J. C., Castrillón Montenegro, O. E., Toro Cardona, J. A., and Orejuela Cabrera, J. P. (2008). Hierarchical production planning model in flexible job shop including a preemption and sequence-dependent setup times. *Ingeniería e Investigacióon*, *28*(2), 72-79. Retrieved from: https://revistas.unal.edu.co/index.php/ingeinv/article/view/14896

Rubaiee, S., and Yildirim, M. B. (2019). An energy-aware multiobjective ant colony algorithm to minimize total completion time and energy cost on a single-machine preemptive scheduling. *Computers and Industrial Engineering*, *127*, 240-252. DOI: 10.1016/j.cie.2018.12.020

Sabbani, I., Omar, B., and Eszetergar-Kiss, D. (2019). Simulation results for a daily activity chain optimization method based on ant colony algorithm with time windows. *International Journal of Advanced Computer Science and Applications*, *10*(1), 425-430. DOI: 10.14569/IJACSA.2019.0100156

Tinarut, P., and Leksakul, K. (2019). Hybrid self-organizing map approach for traveling salesman problem. *Chiang Mai University Journal of Natural Sciences*, *18*(1), 27-37. DOI: 10.12982/CMUJNS.2019.0003

Todosijevic, R., Mjirda, A., Mladenovic, M., Hanafi, S., and Gendron, B. (2017). A general variable neighborhood search variants for the travelling salesman problem with draft limits. *Optimization Letters*, *11*(6), 1047-1056. DOI: 10.1007/s11590-014-0788-9

Vartdal, J. T., Qassim, R. Y., Mokliev, B., Udjus, G., and Gonzalez-Gorbena, E. (2019). Optimal configuration problem identification of electrical power cable in tidal turbine farm traveling salesman problem modeling approach. *Journal of Modern Power Systems and Clean Energy*, *7*(2), 289-296. DOI: 10.1007/s40565-018-0472-7

Wang, Z., Guo, J., Zheng, M., and Wang, Y. (2015). Uncertain multiobjective traveling salesman problem. *European Journal of Operational Research*, *241*(2), 478-489. DOI: 10.1016/j.ejor.2014.09.012

Xu, G., Wang, Y., Liu, S., and Wang, S. (2018). Tensioning-phase box girder deformation prediction model based on ant colony algorithm and residual correction. *Mathematical Problems in Engineering*. DOI: 10.1155/2018/1872578

Yen, C. T., and Cheng, M. F. (2018). A study of fuzzy control with ant colony algorithm used in mobile robot for shortest path planning and obstacle avoidance. *Microsystem Technologies*, *24*(1), 125-135. DOI: 10.1007/s00542-016-3192-9

Zhang, L., Mei, J., and Yan, B. (2018). A new test set compression scheme for circular scan. *Eurasip Journal on Embedded Systems*, *2018*(1). DOI: 10.1186/s13639-018-0085-2

Zhang, S., and Zhang, Y. (2018). A hybrid genetic and ant colony algorithm for finding the shortest path in dynamic traffic networks. *Automatic Control and Computer Sciences*, *52*(1), 67-76. DOI: 10.3103/S014641161801008X

Zhou, A. H., Zhu, L. P., Hu, B., Deng, S., Song, Y., Qiu, H., and Pan, S. (2019). Traveling-salesman-problem algorithm based on simulated annealing and gene-expression programming. *Information*, *10*(1). DOI: 10.3390/info10010007

Ingeniería e Investigación vol. 39 No. 3, December - 2019 (50-61)

DOI: http://dx.doi.org/10.15446/ing.investig.v39n3.77175

Evaluation of a facility location for a food assistance supply chain. The case of *Bienestarina* in Colombia

Evaluación de la localización de instalaciones para una cadena de suministro de asistencia alimentaria. Caso *Bienestarina* en Colombia

Feizar Rueda-Velasco[1], Wilson Adarme-Jaimes[2], Angélica Garzón-Luna[3], Jhonatan Marroquín-Ávila[4], and Gabriel Parada-Caro[5]

ABSTRACT

The evaluation of the strategic supply chain configuration is considered one of the strategic logistics decisions, especially in food assistance supply chains focused on generating better nutritional conditions in vulnerable populations. In Colombia, there is a social program called *Bienestarina*, which aims to promote food and nutritional security in a vulnerable population. Although the government supports the program for improving nutritional support, there are currently inconsistencies in freight flows, lack of coverage in some areas, and delivery delays. Therefore, this work aims to evaluate the current configuration of the supply chain and propose improvements related to the facility location. Such advances would enable the increase in the efficacy of the network and the reduction of malnutrition in the country. For this purpose, a mixed-integer mathematical programming model is presented, which considers the weighted distance criterion for different demand scenarios and supports the location-allocation decision in a social assistance supply chain. The current network configuration was compared with the optimal proposed structure. The comparisons show highly potential improvements in freight flow allocation, suggests several variations in the existing warehouses emplacement, and generates public policy implications to reduce the logistic cost in the system, prioritizing in turn the demand covering.

Keywords: Facility Location problem, Food assistance programs, Humanitarian supply chain.

RESUMEN

La evaluación de la configuración estratégica de la cadena de suministro se considera una decisión fundamental en logıstica, especialmente en cadenas de suministro de asistencia alimentaria cuyo objetivo es mejorar las condiciones nutricionales de poblaciones en situaciones de vulnerabilidad. Colombia cuenta con un programa estatal denominado *Bienestarina*, que busca promover la seguridad alimentaria de los sectores más vulnerables de la población. Aunque el programa es apoyado por el gobierno y contribuye a mejorar las condiciones nutricionales, actualmente se presentan inconsistencias en los flujos de carga, falta de cobertura en algunas áreas y demoras en las entregas. Por lo anterior, este trabajo busca evaluar la configuración actual de la cadena y proponer mejoras relacionadas con la localización de instalaciones. Esta mejora permitirıa el incremento en la eficacia de la red y la reducción de la desnutrición en el paıs. Para este propósito, se presenta un modelo de programación matemática entera mixta que considera el criterio de distancia ponderada para diferentes escenarios de demanda y soporta la decisión de localización-asignación en una cadena de suministro de asistencia social. La configuración de red actual se comparó con la estructura óptima propuesta. Las comparaciones muestran grandes diferencias entre las asignaciones actuales y los escenarios propuestos por el modelo matemático, sugieren cambios en la localización actual de los almacenes, y genera implicaciones de polıtica pública para la reducción del costo logıstico en el sistema, priorizando a su vez la cobertura de la demanda.

Palabras clave: Problema de localización y asignación, Programas de asistencia alimentaria, Cadenas de suministro humanitarias.

Received: January 9th, 2019
Accepted: November 5th, 2019

Introduction

Subnutrition is a growing problem. In 2018, 5,5% of the total Latin American population suffered hunger. The problem is critical, especially in children, where official data report that 4 million children under five years old are in underweight,

[1]Ph.D. (C) in Engineering, Universidad Nacional de Colombia, Colombia. Affiliation: Assistant Professor, Universidad Distrital Francisco José de Caldas, Colombia. E-mail: fjruedav@udistrital.edu.co
[2]Ph.D. in Engineering, Universidad Nacional de Colombia, Colombia. Affiliation: Associate Professor, Universidad Nacional de Colombia, Colombia.
E-Mail: wadarmej@unal.edu.co
[3]Industrial Engineer, Universidad Distrital Francisco José de Caldas, Colombia.
E-mail: jagarzonl@correo.udistrital.edu.co
[4]Industrial Engineer, Universidad Distrital Francisco José de Caldas, Colombia.
E-mail: jmarroquina@correo.udistrital.edu.co
[5]Industrial Engineer, Universidad Distrital Francisco José de Caldas, Colombia.
E-mail: gdparadac@correo.udistrital.edu.co

How to cite: Rueda-Velasco, F., Adarme-Jaimes, W., Garzón-Luna, A., Marroquín-Ávila, J., and Parada-Caro, G. (2019). Evaluation of the Bienestarina Supply Chain Configuration in Colombia. *Ingeniería e Investigación*, *39*(3). DOI: 10.15446/ing.investig.v39n3.77175

700 000 are in acute malnutrition, and 4'8 million suffer chronic malnutrition (FAO et al., 2019)

Given this situation, some Latin American countries such as Argentina, Chile, Ecuador, Peru, Colombia, Venezuela, Costa Rica, Cuba, Mexico, Nicaragua, Dominican Republic, El Salvador, Guatemala, Haiti, Panama and Honduras have created strategies to guarantee an adequate access to nutrition for the most vulnerable populations (UNICEF, 2006), through the production and distribution of products of high nutritional value.

One of the strategies to fight malnutrition is the continuous supply of food to the vulnerable population. That approach delivers food or complementary feeding to enhance the ingest of high nutritional value nourishment (Lopez-Arana et al., 2016). Other strategies are the direct cash transfers to the target population or the indirect cash transfers for alleviating the cost of the food and increasing the variety of consumer products (De Groot et al., 2017).

Continuous supply strategy differs from direct or indirect cash transfers in the logistical efforts to procure, produce, and distribute the food. Those efforts involve a supply chain that connects the product supply with the demand in the target population.

Some examples in Latin American countries are the LICONSA program to distribute low-cost fortified milk in low-income families (Talamantes, 2016), the National Program of Complementary Food in Chile for children under six years old and nursing mothers (Ministerio de Salud de Chile, 2011) and the axis for food access of the Zero Hunger politics in Brazil (Paes-Sousa and Vaitsman, 2014).

In Colombia, the Instituto Colombiano de Bienestar Familiar (ICBF) focuses on the prevention and comprehensive protection of early childhood, childhood, adolescence, and the well-being of families. One of the institutional objectives of the institute is to promote food and nutritional security (Instituto Colombiano de Bienestar Familiar, 2016). Therefore, the institution has implemented programs related to the production and distribution of foods of high nutritional value. The leader program on this axis is called *Bienestarina*.

Bienestarina is a nationwide program financed with public resources for producing and delivering nutritional supplements for children, adolescents, pregnant women, lactating mothers, the elderly, and families that are considered vulnerable or in malnutrition risk. The *Bienestarina* program started in 1976 and has a national scope with an annual budget close to 40 million dollars (Departamento Nacional de Planeación [DNP], 2015). The main product of the program is a powder composed of mixed cereals, milk, vitamins, and essential fatty acids (ICBF, 2019).

As technical system, the *Bienestarina* program has a six echelon supply chain (Figure 1) composed of: 15 suppliers, 2 production plants located in the departments of Valle del Cauca and Atlántico, 21 regional warehouses, approximately 5 000 distribution points (DP) located in 1 056 municipalities and 170 000 executing units that benefit approximately 4'500 000 people (ICBF, 2014).

According to primary data of the system, the freight flow for the year 2015 was approximately 18 000 tonnes (DNP, 2015). From 2016 to 2019, the public policy planned to maintain a production of 22 000 tons (DNP, 2015).

Figure 1. Scheme of the *Bienestarina* distribution chainEDA acquisition circuit.
Source: Authors using 2015 ICBF data (DNP, 2014).

The *Bienestarina* system is a non-profit supply chain with characteristics of a business supply chains and also of humanitarian supply chains.

From the point of view of the business supply chain, the *Bienestarina system* has low variability in the aggregated demand data, stability in the facility network, transport connections, and other support systems, as well as a decision-making structure controlled by a small number of actors.

However, the *Bienestarina* supply chain has different objectives from a business supply chain. The system is not seeking economic profits, it looks for increasing the social welfare of a population living with food insecurity instead. This means that the system cannot limit the level of service or restrict the coverage areas with profit purposes. Hence, the objectives of the *Bienestarina* supply chain match better with humanitarian supply chains.

Despite the social purposes, in the *Bienestarina* Supply chain, the decision-making structure and the facility network are not under stress as in a post-disaster humanitarian context. Hence the analyzed supply chain is in a midpoint between a humanitarian objective and a distribution network operation closer to the business context. According to Holguín-Veras et al. (2012), those features match regular humanitarian logistics or slow-onset disaster supply chain. In other words, the supply chain design and configuration should be analyzed from a regular humanitarian logistics or slow-onset disaster point of view, but this does not mean that malnutrition or sub nutrition problem is a slow-onset disaster itself.

The slow-onset disaster supply chains look for the recovery of society after disasters (Noori and Weber, 2016), famine relief, aid within refugee camps, political crisis, or the regional development of a country (Cozzolino, 2012; Gustavsson, 2003; Kovács and Spens, 2007).

Therefore, the strategic configuration of the *Bienestarina* supply chain should be addressed mainly to reduce the unmet food aid demand, but also to enhance the system

efficiency, cutting the logistic cost. At the same time, lower logistic cost means more resources available to increase the system coverage.

Thus, the mathematical programming efforts addressed to improve the supply chain configuration take relevance, especially in the context of a system like *Bienestarina*, which has been built since 1976 by adding facilities or delivery points to the network without evidence of overall optimizing. This research presents an evaluation of the facility location in the *Bienestarina System*. The evaluation is made using real data and tested though a mixed-integer linear programming model.

In the next sections, a general description of the background in a strategic supply chain facility location is presented. Next, a mathematical model for facility location is described. Then, a comparison between the current system and the optimal structure is made. Finally, conclusions and future work are proposed.

Facility Location for the *Bienestarina* context

Facility Location has been a top research topic in the scientific literature for operations research and supply chain management. The decisions to locate and allocate facilities are a strategic challenge for public and private organizations (Accorsi et al., 2016; Owen and Daskin, 1998) with an impact on the long term performance of a supply chain.

The *Bienestarina* case is not an exception. Moving annually more than 18 000 tonnes between factory plants and delivery points with national scope, every improvement in facility location could impact directly on the system capacity to cover the vulnerable population. As explained before, the system has built the current network throughout more than 40 years of continuous work and adding facilities in an ad-hoc way. Without evidence of an optimization of the network design, comparisons between the current network design and new alternatives based on mathematical models for optimal facility location take relevance.

Despite the system scope and the program relevance to fighting malnutrition, just a few studies exist around the *Bienestarina* program. For example, studies like the one by Avila (2017) and Rivera and Restrepo (2015) find relations between the nutritional situation and the geographical location of facilities for specific regions in Colombia, but not for the whole country.

For this reason, the mathematical model approach for facility location evaluation in the current system should gather elements from different models and references in the literature. The set of elements is divided here into three main issues: (i) Objectives (ii) network structure and (iii) real case evaluation.

(i) *Objectives*

In the literature about supply chains, the most common objectives have been the minimization of costs (Bortolini et al., 2016; Colicchia et al., 2016; Rancourt et al., 2015; Paul and Wang, 2015). Nevertheless, this objective is not the priority in a system with social or humanitarian purposes like *Bienestarina*.

In the humanitarian context, there are objectives like the minimization of deprivation cost (Holguín-Veras et al., 2013) or the maximizing of equity (Ferrer et al., 2018; Huang and Rafiei, 2019). However, those objectives are more proper for emergency contexts, like post-disaster situations.

A system like *Bienestarina* requires high priority to the social purpose in the demand coverage, but also the second priority is reducing the total freight flows (as a representation of transportation cost). In this sense, a more suitable objective could be maximizing demand fulfillment (Marianov and Serra, 2001) and, with less priority, the minimization of weighted distances between demand and supply sources (Dessouky et al., 2013) (Hall et al., 2013; Şahin et al., 2007).

(ii) *Network structure*

Besides the objectives pursued in a non-profit supply chain like *Bienestarina,* there is also the network configuration. The *Bienestarina* extended network has six echelons: suppliers, factories, regional warehouses, delivery points, executing units, and beneficiaries. The direct supply chain encompasses the two factories, the 21 regional warehouses, and around 5 000 delivery points. In order to evaluate the current supply chain, a mathematical model should check the regional warehouse location. Those warehouses could change their current location more easily than production plants. The third element in the supply chain (delivery points) as a representation of the system demand is not subject to location changes.

The warehouse location requirement is coherent with previous studies in the literature. For instance, in business logistics research, the mathematical models fare common or allocating or selecting warehouses from a set of alternatives (Adivar et al., 2011; Owen and Daskin, 1998). In a humanitarian logistics context, the problem is similar, but the facilities activated are pre-positioned facilities for relief storage and response instead of warehouses (Balcik and Beamon, 2008; Li et al., 2014; Trivedi and Singh, 2018; Singh, 2016; Ukkusuri and Yushimito, 2005).

Additionally, a mathematical model for *Bienestarina* warehouse evaluation should involve the freight flows allocation between the three echelons in the supply chain. Such characteristic is also common in a facility location and distribution problem, and some examples could be consulted in the studies by Jaimes et al. (2011), Camacho-Vallejo et al. (2014), and Chaabane and Geramianfar (2015).

Another point for analysis is the distance or time parameters used for building the model. Classical formulations use Euclidian or Manhattan distances. However, in many cases, the Colombian geographic conditions avoid straight crossing for product transportation. Usually, the truck roads cross through mountains, and also rural roads are not always are in good condition. Those conditions suggest using more

accurate distance measures than Euclidean or Manhattan distances.

In the last years, real-time or distances are collected using GIS Data with tools like Google Maps®, which can improve the parameter estimation against standard Euclidean distance calculation. Some examples are the studies conducted by Oleshchenko et al. (2019) and Sabarish et al. (2018). Nevertheless, in these tools like Google Maps®, the distance estimation is not available for all towns or municipalities. Due to this fact, it is necessary to take an alternative way for distance estimation. In the model presented in the next section, the distance is calculated using Google Maps® between plants and main urban centers. For the main urban centers and the location with no distance register in Google Maps®, Manhattan distances were used. This approach allows enhancing the model parameters more accurately.

(iii) Real Case Evaluation

The use of real cases in facility location problems is usual in regular humanitarian logistics literature. Some research on slow-onset disasters has develop research around a strategic facility location for improving the food aid distribution in Kenya (M. É. Rancourt et al., 2015). The research considers the welfare of all stakeholders for allocating distribution centers using GIS information. GIS data is also used as a parameter estimation tool in a facility location model for a new United Nations Humanitarian Response Depot (UNHRD) in Kampala, Uganda (Dufour et al., 2018), for silos as a strategy for national food security in India (Mogale et al., 2018) and for providing water to the refugee camp in Syria (Smadi et al., 2018).

Nevertheless, most of the research defines network planning and the warehouses from scratch and make no comparisons with the current network structure. Only the work by Dufour et al. (2018) made a cost and operational evaluation of introducing a new warehouse in the current system. This fact is not completely useful since most of the food assistance supply chains (like *Bienestarina*) have been operative already for many years, thus comparisons between current structures and new proposals based on mathematical methods may offer significant conclusions about the supply chain performance.

In summary, the efforts to compare and evaluate the facility location in food assistance programs like *Bienestarina* are scarce, even in systems with similar characteristics like regular humanitarian logistics. Hence the model presented in the next section gathers elements from the different references cited here to adapt the objectives, the network structure, and obtain real parameter estimation.

The model results can be used for decision making in the supply chain design of the *Bienestarina* case, but also the modeling process is useful for other food assistance programs. Finally, the research presented is also useful to remark the importance of supply chain design in the performance of social assistance programs.

In the next section, the mathematical formulation for the *Bienestarina* case is presented and then the comparisons with the current supply chain configuration.

Location and allocation model: *Bienestarina* case

A mixed-integer programming model was used to address the problem of optimal localization of intermediate facilities (regional warehouses) in the *Bienestarina* supply chain configuration. The model results give a selection of regional warehouses to be maintained or installed within the system configuration, and the allocation of the DP that will be served by each regional warehouse enabled, or directly by a flow sent from either of the two production plants.

Table 1 shows the indexes, parameters, and variables of the model for the evaluation of the location of intermediate infrastructure, aiming to minimize the weighted distances.

Table 1. Indexes, parameters, and variables of the proposed model

	Reference sets
i	Index identifying the production plant i, where $i = 1, 2, \ldots, m$
k	Index identifying the DP k, where $k = 1, 2, \ldots, l$
l	Index identifying main cities l used to calculate, in a nearer way, distances from regional warehouses and production plants to each DP, where $l = 1, 2, \ldots, 0$
	Parameters
$DII_{i,i'}$	Real distance (Km) from the production plant i to the production plant i', where $i = 1, 2, \ldots, m$ and $i' = 1, 2, \ldots, m$
$DIJ_{i,j'}$	Real distance (Km) from the production plant i to the potential warehouse j, where $i = 1, 2, \ldots, m$ and $j = 1, 2, \ldots, n$
$DJJ_{j,j'}$	Real distance (Km) from the potential warehouse j to the potential warehouse j', where $j = 1, 2, \ldots, n$ and $j' = 1, 2, \ldots, n$
$DIL_{i,l}$	Real distance (Km) from the production plant i to the main city l, where $i = 1, 2, \ldots, m$ and $l = 1, 2, \ldots, 0$
$DJL_{j,l}$	Real distance (Km) from the potential warehouse j to the main city l, where $j = 1, 2, \ldots, n$ and $l = 1, 2, \ldots, 0$
$DLK_{l,k}$	Rectilinear distance from the main city l to the DP k, where $l = 1, 2, \ldots, 0$ and $k = 1, 2, \ldots, l$
$Bin_{l,k}$	Binary matrix indicating (1) if the main city l is the nearest to the DP k or (0) otherwise, where $l = 1, 2, \ldots, 0$ and $k = 1, 2, \ldots, l$
D_k	Bienestarina demand (kg) from the DP k, where $k = 1, 2, \ldots, l$
O_fi	Bienestarina production capacity (kg) of the production plant i, where $i = 1, 2, \ldots, m$
B_j	Bienestarina storage capacity (kg) in the potential warehouse j, where $j = 1, 2, \ldots, n$
Q	Maximum quantity of Bienestarina (kg) to be produced/distributed per month, considering the budget assigned to the program.
M	Big M. Considerably high value to penalize unsatisfied demand.
W	Maximum quantity of potential regional warehouses to be opened.
	Calculated Parameters
$DIK_{i,k}$	Calculated distance from the production plant i to the DP k, where $i = 1, 2, \ldots, m$ and $k = 1, 2, \ldots, l$. It is composed of the real distance from the production plant i to the main city l plus the rectilinear distance from the main city l to the DP k. The relevant main city l is the closest to the DP k.

$DJK_{j,k}$	Calculated distance from the warehouse j to the DP k, where $j = 1, 2, \ldots, n$ and $k = 1, 2, \ldots, l$. It is composed of the real distance from the regional warehouse j to the main city l plus the rectilinear distance from the main city l to the DP k. The relevant main city l is the closest to the DP k.
	Decision Variables
BJ_j	Binary variable indicating (1) if the potential warehouse j is included in the strategic structure of the Bienestarina supply chain or (0) if it is not selected, where $j = 1, 2, \ldots, n$
$BJK_{j,k}$	Binary variable indicating (1) if the product flow from the warehouse j to the DP k is activated or (0) otherwise, where $j = 1, 2, \ldots, n$ and $k = 1, 2, \ldots, l$
$BIJ_{i,j'}$	Binary variable indicating (1) if the product flow from the Production plant i to the potential warehouse j is activated or (0) otherwise, where $i = 1, 2, \ldots, m$ and $j = 1, 2, \ldots, n$
$BIK_{i,k}$	Binary variable indicating (1) if the direct product flow from the production plant i to the DP k is activated or (0) otherwise, where $i = 1, 2, \ldots, m$ and $k = 1, 2, \ldots, l$
$BJJ_{j,j'}$	Binary variable indicating (1) if the flow exchanging products from the Potential Warehouse j to the Warehouse j' is activated or (0) otherwise, where $j = 1, 2, \ldots, n$ and $j' = 1, 2, \ldots, n$
$BII_{i,i'}$	Binary variable indicating (1) if the flow exchanging products from the production plant i to production plant i' is activated or (0) otherwise, where $i = 1, 2, \ldots, m$ and $i' = 1, 2, \ldots, m$
$W_{j,k}$	Quantity of Bienestarina (kg) sent from warehouse j to the DP k, where $j = 1, 2, \ldots, n$ and $k = 1, 2, \ldots, l$
$X_{i,i'}$	Quantity of Bienestarina (kg) sent from the production plant i to the production plant i', where $i = 1, 2, \ldots, m$ and $i' = 1, 2, \ldots, m$
$Z_{j,j'}$	Quantity of Bienestarina (kg) sent from the warehouse j to the warehouse j', where $j = 1, 2, \ldots, n$ and $j' = 1, 2, \ldots, n$
$Y_{i,j'}$	Quantity of Bienestarina (kg) sent from the production plant i to the warehouse j, where $i = 1, 2, \ldots, m$ and $j = 1, 2, \ldots, n$
$V_{i,k}$	Quantity of Bienestarina (kg) sent directly from the production plant i to a DP k, where $i = 1, 2, \ldots, m$ and $k = 1, 2, \ldots, l$
DI_k	Unsatisfied demand (kg) from the DP k, where $k = 1, 2, \ldots, l$

Source: Authors

A linear model of mixed-integer programming

The mathematical formulation of the proposed model is detailed in the following equations:

$$\begin{aligned}\min F = {} & (M * \sum_{k=1}^{l} DI_k) + \sum_{i=1}^{m}\sum_{i'=1}^{m} (X_{i,i'} * DII_{i,i'}) \\ & + \sum_{i=1}^{m}\sum_{j=1}^{n} (Y_{i,j} * DIJ_{i,j}) + \sum_{j=1}^{n}\sum_{j'=1}^{n} (Z_{j,j'} * DJJ_{j,j'}) \\ & + \sum_{j=1}^{n}\sum_{k=1}^{l} (W_{j,k} * DJK_{j,k}) + \sum_{i=1}^{m}\sum_{k=1}^{l} (V_{i,k} * DIK_{i,k}) \\ & + \sum_{j=1}^{n} BJ_j + \sum_{i=1}^{m}\sum_{i'=1}^{m} (BII_{i,i'}) + \sum_{j=1}^{n}\sum_{j'=1}^{n} (BJJ_{j,j'}) \\ & + \sum_{i=1}^{m}\sum_{j=1}^{n} (BIJ_{i,j}) + \sum_{j=1}^{n}\sum_{k=1}^{l} (BJK_{j,k}) + \sum_{i=1}^{m}\sum_{k=1}^{l} (BIK_{i,k})\end{aligned} \quad (1)$$

subject to:

$$\sum_{i'=1}^{m} X_{i,i'} + \sum_{j=1}^{n} Y_{i,j} + \sum_{k=1}^{l} V_{i,k} \leq Of_i + \sum_{i'=1}^{m} X_{i',i} \forall i = 1, \ldots, m \quad (2)$$

$$\sum_{j'=1}^{n} Z_{j,j'} + \sum_{k=1}^{l} W_{jk} \leq B_j * BJ_j \quad \forall j = 1, \ldots, n \quad (3)$$

$$\sum_{j=1}^{n} BJK_{j,k} + \sum_{i=1}^{m} BIK_{i,k} \leq 1 \quad \forall k = 1, \ldots, l \quad (4)$$

$$\boldsymbol{DIK_{i,k} * BIK_{i,k} \leq DJK_{j,k}} \quad \forall i = 1, \ldots, m \wedge \forall j = 1, \ldots, n \wedge \forall k = 1, \ldots, l \quad (5)$$

$$\sum_{i=1}^{m}\sum_{j=1}^{n} Y_{i,j} + \sum_{i=1}^{m}\sum_{k=1}^{l} V_{i,k} \leq Q \quad (6)$$

$$\sum_{j=1}^{n} W_{j,k} + \sum_{i=1}^{m} V_{i,k} = D_k - DI_k \quad \forall k = 1, \ldots, l \quad (7)$$

$$\sum_{j'=1}^{n} Z_{j',j} + \sum_{i=1}^{m} Y_{i,j} = \sum_{j'=1}^{n} Z_{j,j'} + \sum_{k=1}^{l} W_{j,k} \quad \forall j = 1, \ldots, n \quad (8)$$

$$Z_{j,j'} = 0 \quad \forall j = j' \quad (9)$$

$$BJK_{j,k} \leq BJ_j \quad \forall j = 1, \ldots, n \wedge \forall k = 1, \ldots, l \quad (10)$$

$$X_{i,i'} \leq Of_i * BII_{i,i'} \quad \forall i = 1, \ldots, m \wedge \forall i' = 1, \ldots, m \quad (11)$$

$$Y_{i,j} \leq Of_i * BIJ_{i,j} \quad \forall i = 1, \ldots, m \wedge \forall j = 1, \ldots, n \quad (12)$$

$$Z_{j,j'} \leq B_j * BJJ_{j,j'} \quad \forall j = 1, \ldots, n \wedge \forall j' = 1, \ldots, n \quad (13)$$

$$W_{j,k} \leq B_j * BJK_{j,k} \quad \forall j = 1, \ldots, n \wedge \forall k = 1, \ldots, l \quad (14)$$

$$V_{i,k} \leq Of_i * BIK_{i,k} \quad \forall i = 1, \ldots, m \wedge \forall k = 1, \ldots, l \quad (15)$$

$$\sum_{j=1}^{m} BJ_j \leq W \quad (16)$$

$$X_{i,i'}, DI_k, Z_{j,j'}, Y_{i,j}, V_{i,k}, W_{j,k} \geq 0 \quad (17)$$

$$BJ_j, BJK_{j,k}, BIJ_{i,j}, BIK_{i,k}, BJJ_{j,j'}, BII_{i,i'} \in \{0, 1\} \quad (18)$$

Equation (1) shows the objective function, expressed linearly. The objective function combines three purposes: (i) to minimize the unmet demand, (ii) to minimize the total weighted distance, and (iii) to reduce the number of activated warehouses and the flows between production plants or between warehouses, as unnecessary flows.

The objective function prioritizes the unmet demand minimization using a *Big M* as a prioritization value. Next, as a second objective, the model used the minimization of the total weighted demand. The distance expressed in kg*km works as a prioritization value itself: significantly less than the *Big M*, but significantly higher than the sum of binary variables, which represent unnecessary flows. The weighted distances are used here as a measure of the transportation effort to reach the demand, such as an indirect measure of the transportation cost, whose data were not available in this research. The lack of cost data avoids further model adaptations to represent the nature of transportation costs. Nevertheless, the causal relation between traveled distance and transportation costs may allow the cost reduction with the weighted distance minimization.

The first two parts in the objective function (total distances and unmet demand) aims to cover the real context of a long-term humanitarian food supply chain. This minimizes the transportation distances as an efficiency measure and the impact over population nutrition status through an efficacy measure. The third term adapts the model to the real data, which reports some flows between production plants and between warehouses.

Equation (1) also requires the distance parameter calculation, whose importance was explained in the previous section. The proposed model includes two kinds of distance parameters: real transport distances gathered from Google Maps® ($DIL_{i,l}$, $DJL_{j,l}$), and estimated distances using Manhattan distances ($DLK_{l,k}$, $DLK_{l,k}$). Far distances are used in cases where real transport distances are not available, which is usual in small distant territories from main cities. The demand calculation is exposed in Equations (19) and (20).

$$DIK_{i,k} = \sum_{l=1}^{0} [(DIL_{i,l} + DLK_{l,k}) * Bin_{l,k}] \quad (19)$$

$$DJK_{j,k} = \sum_{l=1}^{0} [(DJL_{j,l} + DLK_{l,k}) * Bin_{l,k}] \quad (20)$$

Equation (2) ensures that the quantity of *Bienestarina*, in kilograms, sent from the production plant i does not exceed the sum of the monthly production plus the supplies received from the production plant i'.

Equation (3) guarantees that warehouse j only send product if the binary variable for its activation assumes the value 1. It also ensures that the quantity of products sent does not exceed the capacity of the warehouse. The input flow from warehouse j' is not included to avoid oversizing the storage capacity of the warehouse.

Equation (4) includes the notion of indivisible demand for the DP k, ensuring that all its demand is supplied either by a single warehouse or by a single production plant.

Constraint (5) is included to enable the possibility of activating direct flows from plant i to point k, provided that there is no warehouse closer to the respective DP.

Equation (6) represents an additional constraint on the production capacity of the plants. It constitutes an upper limit of *Bienestarina* (Kg) that can be produced and distributed per month considering the budget assigned to the program.

With restriction (7), the unsatisfied demand of each DP k is calculated as the difference between the demand of the DP and what it receives from a warehouse j or plant i.

The equilibrium between the inflows and outflows of warehouse j is guaranteed by equation (8).

With the logical constraint (9), non-coherent delivery of the product among the same warehouse is avoided.

With constraint (10) it is guaranteed that no flow from warehouse j is activated if the warehouse is not included in the strategic configuration of the *Bienestarina* supply chain.

Constraints (11) to (15) are included to assign the value of one (1) to the binary variables of flows between points, whenever products are sent between these points.

The maximum number of warehouses to be opened is guaranteed with constraint (16).

The non-negativity of the flow variables (*Bienestarina* sent between points), as well as the unsatisfied demand variable of DP k, is shown in equation (17). Finally, equation (18) refers to the binary nature of the variables of activation of flows and opening of warehouses.

Results

This section compares the current *Bienestarina* system structure with the optimal structure suggested by the mathematical model proposed in the previous section.

The model parameters used the real location of production plants, warehouses, and DPs. Figure 2 shows the current facility location in a map of Colombia that describes the scope of the national program. White spaces show zones without delivery points and correspond to less populated zones. The warehouses are located in the center and north parts of the country. The production plant indexes are related in Table 2.

Table 2. Location of production plants

Index	Department/City	Index	Department/City
i1	Valle del Cauca/Cartago	i2	Atlántico/Sabanagrande

Source: Authors

Data used for facility location and real deliveries correspond to the 2015 ICBF reports (ICBF, 2017). In that year, the system produced and distributed around 18 000 tonnes of *Bienestarina*. The distributed quantity not necessarily matches the nutrition demand in the country. Thus, five demand scenarios were built taking as reference the 2016 total population under malnutrition conditions in 1 113 Colombian municipalities. These data were estimated using the official 2016 total population report made by the Departamento Administrativo Nacional de Estadística (DANE) and the last malnutrition report published by the Colombian Ministry of Health with 2010 data.

The five scenarios are defined as follows:

1. The current system using 2015 real deliveries data and 1 056 municipalities with real delivery points.
2. Malnutrition population between 0 to 4 years old in 1 113 Colombian municipalities.
3. Malnutrition population between 0 to 19 years old in 1 113 Colombian municipalities.
4. Total population between 0 to 4 years old in 1 113 Colombian municipalities
5. Total population between 0 to 19 years old in 1 113 Colombian municipalities

These population ranges are chosen for representing the main population groups in the current system, where around 60% of total deliveries are sent to 0-4 years old children, and 80% to people under 20 years old. In order to determine the supply chain structure, scenarios B, C, D, and E are compared with the current system structure.

The purpose is to determine the system capacity to respond to the demand scenarios. Also, to test the current facility

location, the model has the possibility to allocate warehouses in the current positions or in other new alternatives. The set of potential warehouses was composed of 59 alternatives (21 current warehouses, 2 production plants, and 36 of the main cities or municipalities in Colombia).

Therefore, the comparison measures show how many of the current warehouses locations remain in an optimal solution, how many of the freight flow allocations match with the optimal location, and the percentage of the total demand covered in each scenario.

The proposed mathematical model was solved using the General Algebraic Modeling System - GAMS 23,7 optimization software (2019) and the CPLEX solver, in a computer with Intel Core i7 processor, 1 terabit hard drive and 16 gigabit RAM.

Scenario A. Real deliveries data

The real deliveries data were gathered from the 2015 delivery reports (ICBF, 2017). As we mentioned above, in the current structure the system has activated 2 production plants and 21 warehouses, where the production plants serve also as a warehouse.

In order to evaluate the robustness of the warehouse location against deliveries variability, the location model was solved for the months with minimum and maximum demand (Figure 2).

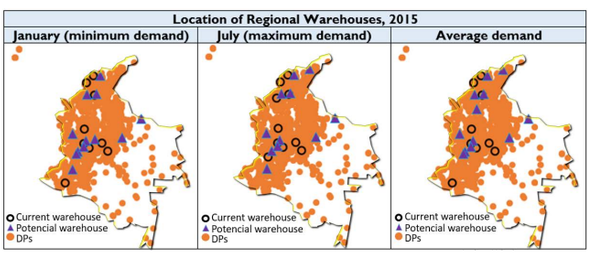

Figure 2. Map of Colombia with the location of the regional warehouses in relevant months of 2015.
Source: Authors

The optimal location of warehouses enabled for each month is represented in Figure 2 in two ways: like black circles without filling, if the selected location is a current warehouse, or like purple triangles, if the selected location corresponds to potential warehouses. The orange circles sections represent the DPs to be assigned. Figure 2 also shows that only 11 of the current warehouse locations are selected in the optimal solution, which means a matching percentage of 52%.

In favor of proving the robustness of the optimal warehouse location, the model was run for every month in the analyzed year. The analysis aims to evaluate the changes in the optimal facility location when facing demand changes.

In Figure 3, the map shows the facility location according to the activation percentage, which considers the number of times that each potential warehouse appeared in the solutions of each model run (relevant months).

Green dots represent the warehouses present in all the runs, which means the set of facilities that remains invariant when facing any demand change. The warehouses marked with a red X are discardable facilities because of their lack of appearance in every solution.

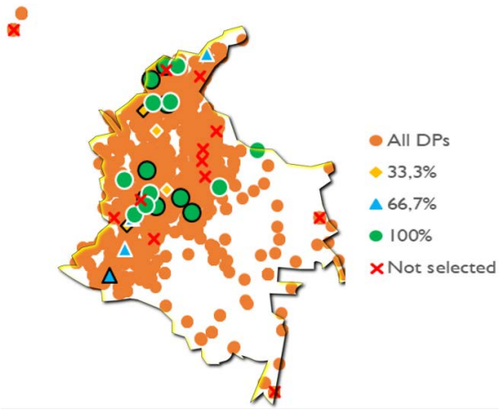

Figure 3. Map of Colombia summarizing the regional warehouses activated in 2015. Scenario 1. The icons with black border are current warehouses, while those with a white border are potential warehouses.
Source: Authors

The analysis for scenario A finishes with the comparison between the current structure and the optimal solutions. The current system performance was calculated through the insertion of the current warehouse and freight flows in the objective function (row "Current" in Table 3). Those results are compared with the model runs in the same three demand calculations as in Figure 2 (minimal demand, maximal demand, and average demand). The comparative results are shown in Table 3.

The row called "Potential" presents the objective function value for the three demand calculations. The comparison process demonstrates the potential reduction of freight flows in optimal solutions. For instance, for the month with maximum demand (July), the total reduction is calculated in 17,33%. The solution also evidences the fulfillment of system purposes. Table 3 shows in any run that the model does not allow unmet demand. Hence, for the three demand calculation, the total contribution of the weighted distance component is more than 99% (Row (1)).

The exposed comparison shows an important gap to be improved, in terms of weighted distance (km*kg). Indeed, if the results are put in a cost context, where the percentage is shown, it would mean a significant reduction in the global logistics cost of the *Bienestarina* Supply Chain.

This section evaluated facilities location with the real deliveries data; however, it could have differences with other demand scenarios. For this reason, scenarios B to E are proposed. Those scenarios are built for covering nutrition in a staggered manner, first focusing on underage population with malnutrition and then in all underage population.

Table 3. Comparative analysis: Current vs. Proposed configuration – Real demand data, 2015

		Scenario	January	July	Average
Objective function (OF) value	Total	Current	409 181'649 446	924 316'978 422	607 051'821 728
		Potential	380 568'010 200	764 102'336 926	547 975'519 592
		Variation	-6,99%	-17,33%	-9,73%
	(1)	Current	99,9999991%	99,9999996%	99,9999992%
		Potential	99,9999990%	99,9999995%	99,9999991%
	(2)	Current	N/A	N/A	N/A
		Potential	N/A	N/A	N/A
	(3)	Current	3 778	3 860	4 992
		Potential	3 671	3 864	4 993
		Variation	-2,83%	0,10%	0,02%
Number of activated flows		Current	3 757	3 839	4 971
		Potential	3 650	3 843	4 972
		Match percentage	40,01%	45,09%	44,50%

(1) % weighted distances/total OF value, (2) Unsatisfied demand and (3) Binary variables activated.

Source: Authors

Comparison of scenarios B to E

The demand parameters used for supply chain configuration modeling were estimated from demographic information registered in the DANE and the malnutrition percentages registered by the Ministry of Health and Social Protection of Colombia.

According to the model presented in a previous section, Table 4 registers a comparison between the current supply chain configuration and the scenarios B to E in terms of objective function value, unsatisfied demand, and number of allocated warehouses.

Results in Table 4 show the performance of the current supply chain configuration in the four scenarios. With 23 active warehouses (2 warehouses in the factories and 21 distributed along the country), the current structure can cover the entire demand for people under 19 years old with malnutrition conditions – scenarios B and C.

Nevertheless, the proposed structure indicates that the system could cover the estimated demand in scenarios B and C with potential warehouses and improve the freight allocation, with a lower weighted distance. Results also demonstrate the need to change the current warehouses location. Indeed, in scenario B, the system could operate with 21 warehouses, where 8 of the current operative warehouses remain (38,09%). In scenario C, the remaining operative warehouses percentage is 38,09% too. Additionally, in both cases, the weighted total distance in the objective function decreased. Thus, an increase in transport efficacy could be expected.

In scenarios D and E, the modeled demand increases to cover the whole population between the indicated age rank. The comparison between the current system configuration and the proposed structure in scenarios C and D presented the same uncovered demand. This fact means a restricted freight flow by the system production capacity and, notably, by the budget constraint of the *Bienestarina* Program. At first glance, it seems that the variation in the value of the objective function in scenarios D and E is not very high. However, by eliminating the effect of the uncovered demand on the objective function (same value for results with the current and the proposed configuration), the proposal structures in scenarios D and E also reduce significantly the weighted total distance compared with the current system configuration, even increasing the number of warehouses.

As in scenarios B and C, the model suggests a modification on the warehouses location, remaining the 42,86% of the current operative warehouses in scenario D, and the 23,81% in scenario E.

Figure 4 depicts the proposal of warehouse location in all scenarios. The solutions in all scenarios illustrate that warehouses are moved to crowded areas, prioritizing the distribution of major freight quantities without reducing covered demand.

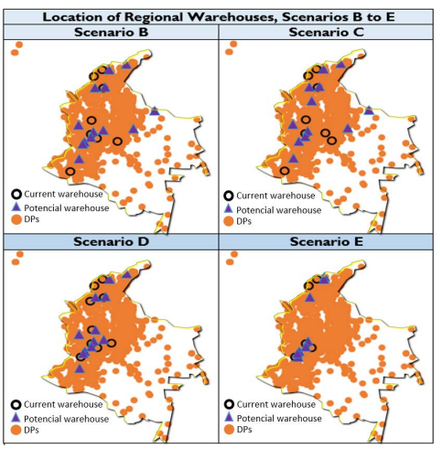

Figure 4. Map of Colombia summarizing the regional warehouses activated in Scenarios B to E: Proposed configuration.
Source: Authors

Finally, the objective function values imply fewer logistics costs and, therefore, more public resources available to invest in production capacity.

Sensitivity analysis. Between humanitarian and commercial purposes

Sensitivity analysis was performed to test the importance of the two primary purposes in the objective function (Equation 1): (i) to minimize the unmet demand and (ii) to minimize the total weighted distance. The first purpose is a typical humanitarian objective and the second purpose is closer to commercial logistics purposes. In the previous section, the objectives were weighted in order to prioritize the humanitarian purpose over the weighed distance minimization (as a representation of the transportation cost).

Table 4. Scenarios B, C, D and E

Scenario	Current Configuration			Proposed configuration					% variation FO value
	Objective function (OF)	Uncovered demand (kg)	# warehouses	Objective function (OF)	Uncovered demand (kg)	# Warehouses			
						Operative	New	Total	
Scenario B Malnutrition 0-4 years old	174 963'620 759	0	18	164 740'780 662	0	8	13	21	-5,84%
Scenario C Malnutrition 0-19 years old	730 651'348 504	0	18	659 040'698 708	0	8	12	20	-9,80%
Scenario D 0-4 years old population	5'766 593'786 490	1 433 191	13	5'663 545'922 572	1 433 191	9	12	21	-1,79%
Scenario D, eliminating the effect of the penalty of uncovered demand on the OF value	607 106'186 490			504 058'322 572					-16,97%
Scenario E 0-19 years old population	44'388 441'682 003	12 210 517	12	44'179 501'541 733	12 210 517	5	8	13	-0,47%
Scenario E, eliminating the effect of the penalty of uncovered demand on the OF value	430 580'482 003			221 640'341 733					-48,53%

Source: Authors

The humanitarian objective was prioritized by the *Big M*, using a value of 3'600 000. The results using this value show a complete demand covering, which is entirely coherent with humanitarian purposes.

In this section, the sensitivity analysis aims to describe the impact in the system structure when the weights in the objective function are changed. Using scenario A in the month with minimum demand, the weight of the *Big M* took three values: 3'600 000, prioritizing the humanitarian objective; 388 505, to give similar weights to the unmet minimization and the distance minimization; and equal to cero (0), to nullify the unmet demand minimization. Table 5 depicts the sensitivity analysis results.

The results show the impact in the system design when the system purposes are changed. In the original Big M value (3'600 000), the humanitarian objective rules the system, the unmet demand is cero, and the number of transportation flows is maximum. With the second Big M value (388 505), the humanitarian and the distance minimization took similar weights, hence the model reduces the freight flows number giving priority to the crowded zones and canceling the flows in rural or remote areas. Besides, the unmet demand increases to 32,14%. Such results describe the change in the system design; the weight of the humanitarian purpose decrease, giving more importance to the classic commercial purposes, which means cutting the longest distance freight flows and the reduction of the service levels in remote areas.

Finally, in the third *Big M value,* the unmet demand effect is canceled, and the model also eliminates all the freight flows. The results are logic because the absence of freight flows removes all traveled distance, and the objective function got the minimum value.

Table 5. Sensitivity analysis results

	Big M Value	M (1)	M (2)	M (3)
		3'600 000	388 505	0
Objective function (OF) value	Total	409 181'649 446	335 823'018 561	21
	(1)	99,9999991 %	57,1546 %	0 %
	(2)	0	143 884'769 275	0
	(3)	3 778	2 341	21
Flows and unmet demand	Number of activated flows	3 757	2 320	0
	% (2)/(1)	0 %	42,8454 %	0 %
	Unmet demand	0	370 355	1 152 297
	% Unmet demand	0 %	32,14 %	100 %

(1) Weighted distances/total OF value (%), (2) Big M * Unmet Demand, (3) Binary variables activated.

M(1), slightly higher than the highest value of the distance between production plants/warehouses and DPs; M(2), average distance of activated paths between production plants, warehouses, and DPs, under the current scenario; M(3), null penalty of unmet demand.

Source: Authors

Conclusions

Bienestarina supply chain is an example of humanitarian food assistance programs and, in a broader way, humanitarian, social assistance programs. This kind of system represents a unique type of supply chain, which does not match entirely with business supply chains or humanitarian supply chains. From the business supply chain, humanitarian social assistance systems take the efficiency orientation, and from the humanitarian supply chain, they takes the purpose of minimizing human suffering. As unique features, this program has the financing structure, sponsored by a

government program; the national scope with a high last-mile access level; and the heterogeneous population as it requires simultaneously distribution in rural, urban, and ethnic territories.

Despite the vast scientific literature on facility location, the evidence of research around slow-onset disasters as malnutrition problems are just a few and also the comparisons between optimal and current supply chain configurations. This research presented a comparison between the optimal structure and the current structure of a humanitarian food assistance program with national scope and a large number of warehouses and delivery points.

With comparison purposes, a mixed-integer programming model was designed for locating the system warehouses and allocating the system freight flows. The model aims to capture food assistance purposes. In this way, the model seeks to assure efficiency in the deliveries via total distance minimization and the food aid covering via unmet demand minimization.

Additionally, the model was adapted to gather a better estimation of real distance parameters using the available Google-Maps® distance and Manhattan distances where Google-Maps® was not available.

The research found a low matching percentage between the current system configuration and the optimal proposal. This fact implies more money in logistics cost and less in food assistance, especially for a program like *Bienestarina,* whose unique public budget should cover production and logistic cost.

For instance, in scenario A, only 52% of the current facilities are in the optimal solution and a potential reduction in 17,33% in the freight flows could be achieved. Results also show the system capacity to cover the demand in all the malnutrition scenarios (A, B, C) and also, enough capacity to cover all children under four years. (Scenario D).

The facility location model was designed to prioritize the humanitarian objectives through the minimization of the unmet demand and also using the minimization of the weighted distances as secondary purpose. The sensitivity analysis shows changes in the results when the model modifies the priorities to give similar weights to humanitarian and commercial purposes. In that case, the model allows unmet demand and cut freight flows leaving unattended rural and remote areas, but also reducing the total traveled distance. This means that in a system led by business purposes, the model reduces the transport cost but sacrifices the demand covering.

These results generate some public policy implications. First, although the program has been incresing its scope and coverage, the growing of the facility network requires optimal planning to achieve the humanitarian objectives and also reduce the transportation cost. Second, the results presented could be used as an input in public tenders for logistics service providers.

With respect to demand calculation, this research had to build a set of scenarios to estimate the number of beneficiaries. That procedure was forced by the absence of data on public demand estimation. The lack of real demand data indicates the incapability of the current system to recognize the target population and, thus, its impacts over nutrition indicators in the country. This weakness could be partially solved through the design of tracking and traceability systems (Rueda-Velasco et al., 2019).

Future work could include the design of supply chain configuration models that minimize deprivation cost (Holguín-Veras et al., 2013), though firstly the deprivation cost for food assistance in Colombia should be calculated. Future studies could also analyze tactical and operative problems like vehicle routing, including time windows, to represent the labor hours in the distribution points.

Supply chain design and configuration with the social scope is a promising research area. Many public programs imply production or transportation of products related to health, food security or other types of humanitarian aid. Usually, this kind of program has the same target population, but its resources and networks are designed and managed independently. Therefore the design of collaborative aid networks can help to improve the public resource allocation and efficacy will be included in future research efforts.

Also, logistics systems as the *Bienestarina* supply chain, have special characteristics, such as social-oriented objectives, high distribution coverage, and connection with a vulnerable population. These features make this kind of system suitable for disaster response, however, effects evaluation on a possible disaster and the design of adaptation procedures toward multi-purpose supply chains should be researched.

Acknowledgements

This research was founded by the "Departamento Administrativo de Ciencia, Tecnología e Innovación (CTeI) - Colciencias" and the Universidad Nacional de Colombia in the joint call for projects #569 (UNAL-UDEC, 2017).

References

Accorsi, R., Cholette, S., Manzini, R., Pini, C., and Penazzi, S. (2016). The land-network problem: Ecosystem carbon balance in planning sustainable agro-food supply chains. *Journal of Cleaner Production*, *112*, 158-171. DOI: 10.1016/j.jclepro.2015.06.082

Adivar, B., Atan, T., Oflaç, B. S., and Örten, T. (2011). Improving social welfare chain using optimal planning model. *Supply Chain Management: An International Journal*, *15*(4), 290-305. DOI: 10.1108/13598541011054661

Ávila, D. (2017). *Diseño y validación de un modelo de distribución de Bienestarina para el Instituto Colombiano De Bienestar Familiar* (*Universidad Industrial de Santander*). Retrieved from http://tangara.uis.edu.co/biblioweb/tesis/2017/166155.pdf

Balcik, B., and Beamon, B. (2008). Facility location in humanitarian relief. *International Journal of Logistics*, *11*(2), 101-121.

Bortolini, M., Faccio, M., Gamberi, M., and Pilati, F. (2016). Multi-objective design of multi-modal fresh food distribution networks. *International Journal of Logistics Systems and Management*, *24*(2), 155. DOI: 10.1504/IJLSM.2016.076470

Camacho-Vallejo, J.-F., González-Rodríguez, E., Almaguer, F.-J., and González-Ramírez, R. G. (2014). A bi-level optimization model for aid distribution after the occurrence of a disaster. *Journal of Cleaner Production*, *105*, 134-145. DOI: 10.1016/j.jclepro.2014.09.069

Chaabane, and Geramianfar. (2015). Sustainable supply chain planning and optimization trade-offs between cost, GHG emissions and service level. In *2015 4th International Conference on Advanced Logistics and Transport* (*ICALT*) (pp. 327-332). IEEE.

Colicchia, C., Creazza, A., Dallari, F., and Melacini, M. (2016). Eco-efficient supply chain networks: development of a design framework and application to a real case study. *Production Planning and Control*, *27*(3), 157-168. DOI: 10.1080/09537287.2015.1090030

Cozzolino, A. (2012). Humanitarian Logistics. *Cross-Sector Cooperation in Disaster Reief* (1st ed.). Springer Science and Business Media. DOI: 10.1007/978-88-470-2658-2

De Groot, R., Palermo, T., Handa, S., Ragno, L. P., and Peterman, A. (2017). Cash Transfers and Child Nutrition: Pathways and Impacts. *Development Policy Review*, *35*(5), 621-643. DOI: 10.1111/dpr.12255

Departamento de Alimentación y Nutrición, and Ministerio de Salud de Chile. (2011). Manual de Programas Alimentarios. In Ministerio de Salud de Chile. Retrieved from http://web.minsal.cl/portal/url/item/caa1783ed97a1425e0400101640109f9.pdf

Dessouky, M., Ordóñez, F., Jia, H., and Shen, Z. (2013). Rapid Distribution of Medical Supplies. In *Patient Flow* (pp. 385-410). Springer, Boston, MA. DOI: 10.1007/978-1-4614-9512-3

DNP. (2014). Documento Conpes 3819: Polítca nacional para consolidar el sistema de ciudades en Colombia. Consejo Nacional de Política Económica y Social República de Colombia Departamento Nacional De Planeación, p. 69. Bogotá D.C.

DNP. (2015). Conpes 3843 Importancia estratégica de los alimentos de alto valor nutricional que serán entregados por el ICBF en las vigencias 2016-2019 (p. 52). p. 52. Bogotá D.C.

Dufour, É., Laporte, G., Paquette, J., and Rancourt, M. É. (2018). Logistics service network design for humanitarian response in East Africa. Omega (United Kingdom), 74, 1-14. DOI: 10.1016/j.omega.2017.01.002

FAO. (2019). El estado de la seguridad alimentaria y la nutrición en el mundo. Retrieved from http://www.fao.org/3/ca5162es/ca5162es.pdf

Ferrer, J. M., Martín-Campo, F. J., Ortuño, M. T., Pedraza-Martínez, A. J., Tirado, G., and Vitoriano, B. (2018). Multi-criteria optimization for last mile distribution of disaster relief aid: Test cases and applications. *European Journal of Operational Research*, *269*(2), 501-515. DOI: 10.1016/j.ejor.2018.02.043

GAMS Development Corporation. (2019). General Algebraic Modeling System (GAMS). Retrieved from https://www.gams.com/download/

Gustavsson, L. (2003). Humanitarian logistics: context and challenges. *Forced Migration Review*, *18*(6), 6-8.

Hall, R., Belson, D., Murali, P., and Dessouky, M. (2013). Modeling patient flows through the healthcare system. In *Patient flow: Reducing delay in healthcare delivery* (pp. 1-44). Springer, Boston, MA. DOI: 10.1007/978-1-4614-9512-3

Holguín-Veras, J., Jaller, M., Van Wassenhove, L. N., Pérez, N., and Wachtendorf, T. (2012). On the unique features of post-disaster humanitarian logistics. *Journal of Operations Management*, 30(7-8), 494-506. DOI: 10.1016/j.jom.2012.08.003

Holguín-Veras, J., Pérez, N., Jaller, M., Van Wassenhove, L. N., and Aros-Vera, F. (2013). On the appropriate objective function for post-disaster humanitarian logistics models. *Journal of Operations Management*, *31*(5), 262-280. DOI: 10.1016/j.jom.2013.06.002

Huang, K., and Rafiei, R. (2019). Equitable last mile distribution in emergency response. *Computers and Industrial Engineering*, *127*, 887-900. DOI: 10.1016/j.cie.2018.11.025

ICBF. (2014). Cartilla Bienestarina. Instituto Colombiano de Bienestar Familiar, 2, 121.

ICBF (2016). Instituto Colombiano De Bienestar Familiar - Icbf. Avance Juridico.

ICBF (2018). Bienestarina Más y Otros Alimentos de Alto Valor Nutricional - Portal ICBF - Instituto Colombiano de Bienestar Familiar ICBF. Retrieved May 16, 2019, from https://www.icbf.gov.co/bienestar/nutricion/bienestarina

ICBF, I. C. de B. F. (2017). Distribución Bienestarina Programas Regulares. Retrieved February 12, 2017, from Nutrición - Bienestarina más y otros alimentos de alto valor nutricional website: https://www.icbf.gov.co/bienestar/nutricion/bienestarina

Jaimes, W. A., Darío, M., and Serna, A. (2011). Modelo para la coordinación de agentes en un sistema logístico de la industria astillera colombiana A coordination agents' model for the Colombian shipbuilding in dustry's logistics system. *Ingeniería e Investigación*, *31*(2), 102-111.

Kovács, G., and Spens, K. M. (2007). Humanitarian logistics in disaster relief operations. *International Journal of Physical Distribution and Logistics Management*, *37*(2), 99-114. DOI: 10.1108/09600030710734820

Li, Z., Liu, X., and Song, Y. (2014). Location-Assignment Model and Algorithm for the Transshipment Container Terminal of Maritime Emergency Materials. In *ICLEM 2014: System Planning, Supply Chain Management, and Safety* (pp. 414-419).

Lopez-Arana, S., Avendaño, M., van Lenthe, F. J., and Burdorf, A. (2016). The impact of a conditional cash transfer programme on consumption in Colombia. *Public Health Nutrition*, *19*(14), 2629-2642. DOI: 10.1017/S1368980016000240

Marianov, V., and Serra, D. (2001). Hierarchical location-allocation models for congested systems. *European Journal of Operational Research*, *135*(1), 195-208. DOI: 10.1016/S0377-2217(00)00314-3

Noori, N. S., and Weber, C. (2016). Dynamics of coordination-clusters in long-term rehabilitation. *Journal of Humanitarian Logistics and Supply Chain Management*, *6*(3), 296-328. DOI: 10.1108/JHLSCM-06-2016-0024

Oleshchenko, L., Bilohub, D., and Yurchyshyn, V. (2019). Internet data analysis for evaluation of optimal location of new facilities. In *XVIII International Conference on Data Science and Intelligent Analysis of Information* (pp. 279-291). Springer, Cham. DOI: 10.1007/978-3-319-97885-7_28

Owen, S. H., and Daskin, M. S. (1998). Strategic facility location: A review. *European Journal of Operational Research*, *111*, 423-447. DOI: 10.1016/S0377-2217(98)00186-6

Paes-Sousa, R., and Vaitsman, J. (2014). Fome zero e brasil sem miséria: Um passo adiante na polítca brasileira de proteção social. *Ciencia e Saude Coletiva*, *19*(11), 4351-4360. DOI: 10.1590/1413-812320141911.08812014

Paul, J., and Wang, X. (2015). Robust optimization for United States Department of Agriculture food aid bid allocations. *Transportation Research Part E: Logistics and Transportation Review*, *82*, 129-146. DOI: 10.1016/j.tre.2015.08.001

Rancourt, M. É., Cordeau, J. F., Laporte, G., and Watkins, B. (2015). Tactical network planning for food aid distribution in Kenya. *Computers and Operations Research*, *56*, 68-83. 10.1016/j.cor.2014.10.018

Rivera, N., and Restrepo, V. (2015). *Diseño de un sistema logístico de acopio y distribución de un producto alimenticio perecedero no refrigerado para el área de influencia del Valle del Cauca* (Universidad Autónoma de Occidente). Retrieved from https://red.uao.edu.co/bitstream/10614/8288/1/T06241.pdf

Rueda-Velasco, F. J., Monsalve-Salamanca, A., and Adarme-Jaimes, W. (2019). Methodology for the Design of Traceability System in Food Assistance Supply Chains. In J. Gonzalez-Feliu, M. Chong, J. Vargas Florez, and J. Padilla Solis (Eds.), *Handbook of Research on Urban and Humanitarian Logistics* (pp. 179-200). DOI: 10.4018/978-1-5225-8160-4.ch009

Sabarish, B. A., Kailassh, B., Baktha, K., and Janaki, Y. (2018). Recommendations of location for facilities using domination set theory. *Proceedings of the 2017 IEEE International Conference on Communication and Signal Processing* (ICCSP), 1540-1544. DOI: 10.1109/ICCSP.2017.8286646

Şahin, G., Sural, H., and Meral, S. (2007). Locational analysis for regionalization of Turkish Red Crescent blood services. *Computers and Operations Research*, *34*(3), 692-704. DOI: 10.1016/j.cor.2005.03.020

Singh, A. (2016). Supplier Selection and Multi-period Demand Allocation in a Humanitarian Supply Chain. In *Managing Humanitarian Logistics* (pp. 189-207). Springer, New Delhi. DOI: 10.1007/978-81-322-2416-7

Smadi, H., Al Theeb, N., and Bawa'neh, H. (2018). Logistics system for drinking water distribution in post disaster humanitarian relief, Al-Za'atari camp. *Journal of Humanitarian Logistics and Supply Chain Management*, *8*(4), 477-496. DOI: 10.1108/JHLSCM-12-2017-0072

Talamantes, C. (2016). *Análisis de los procesos de acopio, producción y distribución de leche Liconsa en México*. Ciudad Juárez, Chihuahua, México.

Trivedi, A., and Singh, A. (2018). Facility location in humanitarian relief: A review. *International Journal of Emergency Management*, *14*(3), 213-232.

Ukkusuri, S. V, and Yushimito, W. F. (2005). Location Routing Approach for the Humanitarian Prepositioning Problem. *Transportation research record*, *2089*(1), 18-25. DOI: 10.3141/2089-03

UNICEF, F. de las N. U. para la I. (2006). *Análisis de Situación de los Alimentos Complementarios Fortificados Para la Niñez entre 6 y 36 Meses de Edad En La Región de América Latina y El Caribe*. UNICEF.

Ingeniería e Investigación vol. 39 No. 3, December - 2019 (62-69)

DOI: http://dx.doi.org/10.15446/ing.investig.v39n3.81426

It is not enough to flip your classroom. A case study in the course of Pavements in Civil Engineering

No basta con invertir tu aula. Un caso de estudio en el curso de Pavimentos de Ingeniería Civil

Yasmany García-Ramírez

ABSTRACT

The flipped classroom, as an active learning model, has given remarkable results in several areas of university teaching; however, its execution can still be improved. This research shows the implementation and improvement of the flipped classroom model in the Pavements course. It evaluates their influence on the students' final grades and on their learning experience. Three groups of students participated in this study, who enrolled in the course of Pavements of the Civil Engineering program. Group A took the course with the traditional model, while Group B took it with a flipped classroom, and Group C experienced it with a reinforced flipped model. Groups took the course in 2017, 2018 and 2019, respectively. Results show that despite using the flipped classroom models, the finals grades did not increase compared to those of the traditional model; however, they improved their learning experience. The students were more satisfied with the method; they even asked for fewer modifications than they did in the traditional model. This research shows that adding little academic tasks to the course would greatly influence the students' opinion.

Keywords: Pavements course, University teaching, Flipped classroom model, Civil Engineering.

RESUMEN

El aula invertida, como un modelo de aprendizaje activo, ha dado resultados notables en diversas áreas de la enseñanza universitaria; sin embargo, su aplicación aún se puede mejorar. Esta investigación muestra la ejecución y mejora del modelo de aula invertida en un curso de Pavimentos. Se evalúa su influencia sobre las calificaciones finales de los estudiantes y sobre su experiencia de aprendizaje. Tres grupos de estudiantes participaron en este estudio, quienes se inscribieron el curso de Pavimentos del programa de Ingeniería Civil. El Grupo A tomó el curso con el modelo tradicional, mientras que el Grupo B lo tomó con el modelo de aula invertida, y el Grupo C lo experimentó con un modelo mejorado de aula invertida. Los grupos tomaron el curso en el 2017, 2018 y 2019, respectivamente. Los resultados muestran que, a pesar del uso de los modelos de aula invertidos, las calificaciones finales no aumentaron en comparación con los puntajes del modelo tradicional; sin embargo, sí mejoró su experiencia de aprendizaje. Los estudiantes estaban más satisfechos con el método, e incluso pidieron menos modificaciones que en el modelo tradicional. Esta investigación muestra que agregar pequeñas acciones académicas en el curso, influiría enormemente en la opinión de los estudiantes.

Palabras clave: Curso de pavimentos, Educación universitaria, Modelo de clase invertida, Ingeniería Civil.

Received: August 1st, 2019
Accepted: October 22nd, 2019

Introduction

For decades, educators have questioned teaching methods entirely based on lectures (Barr and Tagg, 1995). In long lectures, students can get distracted and lose some key concepts or ideas in the topic they are learning. In addition, students only retain some knowledge with this method, and sometimes they do not understand it. Learners are passively absorbing the knowledge organized by the teacher, who does most of the work (Le and Do, 2019). Moreover, nowadays, students have started to be less tolerant of lecture-style presentations (Roehl et al., 2013) and, due to technological advances, students prefer innovative methods than traditional ones (Subramanian and Kelly, 2019). Based on these limitations of this method, new learning approaches have emerged.

Active learning is one of those new concepts that engage the students in their own learning process (Prince, 2004). Students have a more active role, since most of their results depend on them. Instructors are no longer the main actor; they become a guide, who plan, elaborate, and control the activities that students must perform. With these activities, students think about what they are doing, and this promotes the constructive process of knowledge (Bergmann and Sams, 2012; Bonwell, C., and Eison, 1991). Due to its remarkable results, several models have adopted this active learning.

Civil Engineer, Universidad Técnica Particular de Loja, Ecuador. Ph.D. in Civil Engineer, Universidad Nacional de San Juan, Argentina. Affiliation: Assistant Professsor, Universidad Técnica Particular de Loja, Ecuador.
E-mail: ydgarcia1@utpl.edu.ec

How to cite: García-Ramírez, Y. (2019). It is not enough to flip your classroom. A case study in the course of Pavements in Civil Engineering. *Ingeniería e Investigación*, *39*(3). DOI: 10.15446/ing.investig.v39n3.81426

The flipped classroom is one of those models. Its name was given because students have to explore the topic before attending the face-to-face class. They should study from video lectures, screencasts or vodcasts, thus learning concepts out of the classroom (Milman, 2012). In class, there is more time for other engaging activities, such as problem-solving sessions, case studies, collaborative work, observing real situations, discussions, experiments, projects, among others. These academic activities increase their knowledge retention (Blair, 2012; Tucker, 2012). Besides, learning skills are developed when discovering by themselves what they do not know (Le and Do, 2019). Given its promising results, its use is extended to all the educational levels, especially at university level, except in the course of Pavements of the Civil Engineering program.

In this context, this study shows the implementation and improvement of the flipped classroom model in the course of Pavements. It evaluates how the model influences on both the students' final grades and on their learning experience. For this purpose, students who enrolled in the course of Pavements participated in this study. The study considered three groups: group A had the traditional model based on lectures, group B the flipped classroom model, and group C a reinforced flipped classroom model.

To show these results, the rest of this paper is structured as follows. Section 2 shows the literature review about the flipped classroom used in universities, especially in Engineering. Then, Section 3 gives an overview of the experimental development, describing the sample size, model learning description, grading description, course content, data collection, and data processing. Section 4 shows the results considering the students' final course grades and their survey answers. The final part highlights the main conclusions.

Literature review

The flipped model is feasible in universities, since students are used to modern technology (Sohrabi and Iraj, 2016; Subramanian and Kelly, 2019). They also have internet access on most university campuses and homes (Bergmann and Sams, 2012). It allows them to view the web-based instruction at their own pace. They can also watch the digital content as many times as they require. The model favors students who need more time to assimilate knowledge or have attention problems. Another element that promotes the employment of the model is that educators are interested in maximizing their students learning through innovative practices (Hao and Lee, 2016). Based on these elements, the flipped classroom model was used in several areas of knowledge such as Social Sciences, Technology, Engineering, etc.

In Engineering, the teaching-learning approach is represented by technical criteria, within a strong background in Mathematics and Physics (Halbe et al., 2015). Despite this particular background, the flipped model was employed in several Engineering courses with positive results. For example, in Fluid Mechanics, students increased their score in 7,5 points compared with the traditional model group (Webster et al., 2014). In the course of Mechanics of Materials, students in the flipped model performed better than the students in the traditional method (Lee et al., 2015). In an online course of Dynamics, the flipped model improved their learning experience and their problem-solving skills (Fredericks et al., 2013). In Classical Mechanical, most students preferred the flipped classroom model to the traditional one (Bates and Galloway, 2012).

In Civil Engineering, several experiences were conducted employing the flipped classroom model. For example, in the course of Water Resources, students were more involved, and improved their understanding of concepts and problem-solving skills (Li and Daher, 2017). In the course of Statics, learners improved their final grades, became more independent, and they were actively engaged with their learning (García-Ramírez, 2018). Students in the course of Mechanical Engineering, Computing, and Construction Materials admitted that the method had a positive impact on their learning (Gardner et al., 2014). In the course of Transport Engineering, students were satisfied with the flipped model, because they had the opportunity to work at their own pace, interact with their instructor individually, and work collaboratively with their classmates (Karabulut-Ilgu et al., 2016). Despite these positive experiences, in Civil Engineering it has not been employed in the Pavements design field, except for one preliminary study conducted by the author (García-Ramírez, 2019).

Notwithstanding the positive results in Engineering and Civil Engineering, some elements must be considered when applying the flipped classroom model. First, teachers should create quality videos with clear instructions. Second, students cannot ask questions to the teacher during the video (Milman, 2012). Third, students can be distracted by browsing other websites (Roehl et al., 2013). Fourth, in-class and out-class activities must be relevant to the student. Fifth, learners must have devices where they can watch videos. Finally, students should have access to the Internet. The first four elements offer some opportunities to improve the execution of the flipped classroom model.

Experimental development

Sample Size

Three groups participated in this study to answer both research questions. Group A took the course with the traditional model, while Group B took it with a flipped classroom, and Group C experienced it with a reinforced flipped model. Group A had 38 students, Group B had 57 students, and Group C had 70 students. They enrolled in the course in the academic periods of April-August 2017, April-August 2018, and April-August 2019, respectively. All groups were in the fourth year (out of 5) of the Civil Engineering program at the Universidad Técnica Particular de Loja (UTPL). In this course, students learnt how to perform the pavement structural design for highways and airports. The teacher was the same in all groups. Before this course, students had to

approve the courses: Highway Geometric Design, Materials, Soils and Rocks, and Physics.

Learning models descriptions

The learning models used for the three groups are shown in Table 1. In the traditional model, students had to study some material shared through the Virtual Learning Environment (VLE) or in books. Then, they attended the face-to-face class, where they sometimes had to solve reading controls at the beginning of the session. Later, they received a lecture about the week topic. Finally, they participated in a problem-solving session individually o in teams, using a solved example from books. The teacher showed some essential parts to solve it and in the end, the answer to the problem. The teacher helped if they had questions to ask. After in-class activities, students had to solve other problems as homework. They could attend a weekly tutoring session if they had questions when solving or trying to solve the homework.

In the flipped model, students have to watch a pre-recorded lecture (in a video) before attending the class. The videos were uploaded on the Youtube platform and shared through the VLE. To check if they watched them, learners had to solve reading controls at the beginning of the class. Then, the instructor answered questions about the weekly topic and explained their main concept. Afterward, students participated in a problem-solving session individually o in teams, using a solved example made by the teacher, who also showed some essential parts to solve it and in the end, the answer to the problem. The teacher helped them if they had questions about it. They also had to solve another problem as homework. A weekly tutoring session was available if students had questions about the problem and /or the weekly topic.

Table 1. Structure of the Pavements course for all groups in this study

Group	Before class	Face to face class	After class
A	Study some material	Solve reading controls Receive a lecture Problem-solving session	Solve problems as homework Go tutoring
B	Watch a pre-recorded lecture on YouTube	The instructor solve questions about the topic Problem-solving session	Solve problems as homework Go tutoring
C	Watch a pre-recorded lecture on Edpuzzle	Solve reading controls The instructor solve questions about the topic or the field visit Problem-solving session	Solve problems as homework Go field visits to some building project Go tutoring

Source: Authors

In the reinforced flipped classroom model, students had to do the same as in the flipped model, but includingfield visits to a building project related to the course contents. These visits are conducted by the students on their own and without the presence of the teacher. After the visit, they had to make a report about the activities in the construction work. For every activity, photos were mandatory. These photos should include the student, as well as the date and time, to avoid sharing between them or reusing the same photos in their next reports. In this model, the teacher was more involved in their learning, giving feedback in every academic activity, and explaining its aim. So, students knew their mistakes and understood the reason for each activity. Considering that students in group B could skip watching the videos on Youtube, in this case the videos were uploaded on the Edpuzzle platform. In this platform, after students created their users, they had to watch the previously scheduled pre-recorded lecture (start and due date). In this platform, some questions could be added during the video (multiple selections, true/false and short answer) and could set an option to prevent skipping, so students had to watch the whole video. The face-to-face class started with the control reading, and students asked about the field visits or the weekly topic.

Grading description

All three groups had the same grading procedure and grading factors. Reading controls had a weight factor of 20% of the final score grade. The in-class problem-solving session was 15% of the final score, as well as for solving problems as homework. This homework could include up to two more problems related to the week class. The remaining 50% were the midterm exams. Students could get a maximum score of 100 points, and they should have a minimum of 70 points to approve the course.

Course content

The course was 16 weeks long. All three groups had the same course content, as shown in Table 2. This table also included the duration of the pre-recorded lectures. In some weeks, they had no video to watch, because it was the beginning or end of the course, or the midterm exams. Pre-recorded lectures were short according to the literature suggestions (Bonwell, C., and Eison, 1991; Enfield, 2013; García-Ramírez, 2018; Sohrabi and Iraj, 2016). Videos were made using digital slide presentations with voiceovers in Microsoft PowerPoint software.

Data collection

Data collection was performed using two instruments: final score grades and a blind survey at the end of every course. The teacher calculated the student's final scores according to the grading plan. The average grade was estimated in every group, in order to compare it with other groups. A frequency distribution was also made with the individual final score grades to compare the differences between groups. The survey was optional, so 58 students answered it in group A, 55 in group B, and 66 in group C. The questionnaire was composed mostly of several closed-ended questions and a few open questions. Questions were about the course and the applied method.

Table 2. Pavements course structure for all groups in this study

Week	Topic	Duration mm:ss
1	Introduction to Pavements	-
2	Traffic study	32:01
3	Soil study for the design of Pavements	26:10
4	Soil stabilization	29:08
5	Flexible pavement structural design for highways – Asphalt Institute method	21:47
6	AASHTO flexible pavement structural design for highways	26:23
7	SHELL flexible pavement structural design for highways	19:47
8	Midterm exam	-
9	PCA rigid pavement structural design for highways	37:04
10	AASHTO rigid pavement structural design for highways	18:00
11	Articulated pavement structural design for highways method	43:13
12	FAA flexible pavement structural design for airports	24:19
13	PCA and FAA rigid pavement structural design for airports	16:08
14	Failures in Pavements	39:36
15	Maintenance and Rehabilitation - Pavement	-
16	Final exam	-
- There was no pre-recorded lecture to watch.		

Source: Authors

Survey data processing

The survey had three types of questions: numeric (rates), closed-ended, and open. It calculated the average rate from all answers of the numeric questions. In closed-ended questions, it estimated the percentage where students agreed (strongly agree and agree). This information provided an overview of the opinion of the students, since the other results (neither agree nor disagree, disagree, strongly disagree) are their correlative. Finally, in open questions, similar answers were clustered in several categories. When a response had no match with others, it was classified and grouped in the category "Others".

Results

Final course grades

The final average score grades were: 72,82 (group A), 69,68 (group B), and 71,58 (group C). In order to find a statistically significant difference between those values, an analysis of variance (ANOVA) was performed using the statistical software Minitab 14.2 (2005). A 95% level of confidence was used as a parameter of this analysis. Scores from group A did not differ significantly from group B (p-value = 0,066), which means that traditional model had similar scores to the flipped model. Scores from group A also did not differ from scores from group C (p-value = 0,380), which means the flipped method did not increase the grades significantly when compared to the traditional one.

The individual final scores were drawn in a histogram to analyze their distribution in all study groups (Figure 1). Group A had 68% of students with equal or more than 70%, while group B had 49%, and group C had 51%. Most students had between 70 and 79 points in all groups. Students (2%) with the highest score belong to group B. In the range of 80-89 points, there were 13%, 4%, and 30% of students, from group A, B, and C, respectively. Group A had 19% of learners that obtained between 60 and 69 points, that is, close to passing the course. However, it is interesting that the flipped models had more percentage in this range, 33% (group B) and 30% (group C). Even though, more students approved the course under the traditional model, the flipped models had more distributed scores. In addition, they had some interesting trends and behaviors in some ranges that traditional models did not have.

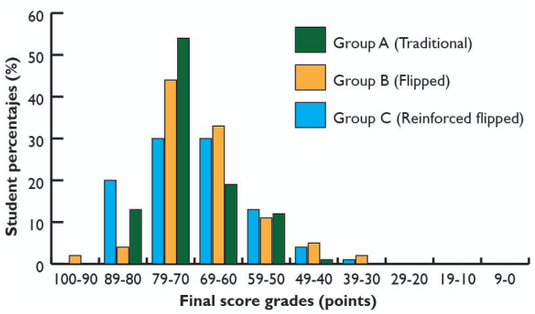

Figure 1. Final score grades and student percentages for all research groups.
Source: Authors

In order to see if groups were academically homogeneous, the difference between the grades was analyzed in the first part of the semester (up to the midterm exam) and compared to the second one (up to the final exam). Most students in group A (76,47%) got the same or a higher grade in the second midterm than in the first one. Students from group B performed a little lower (63,16%), and group C was the lowest (21,74%). These differences could mean that students in group A are better students, in terms of grades, than those in other groups. This could also mean that learners in group A were more motivated than other students in group B and C. These assumptions should be analyzed in future research.

Survey answers

The survey had several parts: rating, selecting options, and responding to open questions. In the rating section, students were asked to rate the course and their self-learning throughout the course. Table 3 shows their average rating values for both questions. The traditional model got a higher average rate than the flipped classroom, and this one got a smaller value compared to the reinforced flipped classroom model. ANOVA analysis was conducted to see if there was a statistical difference between groups of answers. The average rate between group A-B and A-C did not differ statistically (p-value = 0,318 and p-value = 0,126, respectively). However, the average rate between group B-C differs (p-value =0,003),

which suggests that the students' opinion about the method is more positive in the reinforced flipped classroom than in the simple flipped model.

Table 3. Average ratings provided by students in the traditional and flipped model

N° of question	Average rating provided by students (1 = lowest value and 10 = highest value)		
	Group A	Group B	Group C
1	8,86	8,60	9,20
2	7,62	8,25	8,03

1 How many points would you give to the Pavements course?

2 How much self-learning did you do in the Pavements course?

Source: Authors

As expected, concerning self-learning, both flipped classroom models got higher average rates than the traditional one. In addition, an ANOVA analysis was performed with those answers. An average rate differs statistically between groups A-B (p-value = 0,037), but not in groups B-C (p-value = 0,367). This implies that in the flipped models, students are more aware of their self-learning than in the traditional one and, consequently, they consider that they work more than the students of group A.

Students also responded about the methods executed with closed-ended questions. These items had a five-point Likert scale: strongly agree, agree, neither agree nor disagree, disagree, strongly disagree. Table 4 included the percentages of the agreement answers (agree and strongly agree).

Table 4. Survey with five-point Likert scale answers in the traditional and flipped model

N° of question	Percentages of students that agreed (strongly agree and agree)		
	Group A	Group B	Group C
3	98,28	98,18	100,00
4	93,10	90,91	95,45
5	93,10	90,91	96,97
6	87,93	87,27	90,91
7	96,55	96,36	100,00
8	87,93	72,73	95,45
9	79,31	69,09	90,91
10	82,76	72,73	87,88
11	-	-	93,94
12	-	-	86,36

3 The topics of the subject were interesting.
4 In class, the number of problems performed was enough.
5 The problem-solving carried out in class was representative of each topic.
6 The other activities carried out in class (tests, teamwork) were enough.
7 The teacher mastered the topics of the course.
8 The grading of works, lessons, and exams was fair.
9 The learning method was well implemented by the instructor.
10 This methodcan be employed in other courses of Civil Engineering.
11 The field visits helped your learning.
12 The flipped classroom model is better than the traditional one.
- This question was not asked to this group.

Source: Authors

In general terms, topics were interesting for all groups. Most students estimated that in-class and out-class academic activities were good enough and in accordance with their expectations for all three groups. Additionally, most of them thought that the teacher mastered the topics of the subject. Grading had a lower score in the flipped model than in the others, which means that learners were unsatisfied with the grading scores. Interestingly, the reinforced flipped model got the highest score when students answered about the implementation of the method. However, the flipped model had the lowest score, which means that the students evaluate other aspects, independently of the learning method.

The reinforced flipped group has the highest percentage between groups in all of these questions. Besides, when they perceived that the method was well implemented, they suggested that it should be used in other courses of Civil Engineering. Most students under the reinforced flipped model admitted that the visit fields helped in their learning and complemented the other academic activities. Most of them also considered that the reinforced flipped model was better than the traditional one.

Regarding the few open questions that students answered, one question focused on what changes they suggest for the next course of Pavements. Table 5 shows their answers to those questions after processing them. It is remarkable that they suggested fewer modifications in the flipped models than in the traditional one. This means that in the flipped models, students are more satisfied than in the traditional one.

Table 5. Percentage of the students' answers that suggested changes in the course in the traditional and flipped models

N° of question	Percentage of students that suggest changes in the next course of Pavement		
	Group A	Group B	Group C
A	37,93	65,45	84,62
B	15,52	1,82	-
C	18,97	10,91	4,62
D	8,62	-	1,54
E	18,97	21,82	9,23

A: No modifications, B: complements with field visits to the pavement works in the highways around, C: the teacher should solve and explain the problems first, before students solve their problem example, D: teach asphalt mixtures theory or the course should have laboratory practices, and E: others.
- No student suggested this item.

Source: Authors

Some students from the traditional model and few from the flipped model suggested that field visits should be executed to learn more. For that reason, in the reinforced flipped model, field visits were implemented. In the traditional model, some students required that, at the beginning of the class, the teacher should solve and explain a problem, before students solve their problem example. Therefote, in group B, instead of solving the homework problem, the teacher solved a different problem as guiding document, with similar input parameters to their problem example. However, in group B, few students made the same request again. So,

in group C, in addition to the guiding document, feedback was implemented, and very few students complained about it. The teacher did not want to show them how to solve the problem because he/she considered that students could learn more and more permanently if they solved it on their own. Furthermore, some students in group A and C asked for asphalt mixtures theory or including laboratory practices as part of the course teaching plan. Maybe, they made this requirement because previous teachers included those topics. Finally, some students had other requests that ended up in the "other" category.

Students in the flipped classroom models also answered if the videos helped them in their learning process. Most students (98,18%) in group B and group C (98,48%) said that pre-recorded lectures helped them in the course. These answers were clustered in 6 categories, as shown in Table 6.

Two additional open questions were asked in group C in relation to the feedback process and field visits. Most students (83,82%) recognized that they agreed with the feedback given by the teacher. Some of them (10,29%) considered that feedback should include more detailed observations or include videos, documents, or the solved problem. A few students (5,88%) asked for clearer feedback. Concerning the field visits, most students (39,17%) agreed with the frequency and report that they should be done. Other students (16,18%) considered that the teacher should be with them and solve their doubts in-situ. Some students (11,76%) answered that field visits should be arranged in more significant building works. Few students (8,82%) demanded that selfies should not be included in the reports, and others (16,18%) had minor requests that were not categorized.

Table 6. Percentage of the students' answers about the pre-recorded lectures in the flipped models

N° of cluster	Percentage of student that answered about the pre-recorded lectures		
	Group A	Group B	Group C
F	-	20,37	16,42
G	-	9,26	17,91
H	-	18,52	31,34
I	-	38,89	11,94
J	-	3,7	2,99
K	-	9,26	19,40

F: they helped to understand additional information and clear doubts, G: they can be rewatched or paused, H: they helped to know in advance the topic of the next class, I: with them, it is easier to understand than in books, J: they helped learning additional concepts that are used in real life, and K: others.
- This question was not asked in this group.

Source: Authors

Conclusions

This article aimed to show the implementation and improvement of the flipped classroom model in the course of Pavements. It evaluates their influence on the students' final grades and on their learning experience. After analyzing the results, the following conclusions were obtained:

The flipped classroom did not increase the student's final grades compared with the traditional model. Other studies reported improvements in grades with this method. For example, in the Statics course students got 6,5 points more than with the traditional model (García-Ramírez, 2018), or in the Fluid Mechanics course, learners got 7,25 points more than with the traditional model (Webster et al., 2014).

Despite of the unaffected final scores, the student's opinion about the flipped classroom model was positive. This was also observed by previous researchers (Gardner et al., 2014; Karabulut-Ilgu et al., 2016; Li and Daher, 2017). Even though the flipped models obtained lower values in the survey with a five-point Likert scale compared with the traditional approach, most students in the flipped classrooms did not want to change academic issues in the executed method, which means they were satisfied with the model. This was also found in other studies (Bates and Galloway, 2012; Gardner et al., 2014). Their answers in the open questions show wider support to this aspect.

Students have a favorable opinion about the flipped classroom model. First, the model promoted their self-learning, more than the traditional model. This was also found in a previous work by García-Ramírez (2018). Self-learning is a competence that is valuable in the labor market. Besides, the pre-recorded lectures helped their learning process. It must be considered that students learn differently and having online available videos is very helpful for them. This method showed better results than the traditional one in terms of academic experience and not in terms of increasing grades.

The contribution of the paper is basically methodological. First, previous studies only compared two groups (traditional and flipped), while this one compared three, from which the last group made improvements (in the learning methodology and academic activities performed) based on the student requests from the previous groups. Second, academic activities such as field visits (for placing the students in real situations) and timely feedback have not been performed in previous literature related to the flipped model in Engineering. Third, the study employed pedagogical approaches to prevent skipping academic tasks (questions in videos on Edpuzzle or selfies in field visits). Fourth, the methodology used in this study (data collection, processing, and interpretation) can be employed in other course of Civil Engineering. Finally, this research shows that the flipped classroom model is not only about eliminating the lecture method; but it is a process of continuous improvement and commitment between instructors and students.

This study has several limitations. First, groups were not homogenous, since they got different grades in the second part of the semester. Besides, the study was also conducted in one university with a small sample size. Furthermore, it involves just one course that belongs to the Civil Engineering program. In other course from the same area or from other careers, this could have different results.

Despite these limitations, this study extends the understanding of the implications of the flipped classroom model. It showed that the flipped method significantly

improves the learning experience compared to the traditional one. It also showed that the flipped model is accepted positively by students. In addition, the model promoted self-learning and helped students learn at their own pace. Besides, this study had better results on educational activities than on the grading. Finally, it showed that it is not enough to flip the classroom, since teachers have to be more involved in the learning students.

Acknowledgements

The author acknowledges the support of the National Secretariat of Higher Education, Science, Technology and Innovation (SENESCYT) and the Universidad Técnica Particular de Loja from the Republic of Ecuador.

References

Barr, R. B., and Tagg, J. (1995). From Teaching to Learning: A New Paradigm for Undergraduate Education. *Change*, *27*(6), 12-25. DOI: 10.1080/00091383.1995.10544672

Bates, S., and Galloway, R. (2012). The inverted classroom in a large enrolment introductory physics course: a case study. Paper presented at the Higher Education Academy STEM Conference, Imperial College London, United Kingdom. Retrieved from: https://www2.ph.ed.ac.uk/~rgallowa/Bates_Galloway.pdf

Bergmann, J., and Sams, A. (2012). *Flip Your Classroom Reach Every Student in Every Class Every Day*. International Society for Technology in Education.

Blair, N. (January/February, 2012). Technology integration for the new 21st century learner. *Principal*, 8-13. Retrieved from: https://www.naesp.org/sites/default/files/Blair_JF12.pdf

Bonwell, C., and Eison, J. A. (1991). Active learning: Creating excitement in the classroom [ASHE-ERIC Higher Education Report N° 1]. Washington D.C.: The George Washington University. Retrieved from: https://files.eric.ed.gov/fulltext/ED336049.pdf

Enfield, J. (2013). Looking at the Impact of the Flipped Classroom Model of Instruction on Undergraduate Multimedia Students at CSUN. *TechTrends*, *57*(6), 14-27. DOI: 10.1007/s11528-013-0698-1

Fredericks, C., Rayyan, S., Teodorescu, R., Balint, T., Seaton, D., and Pritchard, D. E. (June, 2013). From flipped to open instruction: The mechanics online course. Paper presented at the Sixth Conference of MIT's Learning International Network Consortium, MIT, Cambridge, Massachusetts, USA. Retrieved from: https://linc.mit.edu/linc2013/proceedings/Session5/Session5Fredericks.pdf

García-Ramírez, Y. (2018). Uso del modelo de clase invertida en la materia de Estática en Ingeniería Civil. *Ventana Informática*, *38*, 65-82. DOI: 10.30554/ventanainform.38.2860.2018

García-Ramírez, Y. (2019). Pavements Course: Is the Flipped Classroom Model Effective in All Cases? A Case Study in a Developing Country. In A. Bozzon, F. Domínguez-Mayo and J. Filipe (Eds.) *Proceedings of the 15th International Conference on Web Information Systems and Technologies*. Scitepress Digital Library, 509-516. DOI: 10.5220/0008397705090516

Gardner, A., Willey, K., Vessalas, K., and Li, J. (2014). Experiences with flipped learning in subjects in consecutive stages of a Civil Engineering programme. *Proceedings of the 25th Annual Conference of the Australasian Association for Engineering Education*, Massey University, Wellington, New Zealand. Retrieved from: http://hdl.handle.net/10453/31875

Halbe, J., Adamowski, J., and Pahl-Wostl, C. (2015). The role of paradigms in engineering practice and education for sustainable development. Journal of Cleaner Production, 106, 272-282. DOI: 10.1016/J.JCLEPRO.2015.01.093

Hao, Y., and Lee, K. S. (2016). Teaching in flipped classrooms: xploring pre-service teachers' concerns. *Computers in Human Behavior, 57*, 250-260. DOI: 10.1016/j.chb.2015.12.022

Karabulut-Ilgu, A., Yao, S., Tarmo, P., and Jahren, C. (June, 2016). A Flipped Classroom Approach to Teaching Transportation Engineering. Paper presented at the ASEE Annual Conference and Exposition. New Orleans, LA. Retrieved from: https://www.asee.org/public/conferences/64/papers/16034/view

Le, T. Q., and Do, T. T. A. (2019). Active Teaching Techniques for Engineering Students to Ensure The Learning Outcomes of Training Programs by CDIO Approach. *International Journal on Advanced Science, Engineering and Information Technology, 9*(1), 266-273. DOI: 10.18517/ijaseit.9.1.7959

Lee, S. L., Hackett, and Estrada, H. (2015). Evaluation of a Flipped Classroom in Mechanics of Materials. Paper presented at the ASEE Annual Conference and Exposition. Seattle, WA. Retrieved from: https://www.asee.org/public/conferences/56/papers/11392/view

Li, Y., and Daher, T. (2017). Integrating Innovative Classroom Activities with Flipped Teaching in a Water Resources Engineering Class. *Journal of Professional Issues in Engineering Education and Practice*, *143*(1), 05016008. DOI: 10.1061/(ASCE)EI.1943-5541.0000297

Milman, N. B. (2012). The Flipped Classroom Strategy: What is it and how can it be used? *Distance Learning, 11*(4), 9-11. Retrieved from: https://search.proquest.com/openview/616e91b3df376d82fd5d30c598c665f3/1?pq-origsite=gscholar%26cbl=29704

Minitab, LLC. (2005). Minitab Statistical Software (14.2) [Computer program]. Retrieved from: fromwww.minitab.com

Prince, M. (July, 2004). Does active learning work? A review of the research. *Journal of Engineering Education*, *93*, 223-232. DOI: 10.1002/j.2168-9830.2004.tb00809.x

Roehl, A., Reddy, S. L., and Shannon, G. J. (2013). The flipped classroom: An opportunity to engage millennial students

through active learning strategies. *Journal of Family & Consumer Sciences, 105*(2), 44-49. Retrieved from: https://pdfs.semanticscholar.org/daa3/b94cdc7b52b3381a7c7e21022a7a8c005f84.pdf

Sohrabi, B., and Iraj, H. (2016). Implementing flipped classroom using digital media: A comparison of two demographically different groups perceptions. *Computers in Human Behavior, 60*, 514-524. DOI: 10.1016/j.chb.2016.02.056

Subramanian, D. V., and Kelly, P. (2019). Effects of introducing innovative teaching methods in engineering classes: A case study on classes in an Indian university. *Computer Applications in Engineering Education*, *27*(1), 183-193. DOI: 10.1002/cae.22067

Tucker, B. (Winter, 2012). The Flipped Classroom: Online instruction at home frees class time for learning. *Education Next, 12*(1). Retrieved from: https://www.educationnext.org/files/ednext_20121_BTucker.pdf

Webster, D. R., Majerich, D. M., and Luo, J. (November, 2014). "Flippin' Fluid Mechanics - Quasi-experimental Pre-test and Post-test Comparison Using Two Groups". Paper presented at the 67th Annual Meeting of the APS Division of Fluid Dynamics, San Francisco, CA. Abstract retrieved from: https://ui.adsabs.harvard.edu/abs/2014APS..DFDM33005W/abstract

Suscripción a la Revista *I&I*

Instrucciones de Suscripción:

1. Consignar **$54 000 COP**, valor correspondiente a **1 año** y **tres ejemplares** de la revista en la cuenta **No. 01272007- 4** (No. Concepto **20181015**) a nombre del Fondo Especial de la Facultad de Ingeniería — Suscripción Revista, en cualquier oficina del **Banco Popular** .
2. Enviar una copia del recibo de consignación junto con los siguientes datos:

   Suscripción a nombre de:

   Email:

   Dirección de envío (País, ciudad,...):

   Teléfono celular:

   Fecha: dd/mm/yyy

INGENIERÍA E INVESTIGACIÓN

"*Tecnología e innovación con tradición y excelencia*"

ISSN: 0120-5609 (print)
ISSN: 2248-8723 (online)
E-mail: revii_bog@unal.edu.co
Página web: http://revistas.unal.edu.co/index.php/ingeinv

UNIVERSIDAD NACIONAL DE COLOMBIA

Suscripción a la Revista *I&I*

Instrucciones de Suscripción:

1. Consignar **$54 000 COP**, valor correspondiente a **1 año** y **tres ejemplares** de la revista en la cuenta **No. 01272007- 4** (No. Concepto **20181015**) a nombre del Fondo Especial de la Facultad de Ingeniería — Suscripción Revista, en cualquier oficina del **Banco Popular** .
2. Enviar una copia del recibo de consignación junto con los siguientes datos:

   Suscripción a nombre de:

   Email:

   Dirección de envío (País, ciudad,...):

   Teléfono celular:

   Fecha: dd/mm/yyy

INGENIERÍA E INVESTIGACIÓN

"*Tecnología e innovación con tradición y excelencia*"

ISSN: 0120-5609 (print)
ISSN: 2248-8723 (online)
E-mail: revii_bog@unal.edu.co
Página web: http://revistas.unal.edu.co/index.php/ingeinv

UNIVERSIDAD NACIONAL DE COLOMBIA

Instructions for Authors

Editorial Committee reserves the copyright to printing any material and its total or partial reproduction, as well as the right to accept submitted material or reject it. It also reserves the right to make any editorial modification which it thinks fit. In such event, the author of the submitted material in question will receive the evaluators' recommendations for changes to be made in writing. If an author accepts them, the revised (or rewritten) article must be submitted with the suggested changes having been made by the date fixed by the journal to guarantee its publication in the programmed issue.

The process to be followed for publishing an article in the journal

The article must be uploaded into the journal's OJS website, see the guidelines for article submission in the Authors guide section in our website http://www.revistas.unal.edu.co/index.php/ingeinv/article/view/59291/56815. Any manuscript must be sent using journal's template (6 pages length max.) and must be accompanied by the license agreement, addressed to the journal's editor, Prof. Andrés Pavas, stating that all authors involved in the work in question agree to it being submitted for consideration in the *Ingeniería e Investigación journal*.

Article and License templates are available on:
http://www.revistas.unal.edu.co/index.php/ingeinv/index

Once an article has been received by the journal, the corresponding author will be notified by e-mail and the peer-review process will be begun. Following this evaluation, authors will then be informed whether their article has been accepted or not. If accepted, authors must deal with the respective corrections recommended by the evaluators and the Editorial Committee's final decision. If it is to be published.

Content

All articles being considered by the committee for possible publication in the *Ingeniería e Investigación journal* must consist of the following parts:

- Title, abstract and keywords must be written in Spanish and English. The title must clearly explain the contents of the article in question, written in normal title form and be preferably brief. The abstract should contain around 200 words in Spanish and English, as well as including the methods and materials used, results obtained and conclusions drawn.
- An Introduction must be given. It must describe article's general purpouse, including its main objective, referring to any previous work and the scope of the current article.
- Conclusions must be drawn. This section must provide the implication of the results found and their relationship to the proposed objective.
- Bibliographical references must be given (an explanation and example of how to set them out is given later on).
- Acknowledgements (Optional). These should be brief and mention any essential support received for carrying out the work being reported.
- Appendix (Optional).

Scientific and technological research articles must also include:

- Experimental development. This must be written giving sufficient details for the subject to be fully understood by readers, including descriptions of any procedures involved.
- Results. These must give a clear explanation and interpretation of the findings. If it is necessary, a brief, focused discussion about how given results can be interpreted.

It is required that the bibliographical references for all articles are included at the end of the article, given in alphabetical order of first authors' surnames and mentioned in the text and, since May 2014, it is asked that the authors use the American Psychological Association (APA) style for citation and references:

- Articles published in journals:

Author, A. A., Author, B. B., & Author, C. C. (year). Article title. Journal Title, volume number(issue number), page numbers.

Del Sasso, L. A., Bey, L. G. & Renzel, D. (1958). Low-scale flight ballistic measurements for guided missiles. Journal of the Aeronautical Sciences, 15(10), 605-608

Author, A. A., & Author, B. B. (year). Article title. Journal Title, volume number(issue number), page numbers. Retrieved from http://www.xxxxxxxxxxxxxxxx

Gaona, P. A. (2014). Information visualization: a proposal to improve search and access digital resources in repositories. Ingeniería e Investigación, 34(1), 83-89. Retrieved from http://www.revistas.unal.edu.co/index.php/ingeinv/article/ view/39449

- Books:

Author, A. A. & Author, B. B. (year). Title of work. Location: Publisher.

Turner, M. J., Martin, H. C. & Leible, R. C. (1964). Further development and applications of the stiffness method, Matrix Methods of Structural Analysis. New York: the Macmillan Co.

- Conference papers and symposium contributions:

Uribe, J. (1973, September). The effects of fire on the structure of Avianca building, Paper presented at National Seminar concerning Tall Buildings, Bogotá, Colombian School of Engineering.

- Theses or undergraduate projects:

Patton, F. D. (1906). Multiple modes of shear failure in rock-related materials (PhD thesis, University of Illinois).

Further information can be obtained by:

Contacting the Editorial Team (Email: revii_bog@unal.edu.co) or Prof. Andrés Pavas (Editor-in-Chief.
Email: fapavasm@unal.edu.co)

The *Ingeniería e Investigación* journal's office is located at: Ciudad Universitaria, Facultad de Ingeniería, Edificio CADE. Telefax: (57-1) 3165000 Ext. 13674. Bogotá - Colombia.